NOVEL MECHANISMS OF

PROGRAMMED CELL DEATH

IN THE PROTOZOAN PARASITE *BLASTOCYSTIS*

YIN JING
B.Sc. (Hons.), NUS

A THESIS SUBMITTED

FOR THE DEGREE OF MASTER OF SCIENCE

DEPARTMENT OF MICROBIOLOGY

NATIONAL UNIVERSITY OF SINGAPORE

2009

Acknowledgements

First and foremost, I would like to express my deepest gratitude to my supervisor, Dr Kevin Tan for his guidance and support ever since I was an undergraduate student. He has given me the freedom to explore on my own while always steered me in the right direction whenever I was lost. His expertise, patience and encouragement were invaluable to me in completing this project. I am thankful to him for providing me a well rounded graduate research experience.

I owe my sincere thanks to Dr. Wu Binhui for initiating the purification of legumain and for the many helpful discussions and ideas.

Thank you to all the past and present members of the Tan lab who helped me in one way or another and made the lab a wonderful and pleasant place to work in: Dr. Manoj, Angeline, Jun Hong, Han Bin, Chuu Ling, Vivien, Alvin, Haris, Joshua, Joanne and Lenny. Special thanks to Madam Ng Geok Choo and Mr. Rama for their tireless efforts in maintaining the smooth functioning of the lab.

I am greatly indebted to Mrs. Josephine Howe for her time and help in teaching me transmission electron microscopy techniques. I would also like to thank Kok Tee and Saw from the Flow Cytometry Unit, Hu Xian and Zhang Jie from the Confocal Microscope Unit in National University Medical Institute for their assistance in flow cytometry and confocal microscopy.

Last but not least, I would like to thank my parents and grandparents for their unwavering love and support throughout the years.

Yin Jing

August 2009

Publications

Journals:

Jing Yin, Angeline JJ Ye, and Kevin SW Tan (2010) Autophagy is involved in starvation response and cell death in *Blastocystis*. Microbiology 156: 665-677.

Binhui Wu*, Jing Yin*, Catherine Texier, Michael Roussel, and Kevin SW Tan (2010) *Blastocystis* legumain is localized on the cell surface and specific inhibition of its activity implicates a pro-survival role for the enzyme. Journal of Biological Chemistry 285: 1790-1798. (*equal first author)

Jing Yin, Josephine Howe, and Kevin SW Tan (2010) Staurosporine-induced programmed cell death in *Blastocystis* occurs independently of caspases and cathepsins and is augmented by calpain inhibition. Microbiology (in press). doi: 10.1099/mic.0.034025-0

Conferences:

Yin J and Tan KSW. Proteomic analysis of antibody- and metronidazole-induced programmed cell death in the protozoan parasite *Blastocystis*. In 15th Euroconference on Apoptosis, 26 – 31 October 2007, Portoroz, Slovenia.

Jing Yin and Kevin S. W. Tan. Staurosporine-induced programmed cell death in *Blastocystis.* In 4th International Conference on Anaerobic Protists, 12 – 16 May 2008, Taoyuan, Taiwan.

Binhui Wu, Jing Yin and Kevin S. W. Tan. Identification of cysteine proteases potentially involved in programmed cell death of *Blastocystis*. In 4th International Conference on Anaerobic Protists, 12 – 16 May 2008, Taoyuan, Taiwan.

Table of Contents

Summary

Programmed cell death (PCD) is crucial for cellular growth and development in multicellular organisms. Although distinct PCD features have been described for unicellular eukaryotes, homology searches have failed to reveal clear PCD-related orthologs among these organisms. Previous studies revealed that a surface-reactive monoclonal antibody MAb 1D5 could induce apoptosis-like PCD in the protozoan parasite *Blastocystis*. In the present study, through two-dimensional gel electrophoresis and mass spectrometry, the cellular target of MAb 1D5 was identified as a cell surface-localized legumain, an asparagine endopeptidase that is usually found in lysosomal/acidic compartments of other organisms. Recombinant *Blastocystis* legumain displayed biphasic pH optima in substrate assays, with peaks at pH 4 and 7.4. Activity of *Blastocystis* legumain was greatly inhibited by legumain specific inhibitor Cbz-Ala-Ala-AAsn-EPCOOEt (APE-RR), and moderately inhibited by MAb 1D5, cystatin and caspase-1 inhibitor. It was found that inhibition of legumain activity induced apoptosis-like PCD in *Blastocystis*, observed by increased externalization of phosphatidylserine (PS) residues and *in situ* DNA fragmentation. In contrast to plants, in which legumains have been shown to play a pro-death role, legumain appears to display a pro-survival role in *Blastocystis*. The data strongly suggest that legumain has a key role in the regulation of *Blastocystis* cell death.

Previous studies demonstrated that besides apoptosis, MAb 1D5 could elicit a PCD response in *Blastocystis* independent of caspases-like activity, mitochondria, or both, suggesting the existence of an alternative cell death pathway. In this study, the use of autophagic marker monodansylcadaverine (MDC) and autophagic inhibitors 3-

methyladenine and wortmannin showed the existence of autophagic cell death in MAb 1D5-treated *Blastocystis*. MAb 1D5-triggered autophagy was intensified in the presence of the caspase inhibitor zVAD.fmk and appeared to be dependent on mitochondrial outer membrane permeabilization (MOMP) since the MOMP inhibitor cyclosporine A could abolish MDC incorporation in MAb 1D5-treated cells, even in the presence of zVAD.fmk. This study is the first to report the occurrence of autophagy in *Blastocystis* through induction by a cytotoxic antibody. MDC staining of *Blastocystis* colony forms revealed that autophagy also occurs naturally in this organism. Amino acid starvation and rapamycin treatment are two common triggers of autophagy in mammalian cells and *Blastocystis* was found to rapidly up-regulate MDC-labeled autophagic vacuoles upon these inductions. Confocal microscopic and transmission electron microscopic studies also showed morphological changes suggestive of autophagy. The unusually large size of the autophagic compartments within the parasite central vacuole was found to be unique in *Blastocystis*. These results suggest that the core machinery for autophagy is conserved in *Blastocystis* and plays an important role in starvation response and cell death of the parasite.

The last part of this study reports that staurosporine, a common apoptosis-inducer in mammalian cells, also induces cytoplasmic and nuclear features of apoptosis in *Blastocystis*, including cell shrinkage, PS externalization, maintenance of plasma membrane integrity, extensive cytoplasmic vacuolation, nuclear condensation and DNA fragmentation. Staurosporine-induced PS exposure and DNA fragmentation was abolished by the MOMP inhibitor cyclosporin A and significantly inhibited by the broad cysteine protease inhibitor iodoacetamide. Interestingly, the apoptosis phenotype was insensitive to inhibitors of caspases and cathepsins B and L while

calpain-specific inhibitors augmented staurosporine-induced apoptosis response. While the identities of the proteases responsible for staurosporine-induced apoptosis warrants further investigation, these findings demonstrate that PCD in *Blastocystis* is complex and regulated by multiple mediators.

Chapter 1

Introduction

1.1 Biology of *Blastocystis*

Blastocystis is a protozoan parasite found in the intestines of humans and many other animals. It is often the most common organisms isolated in parasitological surveys (Stenzel and Boreham, 1996; Tan, 2004, 2008; Zierdt, 1991a). The parasite was first described in the early 1900's (Alexeieff, 1911; Brumpt, 1912) and has since then baffled researchers about its life cycle, pathogenesis, biochemistry, cellular and molecular biology. This organism has evoked considerable research interests due to its potential to cause intestinal diseases (Zierdt, 1991b) and the last decade or so has seen significant advances in our understanding of *Blastocystis* biology (Tan, 2008).

1.1.1 Taxonomy and classification

The taxonomic position of *Blastocystis* spp. has been controversial until the recently unambiguous placement of this organism into the stramenopiles (Arisue *et al.*, 2002; Hoevers and Snowden, 2005; Silberman *et al.*, 1996). It was initially suggested to be an yeast or fungus (Alexeieff, 1911; Brumpt, 1912) and the cyst of a flagellate (Haughwout, 1918). Zierdt and colleagues found that *Blastocystis* had some protistan features morphologically and physiologically. They classified this organism as a protist in the phylum Protozoa, subphylum Sporozoa (Zierdt *et al.*, 1967), reclassified later to subphylum Sarcodina (Zierdt *et al.*, 1988). Molecular sequencing studies of small-subunit rRNA indicated that *Blastocystis* is not monophylectic with the yeasts,

fungi, sarcodines or sporozoans (Johnson *et al.*, 1989). Another study by Silberman *et al.* reported the complete sequence of *Blastocystis* small-subunit rRNA gene and showed that it could be placed among the stramenopiles (Silberman *et al.*, 1996). Yet two studies using the sequence of elongation factor-1α (EF-1α) suggested that *Blastocystis* diverged before the stramenopiles and was related to *Entamoeba histolytica* (Ho *et al.*, 2000; Nakamura *et al.*, 1996). However, both studies with EF-1α were criticized by its low statistical significance and other factors, which made the phylogenetic position of *Blastocystis* inaccurate (Tan, 2008; Tan *et al.*, 2002). A recent study used multiple molecular sequence data (including small-subunit rRNA, cytosolic-type 70 kD heat shock protein, translation elongation factor 2 and the non-catalytic 'B' subunit of vacuolar ATPase) and clearly showed that *Blastocystis* is a stramenopile (Arisue *et al.*, 2002).

The Stramenopiles, also called *Chromista* and *Heterokonta*, are a diverse group of unicellular and multicellular protists comprising of heterotrophic and photosynthetic representatives, and are characterized by their flagella and hair-like projections extending laterally from the flagellum (mastigonemes). *Blastocystis* does not have flagella and is non-motile. Therefore, it is placed in a new class called *Blastocystea*, subphylum *Opalinata*, infrakingdom *Heteokonta*, subkingdom *Chromobiota*, kingdom *Chromista* (Tan, 2008). The closest species to *Blastocystis* is *Proteromonas lacertae* (Arisue *et al.*, 2002; Silberman *et al.*, 1996).

The designation of *Blastocystis* subsets has also been bewildering because different studies used different methods to subtype and classify *Blastocystis* sp., which made corroboration, comparison or criticism of publications very difficult. Due to the

urgency of a standard terminology in this research field, a group of investigators from different laboratories came up with a consensus on the terminology of *Blastocystis* subtypes (Stensvold *et al.*, 2007a). In the past, *Blastocystis* isolates from humans was designated *Blastocystis hominis*, whereas *Blastocystis* isolates from other animals was usually named *Blastocystis* sp., or specific names according to the host origin, such as *Blastocystis ratti*. However, this old practice of assigning *Blastocystis* species according to host origin is misleading because of the extensive genetic diversity of this organism even among isolates from one host. Therefore, the current consensus terminology recommends that all mammalian and avian isolates are designated *Blastocystis* sp. and assigned to a subtype from 1 to 9 by a simplified small subunit-rDNA typing method (Stensvold *et al.*, 2007a; Stensvold *et al.*, 2007b). Table 1.1 shows the new designations of some commonly studied *Blastocystis* isolates. Humans can be host to *Blastocystis* spp. originated from various mammals (subtype 1), primates and pigs (subtype 2), rodents (subtype 4), cattle and pigs (subtype 5), and birds (subtype 6 and 7) (Tan, 2008).

Table 1.1 Old and new classification of commonly studied *Blastocystis* isolates based on a consensus terminology* (adapted from Tan, 2008)

Species	Isolate(s)	Culture type	Host	New designation
B. hominis	Nand II	Axenic	Human	*Blastocystis* sp. subtype 1
B. hominis	Si	Axenic	Human	*Blastocystis* sp. subtype 1
B. hominis	B, C, E, G, H	Axenic	Human	*Blastocystis* sp. subtype 7
B. ratti	S1, WR1, WR2	Axenic	Rat	*Blastocystis* sp. subtype 4
Blastocystis sp.	NIH:1295:1	Xenic	Guinea pig	*Blastocystis* sp. subtype 4

*proposed by Stensvold *et al.*, 2007a

1.1.2 Morphology

Blastocystis is a polymorphic organism and four major forms (vacuolar, granular, amoeboid and cyst) are commonly observed in fecal and laboratory culture samples (Stenzel and Boreham, 1996; Tan *et al.*, 2002; Zierdt *et al.*, 1967).

The vacuolar form, also referred to as the central vacuole form, is the predominant cell form seen in stool samples and axenized *in vitro* cultures and considered to be the typical *Blastocystis* cell form (Figure 1.1 A). It is spherical and varies greatly in size, diameter ranging from 2 to 200 μm with average diameters of 4 to 15 μm (Stenzel and Boreham, 1996). The characteristic large vacuole occupies up to 90% of the cell volume, surrounded by a thin rim of cytoplasm containing organelles such as the nucleus, Golgi apparatus, endoplasmic reticulum and mitochondrion-like organelles (Tan *et al.*, 2002).

The granular form (Figure 1.1 B) is morphologically similar to the vacuolar form, except that there are granules in the cytoplasm or more commonly in the central vacuole. The granular form is slightly larger in size, with average diameters of 3 to 80 μm (Dunn *et al.*, 1989a; Zierdt and Williams, 1974). They are usually seen in non-axenized and older cultures (Tan, 2004).

The amoeboid form (Figure 1.1 C) has been rarely identified with conflicting reports on its morphology (Dunn *et al.*, 1989a; McClure *et al.*, 1980; Tan *et al.*, 1996b). Generally it is irregular in shape and often has extended pseudopodia, but appears non-motile despite the observation of pseudopods. They are usually observed in old or

antibiotic-treated cultures (Zierdt, 1973), and in *Blastocystis* colonies grown in soft agar (Tan *et al.*, 1996b).

The cyst form (Figure 1.1 D) was discovered most recently (Mehlhorn, 1988; Stenzel and Boreham, 1991). It is smaller in size (2 to 5 μm) than the other three forms and is surrounded by a thick multi-layered cyst wall. The cyst form has been reported to withstand environmental stress. Unlike the vacuolar and granular form, cysts are able to resist lysis by distilled water, and are able to survive at room temperature for up to 19 days (Zaman, 1998; Zaman *et al.*, 1995). The cyst form has been shown to be the infective stage by several experimental infectivity studies with mice, rats and birds (Abou El Naga and Negm, 2001; Moe *et al.*, 1997; Tan, 2008)

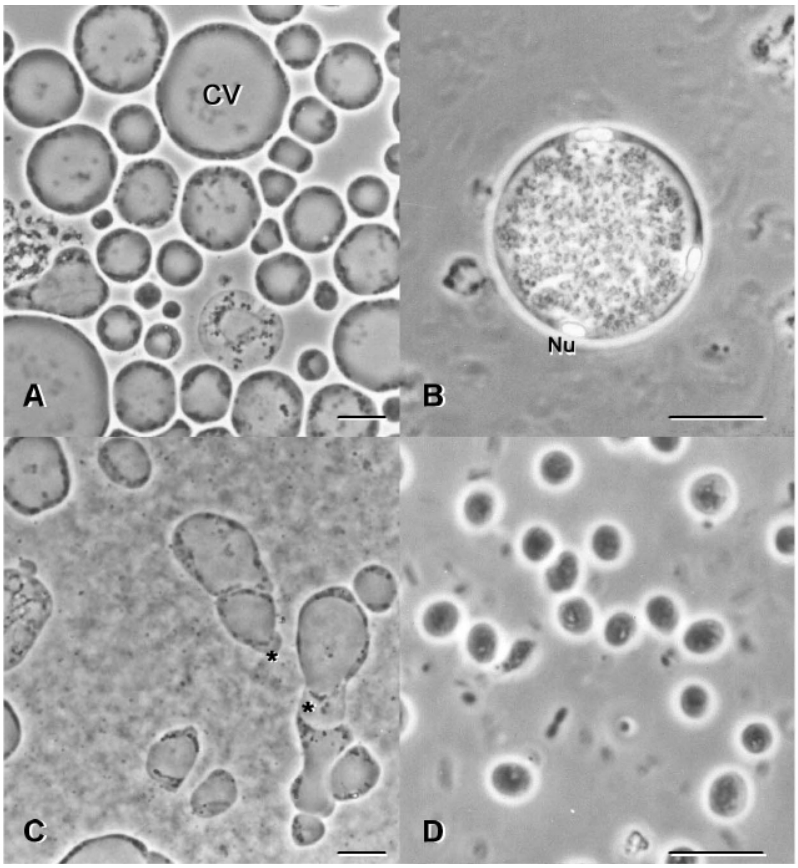

Figure 1.1 Morphological forms of *Blastocystis*. Light micrographs of **(A)** vacuolar forms; **(B)** granular forms; **(C)** amoeboid pseudopod-like cytoplasmic extensions (*); and **(D)** cyst forms. CV, central vacuole; Nu, nucleus. (Tan, 2007)

1.1.3 Life cycle and mode of transmission

A number of conflicting life cycles have been proposed for *Blastocystis* (Boreham and Stenzel, 1993; Singh *et al.*, 1995; Zierdt, 1973) and controversies about these modes of division are due to the lack of experimental proof. Different modes of reproduction such as schizogony (Singh *et al.*, 1995), plasmotomy (budding) (Tan and Suresh, 2007), endodyogeny (Zhang *et al.*, 2007) and sac-like pouches (Suresh *et al.*, 1997) have been postulated based on observations in different studies. However, the only accepted mode of reproduction should be binary fission until proven otherwise (Tan, 2008).

A revised life cycle incorporating information on animal infection studies and the recent phylogenetic studies was proposed (Tan, 2004, 2008). The proposed life cycle (Figure 1.2) suggests that cyst form is the infective stage and the infection by this parasite occurs in humans and animals by fecal-oral route. The cysts develop into vacuolar forms in the large intestines. In the human intestine, vacuolar forms divide by binary fission and may develop into amoeboid or granular forms. Encystations of vacuolar forms may occur in host intestines and intermediate cysts may have a thick fibrillar layer which is lost during the passage in the external environment. Humans are potentially infected by seven or more subtypes (subtype 1 to 7) of *Blastocystis* and certain animals are reservoirs for transmission to humans. Subtype 1 is cross-infective among mammals and birds. Subtypes 2, 3, 4, and 5 are primate/pig, human, rodent and cattle/pig isolates respectively. Subtypes 6 and 7 are mainly avian isolates.

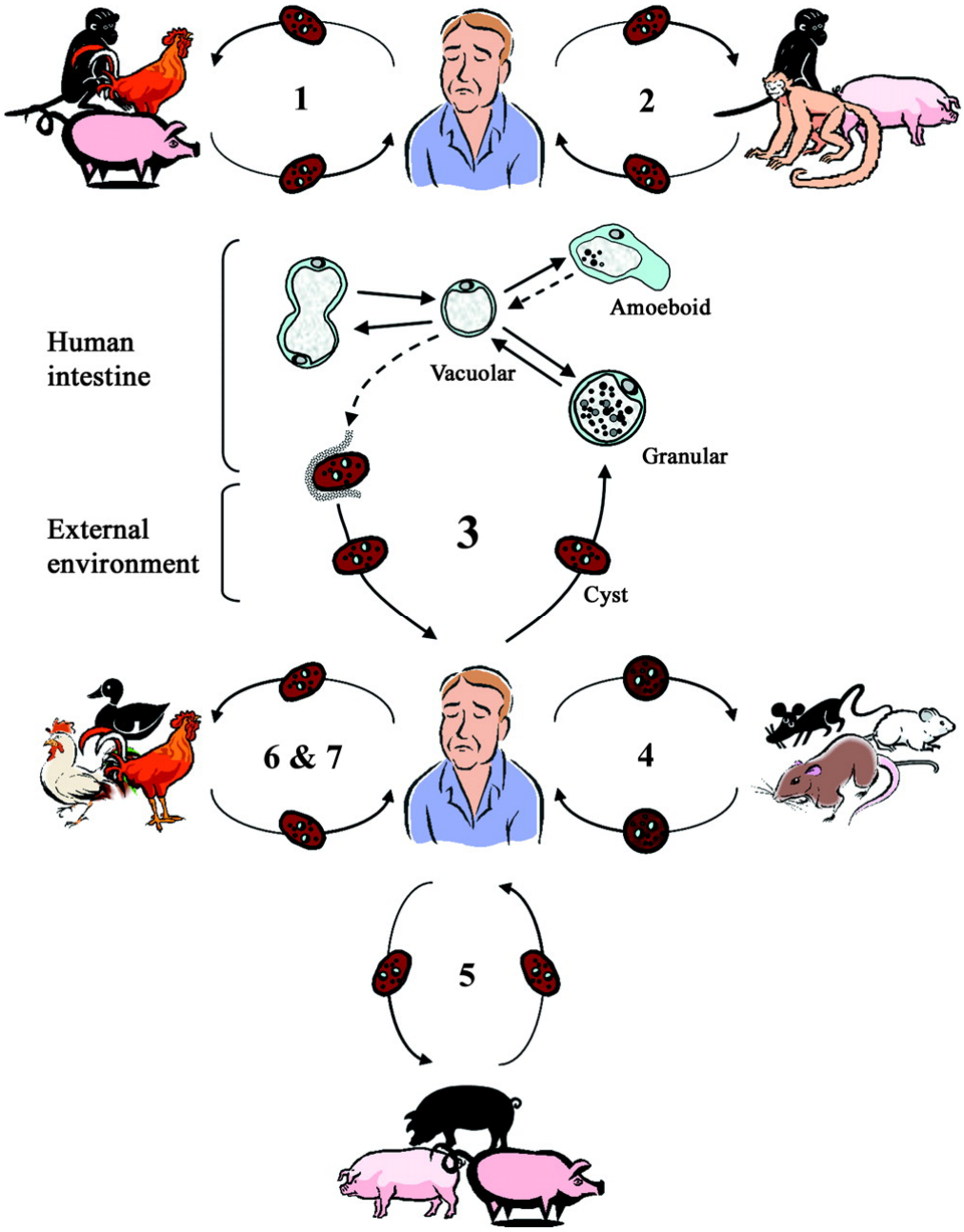

Figure 1.2 Life cycle of *Blastocystis* proposed by Tan, 2008. The proposed scheme suggests that humans are potentially infected by seven or more subtypes (subtype 1 to 7 as shown by the numbers 1 to 7) of *Blastocystis* and that certain animals are reservoirs for transmission to humans. Hypothetical pathways are represented by dotted arrows.

1.1.4 Epidemiology and prevalence

Blastocystis is often the most frequently isolated parasite found in the fecal samples of both healthy individuals and patients suffering from intestinal disorders (Cirioni *et al.*,

1999; Pegelow *et al.*, 1997; Stenzel and Boreham, 1996; Wang, 2004). Prevalence of *Blastocystis* infection is higher in developing countries at a carriage rate up to 60% (Pegelow *et al.*, 1997) and this has been linked to poor hygiene and deficient in sanitation facilities. Increased risk of infection may also be associated with occupations that involve exposure to animals (Rajah Salim *et al.*, 1999).

1.1.5 Pathogenesis

The pathogenicity of *Blastocystis* is currently a matter of debate as there have been numerous studies either implicate or exonerate the parasite as a cause of diseases (Clark, 1997; Stenzel and Boreham, 1996; Tan *et al.*, 2002).

A prospective controlled study suggested that there was no obvious difference in the prevalence of *Blastocystis* in individuals with and without diarrhea and hence *Blastocystis* was not an important diarrhea-causing agent (Shlim *et al.*, 1995). Another case-controlled study (Leder *et al.*, 2005) concluded that there was no correlation between clinical symptoms and *Blastocystis* infection in immunocompetent individuals. However, these studies can be questioned because clinical outcome is multifactorial and influenced by host and parasite factors (Tan, 2008). For example, infections with other established enteric protozoan pathogens such as *Giardia* and *Entameoba* do not always lead to disease. In addition, many of these studies are based on the assumptions that *Blastocystis* is biologically homogenous, but in fact this organism may have inter-subtype and intra-subtype variation in pathogenesis.

In two reports on placebo-controlled treatment of symptomatic but immunocompetent patients with *Blastocystis* as the solely identified pathogen (Nigro *et al.*, 2003;

Rossignol *et al.*, 2005), therapeutic improvement was found concomitant with the clearance of *Blastocystis*. However, critics of these studies may include the existence of some unidentified pathogen.

There are also some *in vitro* studies sought to investigate the effects of *Blastocystis* on mammalian cell cultures. Walderich *et al.* showed that *Blastocystis* could cause cytopathic effects in Chinese hamster ovary and HT 29 cells (Walderich *et al.*, 1998). Puthia *et al.* showed that cysteine proteases of *Blastocystis* were able to cause significant degradation of human secretory immunoglobulin A, compromise barrier function of intestinal epithelial cells, cause host cell apoptosis, and induce proinflammatory cytokines (Puthia *et al.*, 2008; Puthia *et al.*, 2006; Puthia *et al.*, 2005). These studies support a pathogenic role for *Blastocystis*.

It is suggested that because there are no reports unequivocally proving *Blastocystis* is nonpathogenic and there are accumulating epidemiological, *in vitro* and animal studies strongly suggesting the pathogenic potential of the parasite, it would be prudent to consider *Blastocystis* as an emerging protozoan pathogen (Tan, 2008). In the meanwhile, a good animal model should be developed to test Koch's postulates and to fill the gap of our understanding in the pathogenesis of *Blastocystis*.

1.2 Types of cell death

Cell death is a fundamental biological process. Programmed cell death (PCD) is generally opposed to 'accidental cell death', that is necrosis induced by pathological stimuli (Kroemer *et al.*, 2005). PCD is a highly regulated cellular suicide process in

eukaryotes (Hatsugai *et al.*, 2006). PCD is involved in a variety of biological events such as morphogenesis, aging, maintenance of tissue homeostasis and elimination of infected or malignant cells. Thus PCD plays a crucial role in the development and homeostasis of multicellular organisms and deregulation of this process contributes to major pathologies, including cancer, autoimmune diseases, and neurodegenerative diseases (Lenardo *et al.*, 1999; Okada and Mak, 2004; Yuan and Yankner, 2000).

Cell death can occur through different mechanisms resulting in distinct morphologies. Three major morphologies of cell death have been described: apoptotic (or Type I), autophagic (or Type II) and necrotic (or Type III) cell death (Clarke, 1990; Kroemer *et al.*, 2005; Schweichel and Merker, 1973).

1.2.1 Type I cell death – apoptosis

Apoptosis is the most common and well-defined form of PCD. The term 'apoptosis' (meaning 'falling leaves' in Greek) was coined more than 30 years ago to remark on the distinctive morphological features observed in this type of cell death (Kerr *et al.*, 1972). A cell undergoing apoptosis shows a characteristic morphology including rounding-up of the cell, retraction of pseudopods, cellular volume reduction (pyknosis), chromatin condensation, nucleus fragmentation (karyorhexis), little or no ultrastructural modification of cytoplasmic organelles, plasma membrane blebbing, and maintenance of plasma membrane impermeability until late stages of the process (Ameisen, 2002; Kroemer *et al.*, 2005). Blebbing of the plasma membrane leads to the formation of apoptotic bodies, which are engulfed by phagocytes in the absence of any inflammatory response(Henson *et al.*, 2001; Savill *et al.*, 2002).

Apoptosis in mammalian cells is mediated primarily, although not exclusively, by a family of cysteine proteases called caspases (Nicholson, 1999; Salvesen and Dixit, 1999). Caspases cleave their substrates specifically after the aspartate residues. Caspases can be divided into inflammatory caspases and pro-apoptotic caspases, which can be further grouped into initiator and effector caspases (Leist and Jaattela, 2001). They are normally expressed in healthy cells as inactive precursor enzymes. When initiator caspases such as caspases-8 or caspases-9 oligomerize and undergo autoproteolysis, they become active and cleave the precursor form of effector caspases, such as caspases-3, caspases-6 and caspases-7. Activated effector caspases in turn cleave a specific set of cellular substrates, leading to the biochemical and morphological changes associated with apoptosis.

Three major pathways of apoptosis-associated caspase activation (Figure 1.3) have been firmly established – the extrinsic, intrinsic and granzyme B pathway (Taylor *et al.*, 2008). The extrinsic pathway is activated by the binding of extracellular death ligands such as FasL or tumor necrosis factor-α (TNF-α) to transmembrane death receptors on cell surface, inducing the formation of the death-induced signaling complex (DISC). DISC in turn recruits caspase-8 and promotes its autoprocessing and the cascade of procaspase activation that follows (Nagata, 1999; Peter and Krammer, 1998; Wajant, 2002). In the intrinsic pathway, various extracellular and intracellular stresses activate one or more members of the BH3-only protein family. The activation of BH3-only protein above a threshold level overcomes the inhibitory effect of the anti-apoptotic B-cell lymphoma-2 (BCL-2) family members and promotes the pro-apoptotic BCL-2 family members such as BAX and BAK to form pores in the mitochondria outer membrane. Upon mitochondrial outer membrane permeabilization

(MOMP), cytochrome *c* is released and seeds the assembly of apoptosome where caspase-9 becomes active and then propagates the caspase activation cascade (Kroemer *et al.*, 2007). The granzyme B pathway takes place in cytotoxic lymphocyte killing where cytotoxic T lymphocytes (CTL) or natural killer (NK) cells release granules containing granzyme B and perforin to their target cells. Granzyme B enters target cells through pores formed by oligomerization of perforin, and directly activates effector caspases because they have the same specificity as that of caspases to cleave after aspartate residues (Lord *et al.*, 2003; Martin *et al.*, 1996). Granzyme B can initiate mitochondrial events by cleaving the BH3-only protein BID (BH3-interacting domain death agnoist). Truncated BID (tBID) can promote mitochondrial cytochrome *c* release and apoptosome assembly (Barry *et al.*, 2000). In some situations, BID also serves as a link between the extrinsic and intrinsic apoptotic pathways through caspase-8-mediated cleavage to tBID (Yin, 2000).

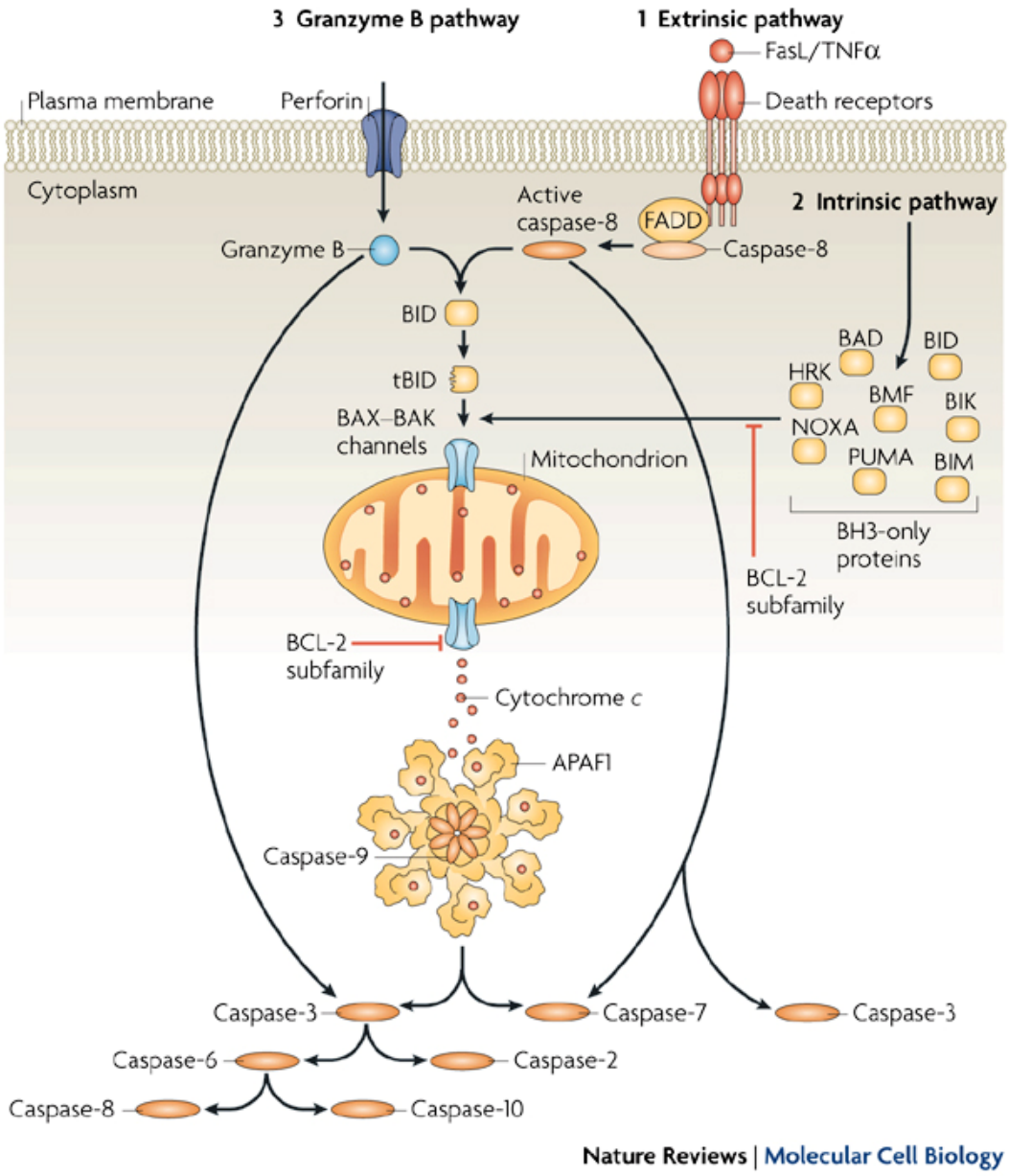

Figure 1.3 Caspase activation pathways (Taylor *et al.*, 2008)

Because of the pivotal roles of caspases in the execution of apoptosis, it has been frequently thought that apoptosis equals caspase activation. However, this belief is challenged by the fact that apoptotic cell death can still occur even when the caspase cascade is blocked, primarily because there are caspase-independent mechanisms of cell death, the main mediators being certain mitochondrial proteins or noncaspase proteases (Abraham and Shaham, 2004; Kroemer and Martin, 2005; Yuan *et al.*, 2003).

The induction of MOMP is a critical event in apoptosis and often defines the point of no return (Kroemer and Reed, 2000). Most pathways upstream of MOMP are independent of caspases. Upon induction of MOMP, mitochondria can release cytochrome *c* and lead to the classical caspase-dependent pathway. However, other caspase-independent effectors such as apoptosis-inducing factor (AIF), endonuclease G and HtrA2/Omi can also be released from mitochondrial intermembrane space and promote caspase-independent death, although the mechanisms are not fully understood (Lorenzo and Susin, 2004; van Gurp *et al.*, 2003). AIF is a flavoprotein which has important function in bioenergetic and redox metabolism and is confined to the mitochondria in healthy cells. When MOMP has occurred, AIF translocates to the nucleus, where it interacts with DNA, triggering chromatin condensation and DNA degradation into large fragments of about 50 kb (Cande *et al.*, 2002; Susin *et al.*, 1999). Endonuclease G is another protein which translocates from mitochondria to the nucleus upon MOMP, and it extensively cleaves nuclear DNA into nucleosomal fragments (Li *et al.*, 2001; van Loo *et al.*, 2001). HtrA2/Omi is a mitochondrial serine protease which can be released into cytosol and induce apoptosis in a caspase-independent manner through its protease activity as well as in a caspase-dependent manner by binding to inhibitor of apoptosis proteins (IAPs) and subsequently activating caspases (Hegde *et al.*, 2002; Suzuki *et al.*, 2001).

Caspase-independent death can also result from stimuli that cause lysosomal membrane permeabilization (LMP) and the consequent release of cathepsin proteases. Lysosomal proteases were considered to only take charge of nonspecific degradation of proteins within lysosomes and contribute to necrotic cell death upon massive lysosomal rupture, but recently it has become evident that upon moderate lysosomal

damage lysosomal proteases have an active and specific role in apoptotic cell death, sometimes without the apparent activation of caspases (Johnson, 2000; Stoka *et al.*, 2007). The cathepsins family consists of cysteine cathepsins (cathepsin B, C, F, H, K, L, O, S, V, X, W), the aspartate protease cathepsin D and the serine protease cathepsin G (Turk *et al.*, 2000). Cathepsin B and D are most stable at physiologic, cytoplasmic pH and are found to be involved in apoptosis. In bile salt-induced apoptosis of rat hepatocytes, cathepsin D and B were found to be activated in a cascade-like fashion downstream of caspases and cathepsin B translocated to the nucleus as the effector protease (Roberts *et al.*, 1999; Roberts *et al.*, 1997). Cathepsin B was also shown to be a dominant execution protease downstream of caspases in several tumor cell lines (Foghsgaard *et al.*, 2001). However, cathepsin B can also be a cell death mediator independent of caspases in WEHI-S fibrosarcoma and non-small cell lung cancer (NSCLC) cells (Broker *et al.*, 2004; Foghsgaard *et al.*, 2001). Cathepsins can induce cell death in a mitochondrion-dependent manner, by cleaving the Bcl-2 family protein Bid and leading to the mitochondrial release of pro-apoptotic factors (Heinrich *et al.*, 2004; Stoka *et al.*, 2001), or by activating Bax with the subsequent release of AIF from mitochondria (Bidere *et al.*, 2003).

The calcium-dependent cytosolic protease calpains have also been described as mediators of apoptosis (Wang, 2000). Calpains can participate in apoptosis signaling downstream or upstream of caspases. For example, caspases have been shown to cause the cleavage of the natural calpain inhibitor calpastatin and lead to the activation of calpain (Porn-Ares *et al.*, 1998). Calpains can act downstream of caspases and contribute to the degradation phase of apoptosis of HL-60 cells (Wood and Newcomb, 1999). In other apoptosis models, calpain activation is upstream of

caspases (Waterhouse *et al.*, 1998) and calpain activates caspase-12 (Nakagawa and Yuan, 2000). However, calpain is also capable to execute cell death in complete absence and independent of caspases in vitamin D-induced apoptosis of the breast cancer cell line MCF-7 (Mathiasen *et al.*, 2002).

1.2.2 Type II cell death – autophagic cell death

Type II, or autophagic cell death is characterized by increased number of autophagic vacuoles in the cytoplasm, without chromatin condensation (Kroemer *et al.*, 2005; Schweichel and Merker, 1973). The autophagic vacuoles are double-membraned and contain degenerating cytoplasmic organelles or cytosol (Levine and Klionsky, 2004b). Type II cell death is morphologically distinct from apoptosis. In classical apoptosis, cytoskeletal elements collapsed early but organelles are preserved until late apoptosis, whereas in autophagic cell death, organelles are degraded early and cytoskeletal elements are preserved until late stage (Bursch *et al.*, 2000). Autophagic cell death proceeds without chromatin condensation or DNA fragmentation, which are characteristics of apoptosis (Levine and Yuan, 2005). *In vivo*, residues of cells undergoing type II cell death are phagocytosed by neighboring cells, just like those of apoptosis, and there is no tissue inflammatory response (Schweichel and Merker, 1973). The term 'autophagic cell death' often misleads people to believe that cell death is occurring through autophagy, but in fact the term simply describes cell death with autophagy because there is no conclusive evidence of a causal relationship between autophagy and cell death (Tsujimoto and Shimizu, 2005).

Autophagy is the major mechanism used by eukaryotic cells to degrade long-lived proteins and perhaps the only known pathway for degrading organelles (Levine and

Klionsky, 2004a). It is believed to be a conserved process in all eukaryotic cells. Autophagy is kept at low basal levels to serve homeostatic functions but is rapidly up-regulated in response to growth-factor withdrawal, starvation, differentiation and developmental triggers (Kuma *et al.*, 2004; Levine and Klionsky, 2004a; Shintani and Klionsky, 2004; Takeshige *et al.*, 1992). Autophagy also plays a role in the destruction of intracellular pathogens (Gutierrez *et al.*, 2004).

At least three forms of autophagy (chaperone-mediated autophagy, microautophagy and macroautophagy) have been recognized, based on their mechanisms, physiological functions and cargo specificity (Kourtis and Tavernarakis, 2009). Macroautophagy has been most extensively studied and is generally simply referred as autophagy. During macroautophagy (hereafter referred to as autophagy), a double-membrane structure called phagophore forms and expands to sequester a portion of cytoplasm in the form of an autophagosome. The autophagosome will fuse with a lytic compartment and the engulfed materials are degraded and the resulting macromolecules are recycled (Figure 1.4) (Klionsky and Emr, 2000; Levine and Klionsky, 2004a).

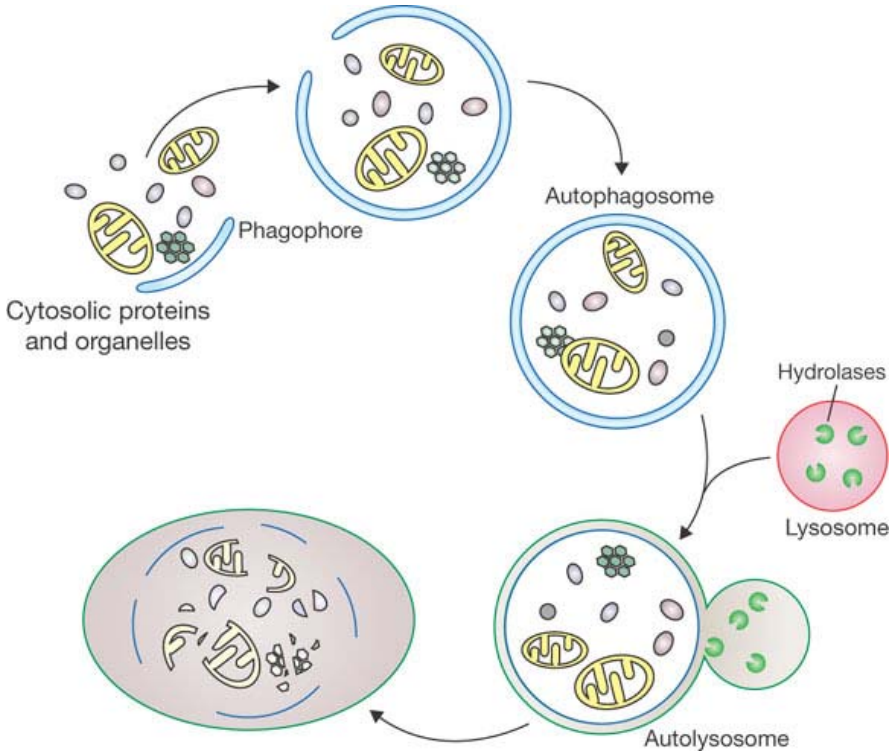

Figure 1.4 Schematic model of the autophagic process (adapted from Xie and Klionsky, 2007).

Our understanding of the molecular basis of autophagy has been significantly advanced by analyses of autophagy-defective mutants in yeasts (Klionsky *et al.*, 2003; Tsukada and Ohsumi, 1993). There are 32 *a*utopha*g*y-related (ATG) genes identified in *Saccharomyces cerevisiae* and other fungi, and many yeast ATG genes have orthologs in mammalian cells (Kanki *et al.*, 2009; Klionsky, 2007; Okamoto *et al.*, 2009). The ATG genes encode proteins required for the induction of autophagy, and the nucleation, expansion, maturation and recycling of autophagosomes (Xie and Klionsky, 2007). Upstream of Atg proteins, several protein kinases regulate autophagy, including at least the phosphatidylinositol 3-kinase (PI3K) and the target of rapamycin (TOR) kinase. TOR is the major inhibitory signal of autophagy during nutrient abundance because it negatively regulates autophagosome formation and expansion (Kamada *et al.*, 2000). The class I PI3K/Akt signaling pathway is activated

by receptor tyrosine kinase and activates TOR to suppress autophagy in the presence of insulin-like and other growth factor (Lum *et al.*, 2005a).

As mentioned above, the exact role of autophagy in type II cell death is still unclear and has been an ongoing debate in the scientific community (Gozuacik and Kimchi, 2004; Kroemer and Levine, 2008; Levine and Yuan, 2005). The presence of autophagic vacuoles in dying cells may result from two possibilities: autophagy is the death execution mechanism, or autophagy is an adaptive response to rescue cells under stress conditions. Theoretically, in order to determine that autophagy observed in a cell is truly a death mechanism, inhibition of autophagy by pharmacological inhibitors or RNA interference (RNAi) would prevent cell death. However, the inhibition of autophagy often shifts the appearance of cell death to another type such as apoptosis and necrosis, instead of effectively enhancing cell survival (Kosta *et al.*, 2004). In some cases, autophagic cell death is prevented while autophagy is still observed (Lee and Baehrecke, 2001). These may suggest that autophagy *per se* is neither sufficient nor required for autophagic cell death (Levine and Yuan, 2005).

There are some studies which indicate that the autophagy pathway is capable of killing cells. Bax-/-, bak-/- murine embryonic fibroblasts (MEFs) fail to exhibit classical apoptosis upon exposure to cytotoxic agents, yet are capable of dying with a type II morphology. This death is blocked by RNAi against autophagy gene Atg5 and Atg6/Beclin 1 (Shimizu *et al.*, 2004). In another study, RNAi directed against Atg6/Beclin 1 and Atg7 suppressed cell death in mouse L929 fibrosarcoma cells treated with the caspase inhibitor zVAD.fmk (Yu *et al.*, 2004). In bax-/-, bak-/- MEFs, autophagy seems to be required for the induction of necrotic death in response to

endoplasmic reticulum (ER) stress (Ullman *et al.*, 2008). However, the physiologic relevance of autophagy gene-dependent cell death in cells whose apoptotic machinery has been crippled is uncertain (Levine and Yuan, 2005). Recent studies of the Drosophila salivary gland development have shown that both apoptosis and autophagy are required for the degradation of these organs (Berry and Baehrecke, 2007), giving the first strong evidence that even in the presence of apoptotic factors, autophagy is required for physiological autophagic cell death during development (Berry and Baehrecke, 2008).

There are also studies supporting that autophagy in the dying cells is a pro-survival mechanism, and type II morphology may result from the failure of cells to adapt. For example, following growth factor withdrawal, bax-/-, bak-/- cells rapidly show reduced ATP levels and compromised bioenergetics and will die if autophagy is inhibited, but bax-/-, bak-/- cells with intact autophagic machinery can sustain viability for several weeks. Although these cells die eventually, at any point before cell death, the addition of growth factor reserves the catabolic responses and maintains cell viability (Lum *et al.*, 2005a).

The exact role of autophagy in cell death and survival is rather complicated and cellular context-dependent. It appears that autophagy probably functions initially as a cytoprotective response, but if cellular damage is too extensive or if apoptosis is compromised, excessive autophagy may be used to kill the cell. Autophagic cell death may be important for complete self-degradation when phagocytes are unavailable (Berry and Baehrecke, 2008). The resources generated by autophagic cell death of individual cells may promote survival of the organism (Galluzzi *et al.*, 2008).

1.2.3 Type III cell death – necrosis

Type III cell death, or necrosis, is usually defined negatively as a type of cell death without signs of apoptosis or autophagy (Kroemer *et al.*, 2005). The morphological features of necrosis include early plasma membrane rupture, cytoplasmic swelling and vacuolation, dilation of cytoplasmic organelles such as mitochondria, ER and Golgi apparatus, as well as moderate chromatin condensation (Edinger and Thompson, 2004; Kroemer *et al.*, 2005). Necrosis is usually a consequence of patho- or supra-physiological condition, such as infection, inflammation, ischemia, mechanical force, heat or cold damage (Zong and Thompson, 2006). The traumatic cell destruction leads to release of intracellular components and triggers inflammatory immune responses (Edinger and Thompson, 2004). Although necrosis has been conceived as a passive and uncontrolled form of cell death, recent evidences suggest that necrosis can also be a regulated event and programmed necrosis may serve to maintain the integrity of tissue and organism (Festjens *et al.*, 2006; Zong and Thompson, 2006).

Table 1.2 summarizes the characteristics of the three different types of cell death (Gozuacik and Kimchi, 2004; Okada and Mak, 2004).

Table 1.2 Characteristics of different types of cell death

	Type I apoptotic	*Type II autophagic*	*Type III necrotic*
Nucleus	Chromatin condensation DNA laddering Nuclear fragmentation	Partial chromatin condensation Nucleus intact until late stages No DNA laddering	Clumping Random degradation of DNA
Cell membrane	Blebbing	Blebbing	Swelling; rupture
Cytoplasm	Cytoplasmic condensation Fragmentation to apoptotic bodies	Increased number of autophagic vesicles	Increased vacuolation Organelle degeneration Mitochondrial swelling
Biochemical features	Caspases are active	Caspase-independent Increased lysosomal activity	Not well characterized
Detection methods	Electron microscopy TUNEL staining Annexin V staining Increase in sub G1 cell population Nuclear fragmentation detection Caspase activity assays	Electron microscopy Test of increased long-lived protein degradation MDC staining Detection of LC3 translocation to autophagic membranes	Electron microscopy Nuclear staining (usually negative) Detection of inflammation and damage in surrounding tissues

1.3 Programmed cell death (PCD) in protozoan parasites

PCD has long been recognized as an essential process to eliminate the unwanted or damaged cells and thus to ensure normal growth and development in multicellular organisms. It was assumed that PCD arose with multicellular organisms (Vaux *et al.*, 1994). However, recently considerable experimental evidences have been accumulated towards the existence of PCD in unicellular eukaryotes. These include non-parasitic organisms, such as yeast (Madeo *et al.*, 2002), the free living slime mold *Dictyostelium discoideum* (Arnoult *et al.*, 2001; Cornillon *et al.*, 1994), the free living ciliate *Tetrahymena thermophila* (Christensen *et al.*, 1998; Kobayashi and Endoh, 2005) and the dinoflagellate *Peridinium gatunense* (Vardi *et al.*, 1999). In parasitic organisms, PCD has been described in the kinetoplastid trypanosomes (Ameisen *et al.*, 1995; Welburn *et al.*, 1996) and *Leishmania* (Arnoult *et al.*, 2002; Bera *et al.*, 2003; Zangger *et al.*, 2002), the apicomplexan parasite *Plasmodium* (Al-Olayan *et al.*, 2002; Deponte and Becker, 2004), trichomonads (Mariante *et al.*, 2006), *Giardia lamblia* (Chose *et al.*, 2003) and *Blastocystis* (Tan and Nasirudeen, 2005).

1.3.1 Occurrence of PCD in unicellular eukaryotes

The baker's yeast *Saccharomyces cerevisiae* is probably the best-known eukaryotic organism and its PCD machinery is also the best studied among unicellular organisms (Frohlich *et al.*, 2007). The first observation that yeast can exhibit apoptotic markers was made on a strain carrying a mutation in the cell division cycle gene CDC48 (Madeo *et al.*, 1997). Mutations or heterologous expression of proapoptotic genes also induce PCD in yeast. Yeast can also undergo apoptosis in some physiological scenarios such as cellular aging, failed mating, or exposure to killer toxins (Buttner *et*

al., 2006). The yeast metacaspase YCA1 has been shown to have similar functions of caspase and mediate apoptosis in yeast (Madeo *et al.*, 2002). Other crucial proteins of the basic molecular machinery executing cell death are also found to be conserved in yeast, such as AIF and HtrA2/Omi (Frohlich *et al.*, 2007). Autophagy genes have been characterized in yeast (Klionsky, 2007) and autophagic cell death can be triggered (Abudugupur *et al.*, 2002). Due to its ease of genetic manipulation and the simplicity of PCD pathway, yeast has been used as a model organism to study the mechanism of PCD and to identify new regulators of PCD from other organisms.

Dictyostelium discoideum grows as a colony of cycling single cells, but upon starvation this slime mold forms multicellular aggregates made of a stalk of dead cells that support the viable spores (Ameisen, 2002). The ease to grow *in vitro*, availability of fully sequenced genome, and well established genetic tools make this protist a good model to study different modes of PCD (Tresse *et al.*, 2007). Apoptotic and non-apoptotic PCD features was observed in stalk cells in an *in vitro* system involving differentiation without morphogenesis (Cornillon *et al.*, 1994), but no DNA fragmentation was detected in this study. However, in another study of similar settings, DNA degradation was detected and a homolog of human AIF of *D. discoideum* was shown to translocate from mitochondria to the nucleus during cell death, and was suggested to be involved in DNA degradation (Arnoult *et al.*, 2001). A vacuolar, autophagic type of cell death was triggered by developmental stimulation of the *D. discoideum* HMX44A strain with no signs of apoptosis, whereas genetic inactivation of the Atg1 autophagy gene switched the mode of cell death to from autophagic cell death to necrotic cell death (Tresse *et al.*, 2007).

Unicellular protozoan parasites cause a wide variety of human diseases. Current treatment of these infections is being challenged by increasing incidence of drug resistance and lack of effective vaccine (Croft *et al.*, 2006; Fidock *et al.*, 2008). Investigation of PCD pathways in these organisms might lead to discovery of novel parasite control strategies (Alvarez *et al.*, 2008; Deponte and Becker, 2004). However, despite the many morphological and biochemical studies of PCD in protozoan parasites, most of the homologs of mammalian molecules involved in cell death signaling are missing in the protozoa and the molecular architecture of PCD in protozoan parasites therefore remains puzzling.

The kinetoplastid parasites of the genera *Leishmania* and *Trypanosoma* cause different forms of leishmaniasis or trypanosomiasis such as Chagas disease (*T. cruzi*) and sleeping sickness (*T. brucei*). Different developmental stages of *Trypanosoma* and *Leishmania* have been shown to die with apoptotic or autophagic features by diverse triggering events (Debrabant *et al.*, 2003). *T. cruzi* epimastigotes during *in vitro* differentiation exhibited cytoplasmic and nuclear morphological features of apoptosis (Ameisen *et al.*, 1995). *T. cruzi* epimastigotes cell death could also be induced by human serum and inhibited by L-arginine-dependent synthesis of nitric oxide (Piacenza *et al.*, 2001), whereas superoxide radicals resulted from mitochondrial calcium overload promotes human serum-induced cell death in *T. cruzi* and overexpression of mitochondrial super oxide dismutase had cytoprotective effects (Irigoin *et al.*, 2009; Piacenza *et al.*, 2007). Reactive oxygen species also induced PCD of procyclic forms of *T. brucei* by activating a calcium-dependent pathway because excess Ca^{2+} was observed in nucleus and Ca^{2+} chelators could inhibit DNA fragmentation (Ridgley *et al.*, 1999). In this system, the nuclease activation was not a

consequence of serine protease, cysteine protease or proteasome activity nor did overexpression of Bcl-2 reverse mitochondrial dysfunction, so it was suggested that proteins involved in trypanosome PCD might be distinct from those in metazoans (Ridgley *et al.*, 1999). *In vitro* cultures of *T. brucei* procyclic forms showed PCD features upon treatment with concanavalin A, a glucose- and mannose-specific lectin binding to glycoproteins (Welburn *et al.*, 1996). The proto-oncogene prohibitin and a receptor for activated protein kinase C was shown to be up-regulated in concanavalin A-induced cell death of *T. brucei* (Welburn and Murphy, 1998). Prostaglandin D2 and its derivatives can induce apoptosis-like PCD in *T. brucei* blood forms with increasing levels of intracellular reactive oxygen species (ROS), and pretreatment with low molecular weight antioxidants abolished formation of ROS, apoptotic features and inhibited cell death (Figarella *et al.*, 2005; Figarella *et al.*, 2006).

Leishmania donovani exhibited apoptotic features in response to various stimuli, such as aging (Lee *et al.*, 2002), oxidative stress (Das *et al.*, 2001), antileishmanial drug amphotericin B (Lee *et al.*, 2002) or the topoisomerase I inhibitor camptothecin (Sen *et al.*, 2004). Autophagic cell death was observed when *L. donovani* was treated with antimicrobial peptides (Bera *et al.*, 2003). *L. major* was found to succumb to the broad-spectrum protein kinase inhibitor staurosporine (Arnoult *et al.*, 2002), heat shock or serum deprivation (Zangger *et al.*, 2002) with apoptotic features. The amastigote form of *L. major* died with DNA fragmentation when treated with nitric oxide, which could be produced by macrophages infected by the parasite (Zangger *et al.*, 2002). Heat stress induced apoptotic-like death in *L. infantum* was found to be partially reversed by expression of the anti-apoptotic mammalian gene Bcl-X_L (Alzate

et al., 2006) and mitochondrial superoxide was found to mediate this cell death (Alzate *et al.*, 2007), suggesting an important role of mitochondria in this model.

Apicomplexan protozoa of the genus *Plasmodium* cause malaria. It was found that the rodent parasite *P. berghei* undergoing differentiation from zygotes to ookinetes exhibited features typical of metazoan apoptotic cells including chromatin condensation, nuclear DNA fragmentation, exposure of phosphatidylserine (PS) from the inner to the outer layer of the cell membrane and caspase-like activity which was blocked by caspase inhibitors (Al-Olayan *et al.*, 2002). Apoptotic like features were also observed in the human parasite *P. falciparum* blood stage cultures after treatment with the antimalarial drug chloroquine (Picot *et al.*, 1997) or the apoptosis-inducer etoposide through a putative role of PfMCA1 metacaspase-like protein (Meslin *et al.*, 2007). However, as it might be difficult to analyze apoptotic markers in *Plasmodium* parasites (Deponte and Becker, 2004), some studies could not detect apoptotic markers during *Plasmodium* cell death (Nyakeriga *et al.*, 2006), but observed secondary necrosis (Porter *et al.*, 2008) and autophagic-like cell death (Totino *et al.*, 2008).

Trichomonads are amitochondrial parasites but possess hydrogenosome, an unusual anaerobic energy-producing organelle. *T. vaginalis* and *T. foetus* showed dramatic changes when treated with drugs and H_2O_2, including apoptotic features such as DNA fragmentation, exposure of PS in the outer leaflet of plasma membrane, hydrogenosomal membrane potential dissipation, and autophagic features such as an abnormal number of oversized vacuoles containing altered hydrogenosomes and misshapen flagella (Chose *et al.*, 2002; Mariante *et al.*, 2006). However, studies

related to trichomonads cell death are relatively few and more investigations are needed to understand how these parasites die without the known "mitochondrial cell death machinery" and the putative role of hydrogenosomes during cell death (Chose *et al.*, 2003).

Blastocystis subtype 7 (previously known as *B. hominis* isolate B) underwent apoptosis-like death when treated with a cytotoxic monoclonal antibody (MAb 1D5) or the drug metronidazole (Nasirudeen *et al.*, 2004; Nasirudeen *et al.*, 2001b; Tan and Nasirudeen, 2005). *Blastocystis* cells displayed a number of morphological and biochemical features of apoptosis such as cell shrinkage and darkening, retention of plasma membrane integrity during initial stages of cell death, externalization of plasma membrane PS residues. DNA and nuclear fragmentation was also shown *in situ* although there was no DNA laddering pattern on agarose gels as seen in many apoptotic cells. Apoptotic bodies-like objects appeared to be deposited into the large central vacuolar space of the parasite by an invagination process (Nasirudeen *et al.*, 2004; Nasirudeen *et al.*, 2001b; Tan and Nasirudeen, 2005). Caspase-3-like antigens and activity was detected during MAb 1D5-induced *Blastocystis* cell death; however, the identity of the caspase-3-like protein is still unknown (Nasirudeen *et al.*, 2001a). Loss of mitochondrial membrane potential was noted in *Blastocystis* cell death (Nasirudeen and Tan, 2004). PCD that is independent of both caspase and mitochondria was also reported (Nasirudeen and Tan, 2005). On the other hand, ageing *Blastocystis* cells grown as colonies seemed to die with autophagic features, showing cytoplasmic vacuolation with myelin and lipid-like inclusions (Tan *et al.*, 2001a).

1.3.2 Implications of PCD in unicellular eukaryotes

The existence of PCD in unicellular organisms may seem counterintuitive, as each cell can survive as an individual and the death of the cell means the death of an organism. However it has been suggested that unicellular organisms can organize themselves as populations and have intercellular communication (DosReis and Barcinski, 2001). A population of protozoan parasites infecting a host is usually founded by a single or a small number of individuals and most of the population share very similar or identical genetic information. Thus it is the entire parasite population of a host but not individual parasites that is subjected to evolutionary pressure (Bruchhaus *et al.*, 2007). PCD may be useful in regulating the number of parasites to avoid damaging a host too early (Al-Olayan *et al.*, 2002; Bruchhaus *et al.*, 2007). PCD can also be a mechanism to control parasite growth under environmental pressure such as nutrient scarcity (Debrabant *et al.*, 2003). Apoptosis-like death of parasites may avoid host inflammatory response leading to the killing of entire parasite population, and thus favour parasite evasion from the host immune system (Lee *et al.*, 2002; Zangger *et al.*, 2002).

1.4 Objectives of the present study

Despite increasing number of studies describing the cytochemical features of PCD in protozoan parasites, knowledge of the mechanism and molecular mediators of PCD in these unicellular organisms is very limited. Previous studies showed that *Blastocystis* succumbed to a cytotoxic monoclonal antibody MAb 1D5 by displaying features that are characteristic of apoptosis (Nasirudeen *et al.*, 2001a; Nasirudeen *et al.*, 2001b; Tan and Nasirudeen, 2005). MAb 1D5 was found to bind to a 30 kD protein of

unknown identity on the plasma membrane (Tan *et al.*, 2001b; Tan *et al.*, 1996a; Tan *et al.*, 1997). The present study aimed to identify the cellular target of MAb 1D5 through two dimensional gel electrophoresis and mass spectrometry based proteomic analysis followed by functional study of the protein. It is hoped that identifying and characterizing this protein would facilitate the discovery of cell death mechanisms in *Blastocystis*.

It was reported that while DNA fragmentation was abolished, MAb 1D5-treated *Blastocystis* pre-exposed to zVAD.fmk and cyclosporine A was not rescued from cell death (Nasirudeen and Tan, 2004, 2005). Therefore, besides apoptosis, other cell death pathways might exist in *Blastocystis* and be triggered upon MAb 1D5 induction. In recent years, autophagic cell death (type II cell death) has received a lot of attention as an alternative PCD pathway (Baehrecke, 2005). The second part of the present study aimed to investigate if MAb 1D5 elicits alternative cell death pathway through autophagy and to characterize the autophagy phenomenon in *Blastocystis*.

Different signaling pathways of PCD can be activated in the same cell in response to different stimuli (Taylor *et al.*, 2008). Besides using cytotoxic antibody to induce PCD in *Blastocystis*, the present study also aimed to investigate if staurosporine, a common inducer of apoptosis in mammalian cells and the pathways of which has been extensively studied, can also elicit a PCD response in *Blastocystis*. Furthermore, by dissecting the mechanisms and regulation of the staurosporine-induced cell death pathway in *Blastocystis* may lead to discovery of novel mechanisms of PCD in this parasite.

Chapter 2

Materials and Methods

2.1 Culture of organism

Blastocystis subtype 7 (previously known as *B. hominis* isolate B) was isolated from a local patient stool sample and axenized (Ho *et al.*, 1993). Cells were cultured in Iscove's modified Dulbecco's medium (IMDM) containing 10% inactive horse serum and incubated anaerobically at 37 °C in an Anaerojar (Oxoid, UK). Cells were subcultured at 3 to 4 days intervals and 4-day old cells at log-phase were used for all experiments.

2.2 Preparation of monoclonal antibody (MAb) 1D5

In this study, monoclonal antibody (MAb) 1D5, a surface-reactive IgM antibody, was used to induce PCD in *Blastocystis.*

2.2.1 Hybridoma culture

The hybridomas secreting MAb 1D5 were produced previously (Tan *et al.*, 1996a). Briefly, three female BALB/c mice were immunized with 0.5 ml aliquots of the extract of *Blastocystis* subtype 7 (500 µg protein/ ml) emulsified in Freund's complete adjuvant. Following booster immunization, spleen cells were harvests and fused with P3.X63.Ag8.U1 (P3U1) myeloma cells. The resultant hybridomas were selected by limiting dilution. Hybridoma cells were cryopreserved in IMDM containing 10% fetal

bovine serum in the presence of 5% dimethylsulfoxide (DMSO) and kept in liquid nitrogen tank in the Department of Microbiology, National University of Singapore. Cryopreserved hybridoma cells were thawed and cultured in IMDM supplemented with 10% fetal bovine serum. Culture supernatant was collected when the medium became acidic (orange to yellow in color) but before cells died and stored under sterile conditions at −20 °C.

2.2.2 Purification of antibody

MAb 1D5 was purified from hybridoma supernatants using Affiland Monoclonal IgM purification kit (Affiland S.A., Belgium). Briefly, 75 g of Precipitating Agent was added to 300 ml of hybridoma supernatant for 15 min with mild agitation. The mixture was allowed to stand for 30 min at 4 °C and spun at 3000×g for 10 min to collect the pellet. The pellet was dissolved in 30 ml of MAb IgM Binding Buffer and loaded to a pre-equilibrated Monoclonal IgM Binding Gel (Sepharose^{TM} fast flow) column at a flow rate of 50 ml/h. MAb IgM Elution Buffer was used to elute MAb 1D5 and the Optical Density (OD) of the eluent at 280 nm was monitored. Twenty-one fractions of 2 ml eluent were collected (Figure 2.1 A) and 10 µl of each fraction was treated with β-mecaptoethanol, separated by SDS-PAGE and stained with Coomassie blue (Figure 2.1 B). Fractions A5 to A12 and B1 to B3 were protein containing fractions because of their high OD value (Figure 2.1 A) and also higher amount of proteins as seen on SDS-PAGE (Figure 2.1 B). To confirm these were indeed MAb 1D5, fraction A5 and A10 were checked by Western blotting using anti-mouse Ig and the results showed two reactive bands of molecular weight 25 kD and 50 kD, corresponding to the light chain and heavy chain of IgM.

A

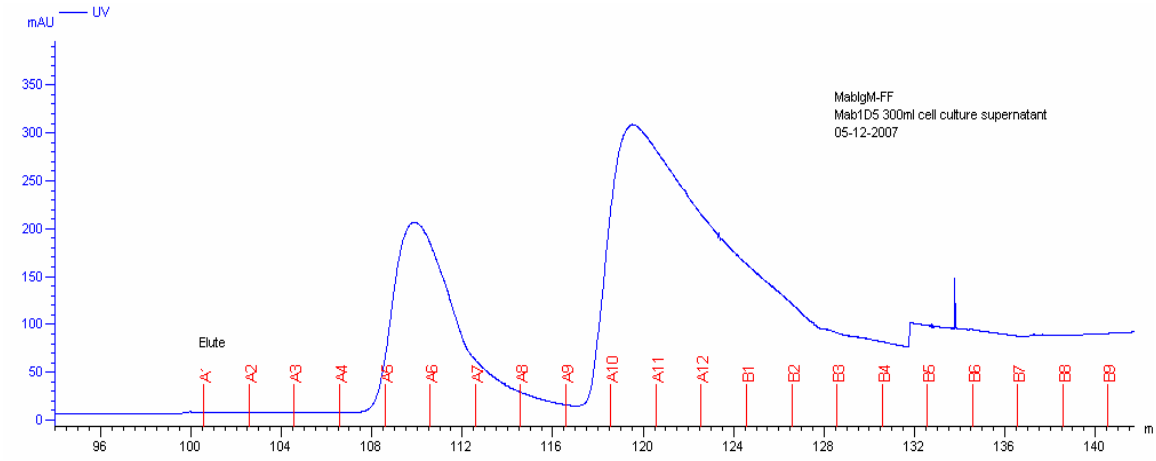

B

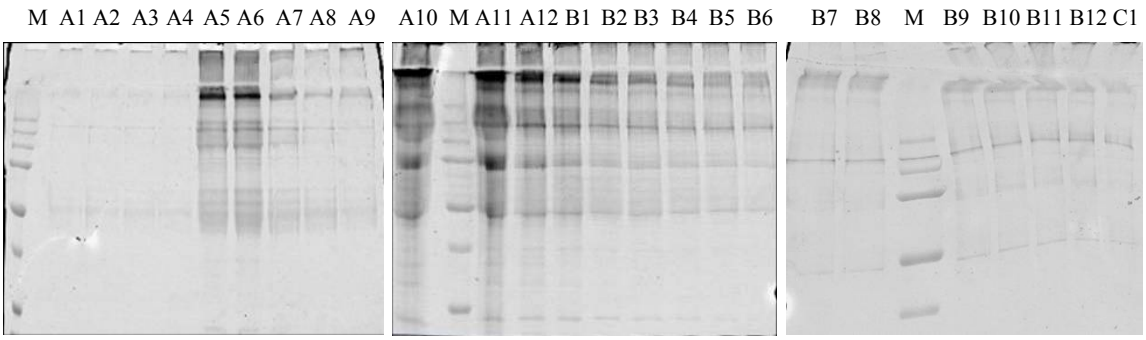

C

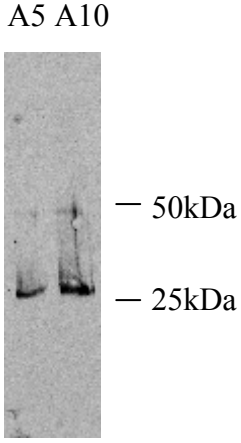

Figure 2.1 Purification of MAb 1D5. **A**, OD plot of elution fractions. **B**, elution fractions were loaded onto 10% SDS-PAGE gels and stained with Coomassie blue. M, molecular weight marker (bands from top to bottom indicate 250, 150, 100, 75, 50, 37 and 25 kD respectively). **C**, elution fraction A5 and A10 were separated on a 10% SDS-PAGE gel and transferred to a PVDF membrane and probed with rabbit anti-mouse Ig antibody.

Fractions A5 to A12 and B1 to B3 were pooled and the buffer of the eluant was changed to PBS and concentrated with a centrifugal filter unit (Amicon, Millipore). The protein concentration was assayed to be 16 μg/ml. The purified MAb 1D5 were stored at -20°C for experiments in this project and future use.

2.3 2-D proteomics

2.3.1 Sample preparation

Blastocystis cells were collected by centrifugation at 2000×g for 10 min and washed three times with 1×PBS (137 mM NaCl, 2.7 mM KCl, 2 mM KH_2PO_4, 10 mM Na_2HPO_4). The final cell pellet was stored at -80 °C until further use. HALT Protease Inhibitor Cocktail, EDTA-free (Pierce) was added to the cell pellet before cells were lysed. The cell pellet was treated with different sample preparation methods.

Method 1 Freeze-thaw

Cell pellet was resuspended in equal volume of PBS with protease inhibitor cocktail. The suspension was subjected to three cycles of alternate freezing (2 min in liquid nitrogen) thawing (37˚C water bath) and centrifuged at 16000×g for 10 min at 4 °C.

Method 2 Triton-X100

Cells were lysed by 0.5% (v/v) Triton-X100 in the presence of protease inhibitor cocktail and allowed to sit on ice for 30 min with occasional shaking. 2-D sample buffer (7 M urea, 2 M thiourea, 4% CHAPS, 50 mM DTT, 0.2% Bio-lyte® 3/10 ampholytes, 0.02% bromophenol blue) was added to the lysate for 10 min on ice, and clear supernatant was collected after centrifugation at 16000×g for 10 min at 4 °C.

Method 3 Trichloroacetic acid (TCA) precipitation

Cell pellet was subjected to three cycles of freezing and thawing. Total proteins from clear cell lysate were precipitated by adding 100% (w/v) TCA to sample so that the final TCA concentration is 10% (w/v). The precipitation process was carried out at 4 °C for 2 h and protein pellet was collected by centrifugation at 16000×g for 15 min at 4 °C. The pellet was washed twice with ice-cold acetone and allowed to air dry at room temperature.

Method 4 DOC-TCA precipitation

Lysates from freeze-thawed parasites was mixed with 1/100 of its volume of 2% DOC (sodium deoxycholate), incubated on ice for 30 min, and 100% (w/v) TCA was added to bring the sample to a final TCA concentration of 10% with immediate vortex. The sample was sat on ice for 2 h to precipitate proteins and protein pellet was collected by centrifugation at 16000×g for 15 min at 4 °C. The pellet was washed twice with ice-cold acetone and allowed to dry at room temperature.

Method 5 TCA/acetone precipitation

To 1 volume of freeze-thawed parasite lysates, 8 volumes of 11.3% (w/v) TCA/acetone was added to bring the final concentration of TCA to 10% (w/v). Protein precipitation was carried out at -20 °C for 2 h and protein pellet was collected by centrifugation at 16000×g for 15 min at 4 °C. The pellet was washed twice with ice-cold acetone and air dried at room temperature.

Method 6 Chloroform/MeOH precipitation

To 1 volume of freeze-thawed parasite lysates, the following reagents were added sequentially with vortexing: 4 volumes of methanol, 1 volume of chloroform and 3 volumes of water. After centrifugation at 16000×g for 2 min, aqueous top layer was removed and 4 volumes of methanol were added with vortexing. Protein pellet was collected by centrifugation of the mixture at 16000×g for 2 min and air dried at room temperature.

Following each method described above, sample buffer (7 M urea, 2 M thiourea, 4% CHAPS, 50 mM DTT, 0.2% Bio-lyte® 3/10 ampholytes, 0.02% bromophenol blue) was added to the solution or pellet. Protein concentration was estimated by a modified Coomassie Plus protein assay kit (Pierce) with BSA as standard because urea found in the lysis solution is a compound that interferes with protein estimation.

2.3.2 2-D electrophoresis

For 2-D electrophoresis in mini gel format, 200 µg proteins in 125 µl of 2-D sample buffer were loaded into a 7 cm immobilized pH gradient (IPG) strip (Bio-Rad). After active rehydration for 12 h at 50 V, isoelectric point focusing (IEF) was performed in a Bio-Rad Protean IEF Cell under the following conditions: linear voltage ramp to 150 V over 20 min; linear voltage ramp to 300 V over 20 min; linear voltage ramp to 600 V over 20 min; linear voltage ramp to 1200 V over 1 h; linear voltage ramp to 4000 V over 1.5 h; 4000 V for 12000 Vh. The IEF was performed at 20 °C at a maximum of 50 mA per strip. For big gel 2-D electrophoresis, 550 µg proteins in 300 µl of 2-D sample buffer were loaded into a 17 cm IPG strip. Active rehydration was carried out in Bio-Rad Protean IEF Cell for 12 h at 50 V, followed by IEF using the following parameters: linear voltage ramp to 250 V over 30 min; linear voltage

ramp to 500 V over 1 h; linear voltage ramp to 2500 V over 1.5 h; linear voltage ramp to 10000 V over 2.5 h; 10000 V for 40000 Vh. After IEF, IPG strips were soaked in equilibration buffer (6M urea, 2% SDS, 0.375 M Tris-HCl pH 8.8, 20% glycerol) supplied with 2% (w/v) DTT for 15 min and then in equilibration buffer containing 2.5% (w/v) iodoacetamide for 15 min. IPG strips of 7 cm length were then mounted onto a precast 8-16% Bio-Rad Ready Gel® using Easymelt agarose (Bio-Rad) and second dimension electrophoresis was performed in Bio-Rad Mini-PROTEAN® 3 electrophoresis cell at constant voltage of 200 V. IPG strips of 17 cm length were mounted onto home-made 12% Laemmli SDS-PAGE gel (18×16 cm) and second dimension electrophoresis was performed in Bio-Rad Protean II xi electrophoresis cell at 16 mA/gel for 30 min and then 24 mA/gel for another 6 h at 4°C. Gels were stained using Coomassie Brilliant Blue (CBB). Stained gels were scanned with Bio-Rad GS-800 densitometer and analyzed with PD Quest 7.1 software (Bio-Rad).

2.3.3 In-gel protein digestion and protein identification by MALDI-TOF mass spectrometry

Protein spots were manually excised from Coomassie blue-stained 2-D gels and were in-gel digested with trypsin. Briefly, gel pieces were soaked in 50% (v/v) acetonitrile (ACN) with 50 mM ammonium bicarbonate (NH_4HCO_3) and incubated at 37 °C for 30 min to wash off the stain. The gel spots were then dried in Speedvac vacuum centrifuge (Savant Instruments) for 5 min. A digestion solution of 3.3 ng/µl sequencing grade modified trypsin (Promega) in 50 mM NH_4HCO_3 was added to the dried gel piece and incubated at 37 °C overnight. Peptides were extracted using 0.1% (v/v) trifluoroacetic acid (TFA; Sigma) in 50% ACN, sonicated at 37 °C for 10 min and then dried in a Speedvac evaporator. Peptides were mixed with an equal volume

of CHCA matrix solution (5 mg/ml α-cyano-4-hydroxycinnamic acid in 0.1% TFA, 50% ACN) and spotted onto a 384-well MALDI sample plate (384 opti-TOF, ABI) followed by air-drying. MS and MS/MS (10 most intense ions from each sample were selected for MS/MS) analyses were carried out using the ABI 4800 MALDI-TOF/TOF Mass Spectrometer (Applied Biosystems). Peptides derived from trypsin were used as an internal standard. Data from MS and MS/MS acquisitions were used in a combined search against the NCBI nonredundant protein database and an in-house *Blastocystis in silico* translated protein database using MASCOT (Version 2.1; Matrix Science, London, UK). Mascot scores greater than 54 were considered to be significant ($p<0.05$).

The genomic sequence contigs of Mascot hits were retrieved. The program GENSCAN was used to predict the locations and exon-intron structures of genes in genomic sequence contigs (http://genes.mit.edu/GENSCAN.html). Parameters used were Arabidopsis for organism and suboptimal exon cutoff of 1.00. In case of multiple genes predicted within the same contig, the most probable gene for the chosen protein spot was verified by the presence of matched peptides. The predicted protein sequence was searched against the *Blastocystis* EST database (http://tbestdb.bcm.umontreal.ca/searches/organism.php?orgID=BH) stored locally using StandAlone Basic Local Alignment Search Tool (BLAST) version 2.2.18.

2.4 Western blotting

Two-dimensional gel electrophoresis was carried out as described in section 2.3.2. For one-dimensional sodium dodecylsulphate-polyacrylamide gel electrophoresis (1D

SDS-PAGE), *Blastocystis* cells were lysed in buffer (25 mM TRIS pH 7.5, 150 mM NaCl, 0.1% Triton X-100, 1 mM DTT, 1 mM EDTA, 1 mM EGTA, 10 mM NaF, 20 mM β-glycerophosphate, 1 mM Na_3VO_4, Roche complete protease inhibitor) and the soluble fraction obtained by centrifugation (16000×g, 10 min) at 4 °C. Total protein concentration was estimated by Bradford assay, and 50 µg of total protein or 5 µg of purified protein was electrophoresed on a 10% SDS-PAGE gel. Following 1-D or 2-D electrophoresis, proteins were transferred onto a PVDF membrane (GE Healthcare) by semi-dry blotting (Bio-Rad), blocked with 3% BSA in TBS-T (triethanolamine-buffered saline with 0.1% Tween 20), incubated with primary antibody, washed, incubated with secondary antibody and visualized by chemiluminescence (ECL plus, GE Healthcare) and exposed to an X-ray film (Kodak).

2.5 Comparison of sequences

The catalytic domain and C-terminal extension of *Blastocystis* legumain was amplified by PCR from a constructed cDNA library of *Blastocystis* subtype 7. Conceptual translation of the nucleotide sequence had 330 amino acids and the sequence was submitted to GenBank (accession number: ACO24555). Sequences of legumains from other species were retrieved from GenBank as the following: mouse (NP_035305), rat (NP_071562), human (AAH03061), bovine (NP_776526), frog (NP_001005720), zebra fish (NP_999924), *Schistosoma* (CAB71158), rice (BAC41386), tobacco (CAE84598), *Haemonchus* (CAJ45481) and *Trichomonas* (AAQ93040). Multiple sequence alignment was performed with ClustalW search engine and manually refined with program Vector NTI (Invitrogen).

2.6 Biochemical characterization of recombinant legumain

2.6.1 pH optimum for enzymatic activity

To measure the pH optimum of *Blastocystis* legumain enzymatic activity, purified recombinant legumain (10 μg) was placed in wells of a 96-well microplate. The reaction was started by adding legumain specific substrate Z-Ala-Ala-Asn-NHMec (finial concentration 10 μM) in assay buffers of different pH supplemented with 1 mM dithiothreitol, 1 mM EDTA and 0.1% CHAPS. The series of buffers used were: 50 mM citric acid-sodium citric, pH 3, pH 4, pH 5; 50 mM MES, pH 5.5, pH 6, pH 6.5; 50 mM Tris-Cl, pH 6.8, pH 7, pH 7.5, pH 8, pH 8.8. The plate was incubated at 30 °C for 30 min. Readings of fluorescence (excitation 353 nm; emission 442 nm) was taken by a TECAN fluorescence plate reader. Results were corrected by substracting the value obtained with legumain-heated inactive control.

2.6.2 Pharmacological inhibitors of enzymatic activity

Purified recombinant legumain was tested for its enzymatic activity in the presence of different inhibitors. The activity assay was carried as described in the previous section with PBS as reaction buffer. Inhibitors used were MAb 1D5 (1.2 μg/ml); non-specific IgM control (2 μg/ml); legumain-specific inhibitor Cbz-Ala-Ala-AAsn-RR-COOOEt (APE-RR, 1 mM); Z-Ala-Ala-Asn-NHMec (10 μM); cystatin (200 μg/ml); caspase-1 inhibitor Ac-YVAD-CMK (4 μM); and cathepsin B inhibitor Z-FA-FMK (400 μM).

2.7 Subcellular localization of legumain by immunofluorescent staining

Cells (1×10^7) were washed with cold PBS and incubated in IMDM medium containing 5 μg fluorescein diacetate (FDA) at 37 °C for 10 min. Cells were then washed and fixed with 3.7% (v/v) formaldehyde on ice for 30 min. To permeabilze cell, cell were incubated with 0.1% Trixton X-100 for 5 min. Cells were incubated with primary antibody (MAb 1D5 or anti-legumain, 1.2 μg/ml in PBS containing 3% BSA) for 2 h at room temperature, washed and incubated with AlexaFluor 594-conjugated secondary antibody (anti-mouse IgM or anti-goat IgG, 2 μg/ml in PBS containing 3% BSA) for 1 h at room temperature. The cells were washed and stained with DAPI and viewed using a confocal microscope (Olympus FV500).

2.8 Apoptosis detection assay

2.8.1 Annexin V-FITC and PI staining

Membrane permeability and exposure of phosphatidylserine (PS) were analyzed using an Annexin V-FITC apoptosis detection kit (BioVision). In brief, cells were washed with cold PBS and resuspended in 500 μl calcium-containing binding buffer. Five micro liter of Annexin V-FITC and propidium iodide (PI) each were added to the cell suspension and incubated at room temperature for 10 min. The cells were washed, re-suspended in 500 μl of PBS and analyzed by a flow cytometer (DAKO CyAn ADP) with 488 nm argon-ion laser. Annexin V-FITC was detected using an emission filter of 530-540 nm and PI was detected using an emission filter of 613-620 nm.

2.8.2 TUNEL assay

Terminal deoxynucleotidyl transferase-mediated dUTP nick-end labeling (TUNEL) was performed using APO-BrdU kit (Invitrogen). In brief, cells were harvested, washed with cold PBS and fixed with 1 ml 3.7% (v/v) formaldehyde on ice for 30 min. After two washes with PBS, the pellet was re-suspended in 1 ml of 70% cold ethanol at -20 °C for 30 min to permeabilize cells. The cells were washed and incubated with 50 µl labeling solution containing 5‑bromo‑2'‑deoxyuridine 5'‑triphosphate (BrdUTP) and terminal deoxynucleotidyl transferase at 37 °C for 1 h. After rinsing, cells were stained with AlexaFluor 488 conjugated anti-BrdU antibody at room temperature for 30 min. The cells were washed, re-suspended in 500 µl of PBS and analyzed by a flow cytometer (DAKO CyAn ADP) using a 488 nm argon-ion laser. Green fluorescence was detected using an emission filter of 530-540 nm.

2.9 Autophagy detection assay

2.9.1 Cell treatments

Blastocystis cells were subjected to various treatments for the assessment of autophagy.

For MAb 1D5 treatment, cells were pre-treated with 50 µM zVAD.fmk and/or 10 µM cyclosporine A for 30 min, and were then exposed to MAb 1D5 or non-specific IgM, and incubated anaerobically for 24 h at 37 °C.

To test for the presence of autophagy in *Blastocystis* colonies, cells were grown in soft agar as previously described (Tan *et al.*, 1996b) with minor modifications.

Approximately 1×10^4 cells taken from day 4 log-phase cultures were mixed in 1 ml of IMDM, added to 20 ml of the mixture of 0.36% Bacto agar and 0.1% sodium thioglycollate in IMDM supplemented with 10% horse serum at 40 °C, and poured into a 100 × 15 mm Petri dish (Nunclon). After gentle swirling to ensure good separation of cells, the Petri dish was kept at -20 °C for 10 min to allow the agar to set and then incubated in an anaerobic jar at 37 °C for 10 days.

For amino acid starvation, 1×10^7 *Blastocystis* cells washed three times with PBS and incubated in 5 ml of Hank's Buffered Salt Solution (HBSS). The tubes were then incubated anaerobically at 37 °C for different time intervals (1, 2 or 3 h).

Rapamycin treatment was done by incubating 1×10^7 *Blastocystis* cells with 100 nM, 500 nM or 1000 nM rapamycin (Sigma) in 5 ml IMDM supplemented with 10% horse serum and were incubated anaerobically at 37 °C for 3 h. DMSO control was also included.

To test the effect of the autophagy inhibitors 3-MA and wortmannin on *Blastocystis*, cells were pre-treated with 20 mM 3-MA (Sigma) or 50 µM wortmannin, and were incubated for 3 h prior to exposure to MAb 1D5, amino acid starvation or rapamycin treatment as described above.

2.9.2 Monodansylcadaverine (MDC) staining

Following various treatments, cells in liquid culture were spun down, washed once with PBS and resuspended in 500 µl PBS. Then 10 µl of 5 mM MDC (Fluka) in PBS was added to the suspension and incubated at 37°C for 15 min. After incubation, the

cells were washed thrice with PBS and mounted onto glass slides with coverslips. Cells were then visualized with a fluorescence microscope (Olympus BX60) using excitation filter of 360 nm and emission filter of 525 nm. The images were captured by a CCD camera (Olympus DP70). The percentage of MDC positive cells were determined by scoring 500 cells per group.

To stain colony cultures of *Blastocystis*, colonies embedded in the agar were removed by a sterile inoculating loop and stained with 0.05 mM MDC in PBS for 30 min. After which, the colonies were washed in 1 ml PBS twice with 5 min interval between each wash. The colonies were then placed on a slide and pressed gently with a coverslip. The colonies were viewed under fluorescent microscope to examine the uptake of the stain by cells at the center and periphery of the colony.

2.9.3 Confocal microscopy examination of MDC and Lysotracker Red costaining

Following various treatments, the cell pellet was stained with 0.05 mM MDC for 15 min at 37 °C and then with 50 nM Lysotracker Red DND-99 (Molecular Probes) for a further 30 min at 37 °C. After incubation, the cells were washed thrice with PBS and mounted onto glass slides with coverslips. Fluorescent images were obtained by using a confocal microscope (Olympus Fluoview FV500). MDC was excited at 405 nm, and emission was collected in the 505 nm to 525 nm bands and Lysotracker was excited at 543 nm, and emission was collected in the 584 nm to 654 nm bands.

2.10 Transmission electron microscopy (TEM)

The ultrastructural features of *Blastocystis* cells under various treatments were examined using transmission electron microscopy. Briefly, cells were fixed with 2% glutaraldehyde and 2% paraformaldehyde in PBS for 3 h at 4 ºC. The cells were then pelleted at 1000×g for 5 min, washed twice with PBS and twice with deionized water. After each washing step, cells were spun at 1500×g and the supernatant was discarded. Cells were then postfixed for 2 h with 1% osmium tetroxide containing 1% potassium ferro-cyanide at room temperature and dehydrated with graded ethanol series (25%, 50%, 75%, 95% and 100%). Infiltration of embedding media was done by passing cells through three changes of mixtures of ethanol and the embedding media (LR White resin), and four changes of absolute LR White embedding media. After the last change of LR White, cells were resuspended in 100 – 200 µl LR White. The suspension was then transferred to a BEEM capsule and centrifuged at 1500×g for 15 min to collect the cells at the bottom tip of the capsule. Capsules were then incubated for 48 h at 50ºC to allow polymerization of the embedding media. Cells were embedded into a microtome (Reichert-Jung) and sliced into 90 nm sections. Ultrathin sections were collected on a 200 mesh copper grid, stained with uranyl acetate and lead citrate each for 9 min and examined using an EM208S transmission electron microscope (Philips).

2.11 Treatment with staurosporine to induce cell death

Staurosporine (Sigma) was used to induce cell death in *Blastocystis*. Cells were inoculated into IMDM in a concentration of 2×10^6 cells per ml. Staurosporine (1 mM stock in DMSO, Sigma) was then added to a final concentration of 1 µM and

incubated with cells for 3 h or 12 h for flow cytometry analysis (as described in section 2.8) and ultrastructural studies (as described in section 2.10). Necrotic control was done by heating cells at 80 ºC for 15 min. The effect of protease inhibitors or cyclosporine A on staurosporine-induced cell death was tested by addition of protease inhibitors or cyclosporine A 30 min before the addition of staurosporine. The protease inhibitors used were: N-Benzyloxycarbonyl-Val-Ala-Asp(O-Me) fluoromethyl ketone (z-VAD.fmk); Z-Phe-Ala fluoromethyl ketone (z-FA.fmk); Z-Phe-Phe-fluoromethyl ketone (z-FF.fmk); (L-3-*trans*-(Propylcarbamyl)oxirane-2-carbonyl)-L-isoleucyl-L-proline methyl ester (CA-074Me); Z-Leu-Leu-Leu-fluoromethyl ketone (z-LLL.fmk); N-acetyl-L-leucinyl-L-leucinyl-L-norleucinal (ALLN); epoxomicin; (2S,3S)-*trans*-Epoxysuccinyl-L-leucylamido-3-methylbutane ethyl ester (E64D) (all were obtained from Sigma, diluted in DMSO, and used at 50 μM unless otherwise stated). Iodoacetamide was purchased from Bio-Rad and diluted in water. Cyclosporine A (Sigma) was diluted in DMSO and used at 10 μM.

2.12 Calpain activity assay

The calpain activity assay was performed using the Calpain Activity Assay Kit (Biovision) according to the manufacturer's protocol. Briefly, cells were treated with staurosporine for 3 h in the presence of different inhibitors. An equivalent number of cells (2×10^6) were pelleted, and the pellets resuspended and incubated in the supplied extraction buffer on ice for 20 min. After a brief centrifugation at 10000×g for 1 min, the clear lysates were transferred to a 96-well microplate, mixed with a fluorogenic calpain substrate Ac-LLY-AFC and incubated for 1 hour at 37 °C in the

dark. Fluorescence intensity was determined at 400 nm excitation and 505 nm emission by a TECAN fluorescence plate reader.

2.13 Reproducibility of results and statistical analysis

All experiments were repeated at least twice, except for transmission electron microscopy analysis, which was performed once. Quantitative data were statistically evaluated using the Student's *t*-test and the level of significance was set at $p<0.05$.

Chapter 3

Mechanisms of MAb 1D5-Induced PCD in *Blastocystis*

3.1 Identification of legumain as MAb 1D5 targeted protein through 2-D proteome analysis

The total set of proteins expressed from the genome of the cell at a given time is called the proteome (Anderson and Anderson, 1998). Two-dimensional gel electrophoresis (2-DE) is a powerful and most commonly used method for proteomic analysis (Gorg *et al.*, 2004; O'Farrell, 1975). Complex protein mixtures extracted from cells and tissues can be separated first according to their isoelectric point and then by molecular weight. Thousands of protein spots can be separated on a 2-D gel in a highly reproducible manner. Unknown proteins of interest can be excised from the gel and digested by trypsin followed by mass spectrometric analysis giving a pattern of digested peptides which can be matched to the theoretical patterns derived from known protein databases and thus the identity of the unknown protein can be ascertained (Gorg *et al.*, 2004).

3.1.1 Optimization of sample preparation for 2-D proteomics

The choice of a suitable sample preparation method is of ultimate importance for a successful 2-DE analysis of the proteome and has to be adapted and optimized for specific cells and tissues (Shaw and Riederer, 2003; Weiss and Gorg, 2008). Most sample preparation protocols consist of a two-step process: cell disruption and

solubilization of proteins. Some samples may require an in-between step to remove interfering compounds.

In the initial trial of sample preparation, *Blastocystis* cells were disrupted by freeze-thaw cycling or by detergent lysis using Triton X-100 and protein solubilization was carried out in a commonly used 2-D sample buffer consisting of chaotropes (7 M urea and 2 M thiourea), zwitterionic detergent (4% CHAPS), reducing agent (50 mM DTT), and carrier ampholytes (0.2% Bio-lyte® 3/10 ampholytes). The protein samples were separated in the first dimension on a 7 cm IPG strip and in the second dimension on an 8-16% gradient mini gel. As visualized by Coomassie blue staining (Figure 3.1.1), only a minimal amount of proteins were resolved at the acidic and lower molecular weight region. The scarcity of resolved protein spots may be due to poor solubilization of proteins or impeded entry of proteins to IPG strips caused by interfering compounds. Horizontal streaks seen on the gels also indicated incomplete isoelectric focusing.

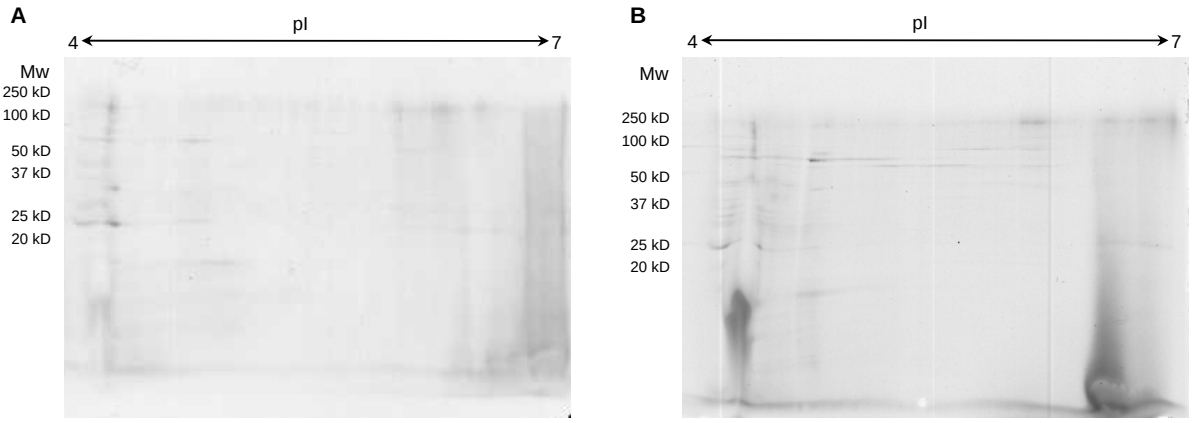

Figure 3.1.1 Coomassie blue-stained 2-D gels of *Blastocystis*. Cells were subjected to freeze-thaw cycling **(A)** or Triton-X 100 lysis **(B)** and then solubilized in 2-D sample buffer. Extracted proteins were then separated by IEF in the first dimension using a pI 4-7 gradient IPG strip followed by 8-16% gradient SDS-PAGE gel in the second dimension.

Precipitation is the most common method to separate proteins from contaminants in the sample and to concentrate proteins. Four precipitation methods, namely TCA (trichloroacetic acid) precipitation, DOC (sodium deoxycholate)-TCA precipitation, TCA/acetone precipitation and chloroform/methanol precipitation, were evaluated using mini-gel format 2-D electrophoresis in order to choose the most reliable one for the best protein separation. With regard to the concern of protein loss during precipitation and the consequent washing, it was found out through Bradford assay that the various precipitation methods were equally satisfactory and at least 70% of the protein levels in crude lysates were recovered in each case. Figure 3.1.2 shows the representative results of 2D electrophoresis analysis by the four different precipitation methods. The TCA/acetone precipitation method (Figure 3.1.2 A) constantly yielded the most satisfactory result because the protein spots were best resolved. DOC-TCA precipitation (Figure 3.1.2 B) performed well to resolve proteins at the acidic region, but proteins near the neutral region were missing in the precipitate. TCA precipitation alone (Figure 3.1.2 C) was not as effective as the combination of TCA and acetone based on the observation of a great amount of horizontal streakings. Chloroform/methanol precipitation (Figure 3.1.2 D) appeared to fail in removing interfering compounds from *Blastocystis* proteins, since proteins did not enter IPG strip as effectively as the other three precipitation methods and the resulted 2D gel was virtually blank. Thus, the method of choice for precipitation of *Blastocystis* proteins is using TCA/acetone because of its good quality, reproducibility and quantity of detectable spots on the gel.

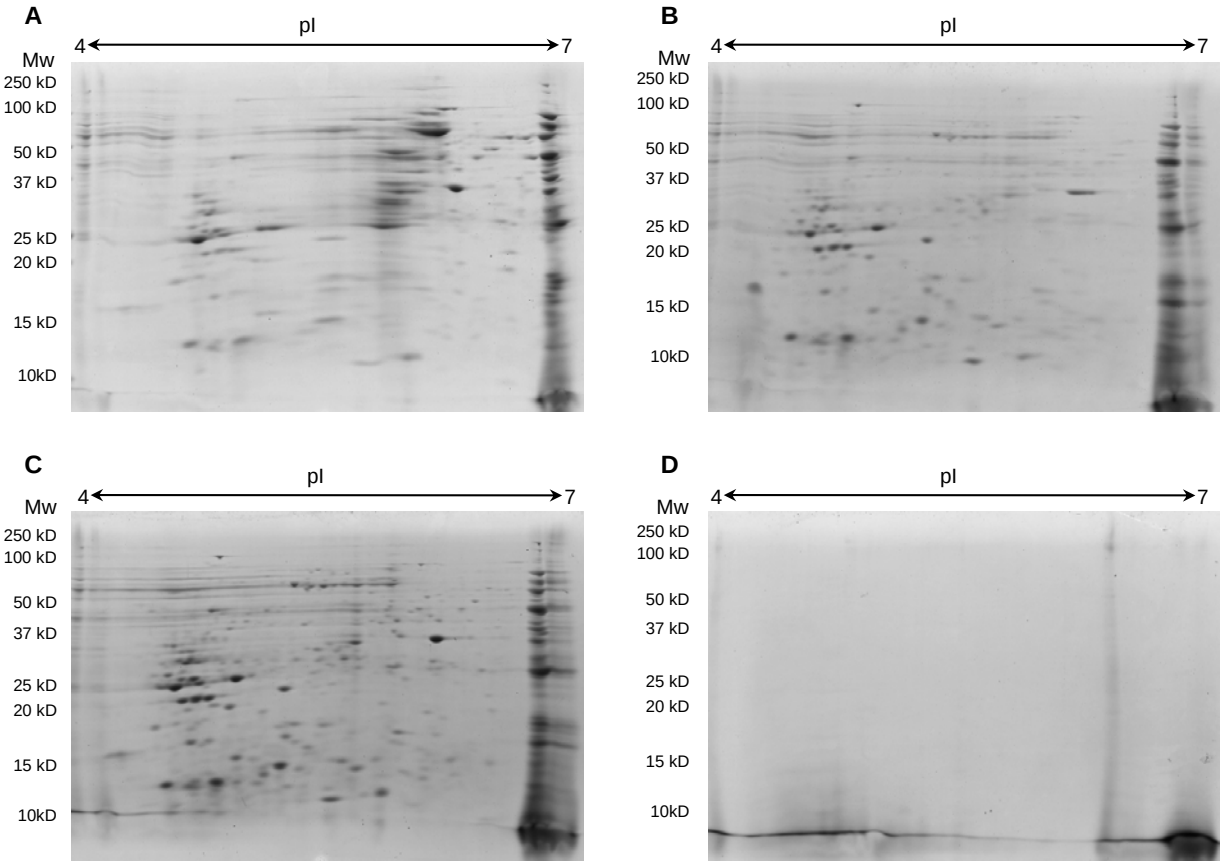

Figure 3.1.2 Two-dimensional electrophoresis analyses of *Blastocystis* cell lysates following precipitation with TCA **(A)**, DOC-TCA **(B)**, TCA/acetone **(C)**, and chloroform/methanol **(D)**. In each case, 200 µg of solubilized protein was loaded to a pI 4-7 gradient IPG strip (7 cm) and separated by IEF in the first dimension followed by 8-16% gradient SDS-PAGE gel in the second dimension. The gels were stained with Coomassie blue.

3.1.2 Construction of 2-D proteome map of Blastocystis subtype 7

Having established a standardized and reproducible method for the preparation of *Blastocystis* proteins for 2-D electrophoresis, a 2-D proteome map was created for *Blastocystis* subtype 7 (Figure 3.1.3). Proteins of *Blastocystis* subtype 7 vacuolar forms were precipitated using TCA/acetone, resolubilized and separated on 4-7 linear and 3-10 linear immobilized pH gradient strips of 17 cm length. The second dimension was separated on a 12% acrylamide gel. Coomassie blue-stained gels showed protein spots with a wide range of molecular weights, isoelectric points and

relative intensities. It was observed that majority of separated proteins had isoelectric points between pH 4 and 8.

The number of protein spots was counted using the PDQuest software. A total of 1134 spots were found on the pH 4-7 gel and 968 spots were detected on the pH 3-10 gel.

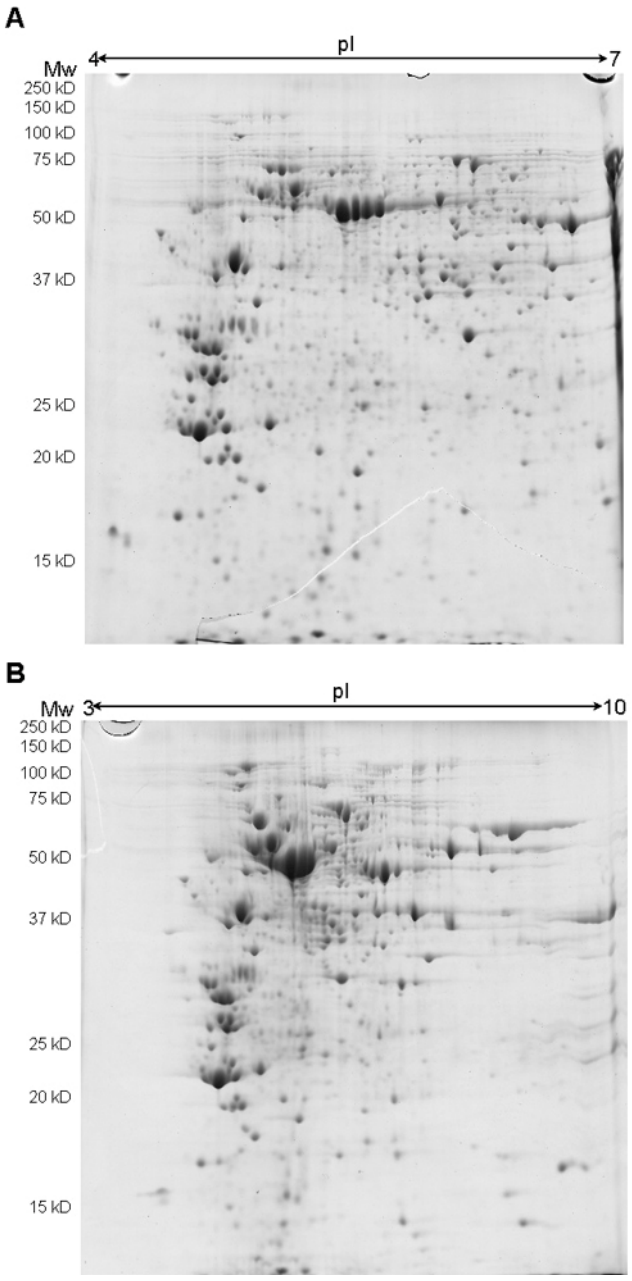

Figure 3.1.3 2D gels of TCA/acetone precipitated *Blastocystis* cell extracts, separated by IEF in 17 cm IPG strips in the pH range 4-7 (A) and 3-10 (B), followed by separation in the second dimension using 12% SDS-PAGE gels. Protein detection was by Coomassie blue staining.

3.1.3 Identification of some landmark protein spots

Sixteen protein spots (Figure 3.1.4) were excised and digested with trypsin. Their mass spectra were acquired with MALDI-TOF-TOF MS and the peak list was submitted for database searching using Mascot program against an in-house database of *in silico* translated draft genome database of *Blastocystis*. The sequence contigs of significant matches were retrieved and putative genes were predicted using GENESCAN program. The putative coded proteins were searched against NCBI Conserved Domain Database and the *Blastocystis* EST database to provide the possible functions of these proteins (Table 3.1.1). It was found that several clearly resolved spots appeared to be encoded by the same genes, such as spot 1 and 2, spot 5 and 6, and spot 7 and 8, which may be due to different posttranslational modifications. The identified proteins have various cellular functions. There are metabolic enzymes involved in different metabolic pathways, such as lipid metabolism (long-chain acyl-CoA synthetases, acyl-CoA synthetase, acetyl/propionyl-CoA carboxylase), amino acid metabolism (urocanate hydratase, and aminoacyl-histidine dipeptidase), and nucleotide metabolism (IMP dehydrogenase). Three protein spots (spot 13, 14 and 15) were found to belong to the C1 cysteine protease family. Other identified proteins have roles in protein synthesis (EF-2), vesicular trafficking (Rab), regulation of intracellular calcium homeostasis (calreticulin) and interaction with cytoskeletal proteins (calponin homology domain protein).

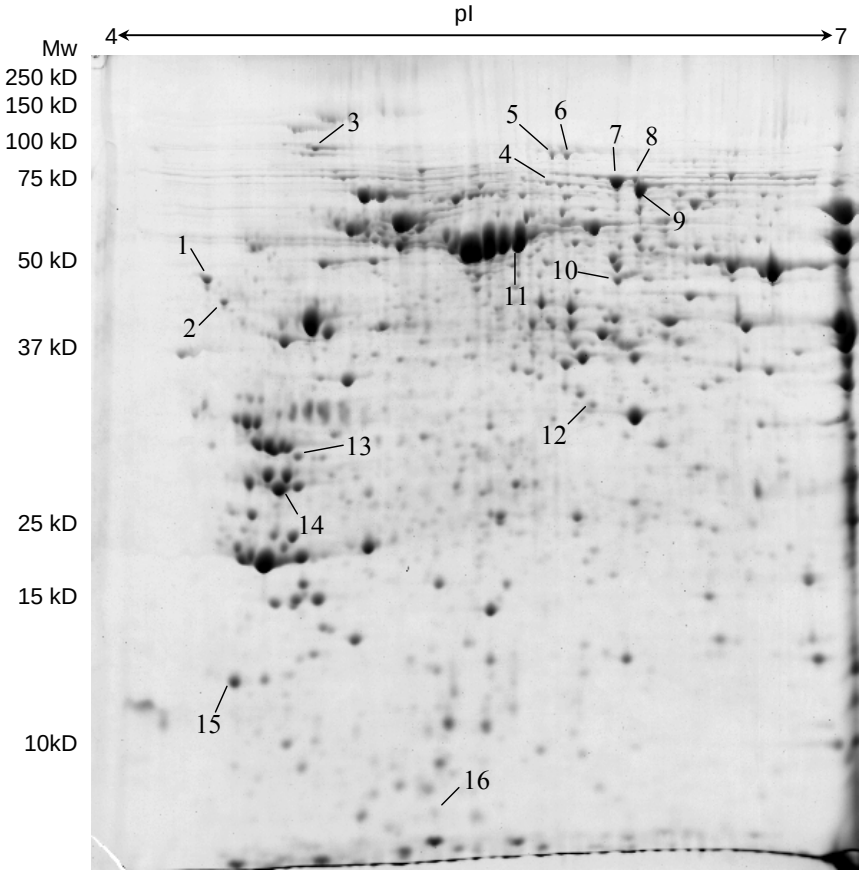

Figure 3.1.4 2-D electrophoresis map of *Blastocystis* proteins identified by mass spectrometry and database searching. Numbers indicate identified proteins (see Table 3.1.1).

Table 3.1.1 Identification of selected proteins of *Blastocystis* subtype 7

Spot number	Measured Mw (kD)	Measured pI	Matched contig	MASCOT Score*	Predicted conserved domain(s)	Matched EST cluster	Annotation of EST
1	47	4.35	Contig 0187	132	Calreticulin	BHL00002741	Calreticulin domain containing protein
2	44	4.4	Contig 0187	163	Calreticulin	BHL00002741	Calreticulin domain containing protein
3	100	4.8	Contig 1593	329	Calponin homology domain	BHL00003062	Calponin homology domain protein
4	70	5.9	Contig 1161	161	FAA1, Long-chain acyl-CoA synthetases (AMP-forming) [Lipid metabolism]	BHL00000659	Grlacs gonadotropin-regulated long chain acyl-CoA synthetase
5	90	5.9	Contig 2221	114	Acyl-CoA synthetase	BHL00001756	Acetyl-CoA synthetase
6	90	6	Contig 2221	165	Acyl-CoA synthetase	BHL00001756	Acetyl-CoA synthetase
7	75	6.2	Contig 1903	490	Acetyl/propionyl-CoA carboxylase, alpha subunit	BHL00001817	Propionyl-CoA carboxylase alpha chain, mitochondrial precursor related cluster
8	75	6.3	Contig 1903	485	Acetyl/propionyl-CoA carboxylase, alpha subunit	BHL00001817	Propionyl-CoA carboxylase alpha chain, mitochondrial precursor related cluster

(Table continues on following page.)

Table 3.1.1 (Continued from previous page.)

Spot number	Measured Mw (kD)	Measured pI	Matched contig	MASCOT Score*	Predicted conserved domain(s)	Matched EST cluster	Annotation of EST
9	70	6.3	Contig 1865	368	Urocanate hydratase [Amino acid transport and metabolism]	BHL00001712	Probable urocanate hydratase related cluster
10	45	6.2	Contig 1990	77	Inosine-5-monophosphate dehydrogenase (IMP dehydrogenase)	BHL00001840	Inosine-5-monophosphate dehydrogenase 1 related cluster
11	60	5.7	Contig 2160	136	aminoacyl-histidine dipeptidase	BHL00001818	Aminoacyl-histidine dipeptidase related cluster
12	30	6	Contig 2380	107	EF-2	BHL00000235	T6H22.13 elongation factor 2, putative / EF-2, putative [EC:3.6.5.3] [KO:K03234]
13	29	4.7	Contig 1743	347	Peptidase_C1A_Cathepsin X	BHL00001238	Cathepsin Y related cluster/Cathepsin Z precursor related cluster
14	28	4.6	Contig 2138	80	Cathepsin B group	BHL00000346	Cathepsin B precursor related cluster
15	17	4.35	Contig 1531	98	Peptidase C1 family and, Cathepsin propeptide inhibitor domain (I29)	BHL00000315	Cysteine protease related cluster
16	12	5.2	Contig 2304	54	Rab subfamily of small GTPases	BHL00001604	Rab family GTPase Rab8 related cluster

* Protein scores greater than 54 are significant ($p<0.05$)

3.1.4 Identification of legumain as MAb 1D5 targeted protein

To identify the MAb 1D5 targeted protein(s), *Blastocystis* proteins were separated by 2-D electrophoresis and transferred to a PVDF membrane which was subsequently probed with MAb 1D5 for immunoblot analysis. In the broad range pI 3-10 gel blot (Figure 3.1.5 A, left) one prominent and big spot could be visualized after film developing, and there were some fainter spots in the pI range of 4 to 7. The narrow range pI 4-7 gel blot (Figure 3.1.5 A, right) separated these spots better, and it was observed that besides the prominent big spot (arrow pointed), MAb 1D5 also recognized a tiny spot (dashed arrow pointed). All the other fainter spots were likely to be nonspecific binding of MAb 1D5 or the secondary antibody because their intensity was much lower. The Western blot was matched against CBB stained 2-D gel, and the big spot was found to be matched to three close spots of the same molecular weight but different pI. The molecular weight of the three spots was 30.5 kD, consistent with 1-D Western blot result from previous studies (Tan *et al.*, 1996a; Tan *et al.*, 1997). pI value of the three spots were 4.55, 4.6 and 4.75. It was likely that because the chemiluminescence signal was very strong so the three spots appeared as one in the Western blot. However, the attempt to match the tiny spot to CBB stained 2-D gel was failed because the protein spot distribution in nearby region was complex and the original spot may be of low quantity to be detected by CBB staining. Using a micro-range of IPG strip (pI 4.7-5.9) might help to better resolve proteins in this region and to locate this spot.

The three MAb 1D5 reactive protein spots were excised from CBB stained 2-D gel, digested by trypsin and analyzed by MALDI-TOF mass spectrometry (Figure 3.1.6). Base peaks of the three spots were all 1540, suggesting that the three spots had the

same most intense ion. The rest of mass peaks of mass-to-charge ratio (m/z) were also highly identical among the three samples. Therefore, the three spots should represent the same protein with slightly different charges.

Individual peaks from the mass spectrum were further analyzed by tandem mass spectrometry (MS/MS) and seven tryptic peptides were sequenced in total (Table 3.1.2).

Table 3.1.2 MS/MS sequenced peptide of MAb 1D5 reactive protein

Molecular weight (Dalton)	Peptide sequence
937	DDFQATLK.K
1149	TETLNEQWK.R
1540	HQADVAHAYQIMR.R
1250	YQHTTGSEKAK.W
1597	WEKLYLEEMSLR.Q
2026	FNYDHQSSVAWDSRDAK.F
2028	GVVVDYEGEDVTPENFMK.V

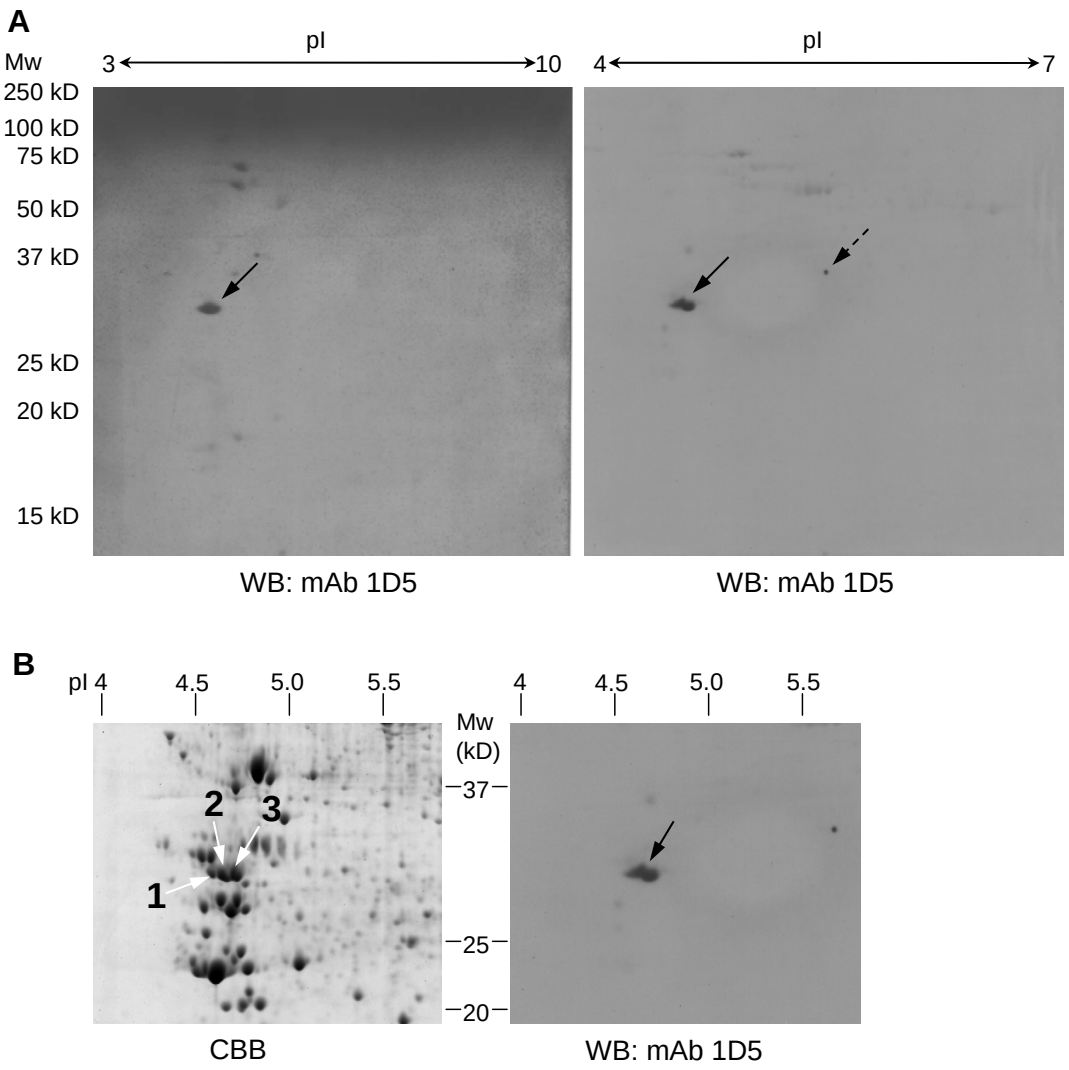

Figure 3.1.5 Identification of MAb 1D5 targeted protein by Western blotting of 2D electrophoresis gel. **A**, Western blot analysis of total proteins separated on pH3-10 range (left) and pH4-7 range (right) IPG strips probed with MAb 1D5. One prominent and big spot could be visualized (arrow) and there was also a tiny spot (dashed arrow). **B**, a Coomassie blue (CBB) stained 2D electrophoresis gel area matched with immunoblot probed by MAb 1D5. The prominent big spot on the blot (black arrow) was matched to three close spots (white arrows) on the CBB stained gel, which were excised for mass spectrometric identification.

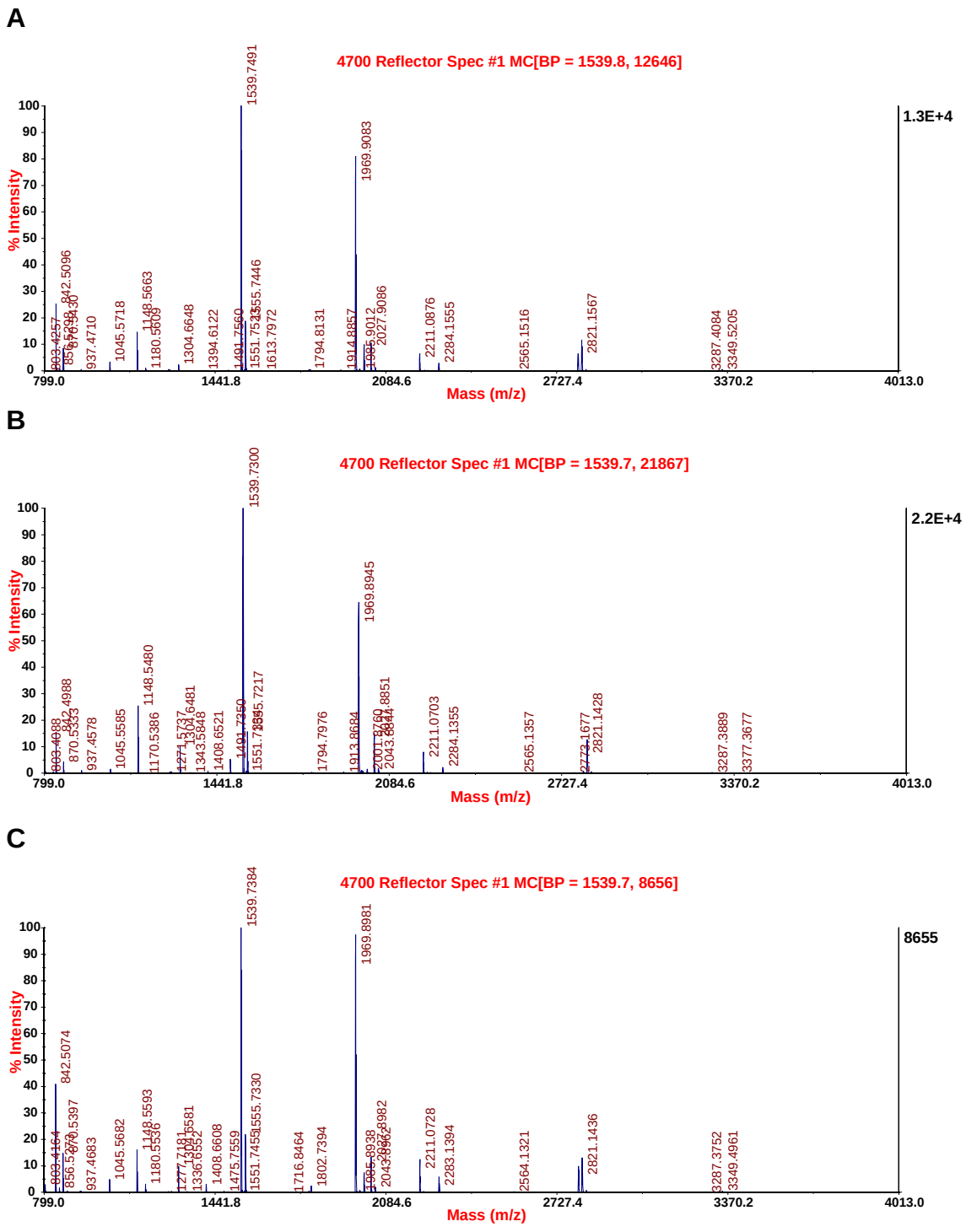

Figure 3.1.6 Mass spectrum of MAb 1D5 reactive protein spots from Figure 3.1.5 B (**A**, spot 1; **B**, spot 2; **C**, spot 3). The spots were excised from Coomassie blue stained 2-D gel, digested by trypsin and analysed by MALDI-TOF mass spectrometry.

Mascot searches of the acquired peptide mass fingerprinting results against the in-house *Blastocystis* database showed an excellent match with Contig 1466. Three genes were predicted in this genome sequence contig by the program GENSCAN (http://genes.mit.edu/GENSCAN.html) (Figure 3.1.7; Appendix I). One predicted gene (gene 2 in Figure 3.1.7 A) was found to cover all the seven sequenced peptides of MAb 1D5 target protein (Figure 3.1.7 B). Therefore, MAb 1D5 targeted protein should be encoded by this putative gene. Conserved domain analysis of the putative gene showed a complete peptidase C13 domain and incomplete NIF (NLI interacting factor-like phosphatase) superfamily domain. BLAST searches using the predicted gene as query sequence returned a list of legumain sequences from species such as corn, zebra fish, bovine and rat, suggesting that the protein analyzed might be a legumain.

A

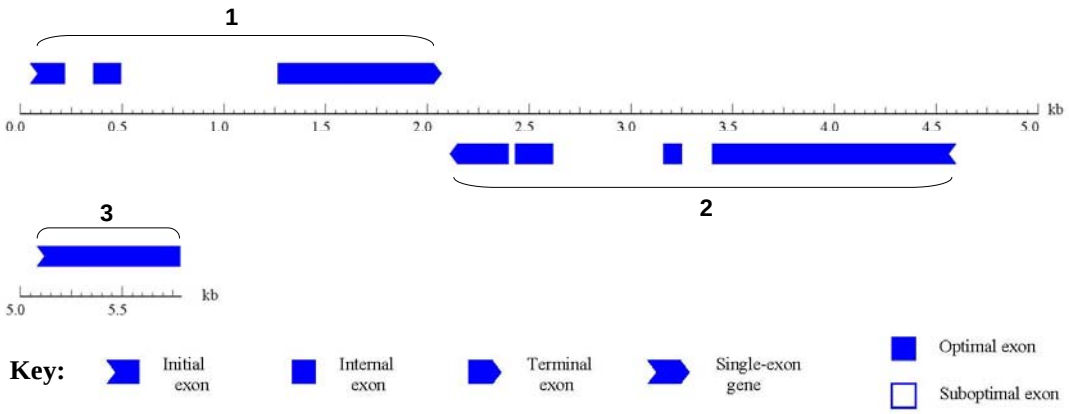

B

```
>Contig1466|GENSCAN_predicted_peptide_2|563_aa
MKFVSIALLRVLALAAADNWAVLVAGSDGFWNYRHQADVAHAYQIMRRGGIPADHIVTMM
YNDVASSSFNPFPGELYNHPGDESPDVYKGVVVDYEGEDVTPENFMKVLLGDESTGKKVL
KTNENDNIFMFFSDHGGPNVLCFPNGDLSKDDFQATLKKMHEQKKYKHFVLYIEACYSGS
MGVGFPEDLGISIVTAANDSESSWGWYCGEEAVVKGKDIGSCLGDEFSVFWMEDTDKGEQ
RTETLNEQWKRIHDGVTKSHASRYGDVSFESDLIGEYVGYPEEKFNYDHQSSVAWDSRDA
KFLFLLYKYQHTTGSEKAKWEKLYLEEMSLRQQIDRYINSFAKESKLYSARVSGEINMEC
YMAGIEQMVAIFGHNDYQYKYYNVLANMASLRRSISKNTLEDDVLRTSTLRQSDIEKEFL
EYCSRFCEIVVFTASKQEYADRMLDFLDPEKKFIKHRLFRESCTKIGKVYVKDLNRLGRD
LRRTVIIDNSIVSFGYHLDNGIPICSWFDNWKDQEVGFLVGIECSYTTRLASCTLYKQCK
TFVPILLICLDSVKPSIASFVNE
```

C

Figure 3.1.7 Bioinformatic analyses of Contig1466 from *Blastocystis* draft genome. **A**, three genes were predicted from the nucleotide sequence of Contig 1466 by the program GENSCAN. Genes 1 and 2 were complete and gene 3 was incomplete. **B**, *in silico* translated peptide sequence of the predicted gene 2. Sequenced peptides of MAb 1D5 target protein were marked in red. **C**, conserved domain analysis of gene 2 showing a complete peptidase C13 domain and incomplete NIF (NLI interacting factor-like phosphatase) superfamily domain.

3.2 MAb 1D5 targets a novel cysteine protease legumain at cell surface to trigger *Blastocystis* cell death

3.2.1 Characterization of the cysteine protease legumain in Blastocystis

A cDNA library was constructed for *Blastocystis* subtype 7 using CloneMiner™ cDNA Library Construction Kit (Invitrogen). Primers were designed to amplify part of the predicted legumain gene, starting from the N-terminus of the predicted gene product till the last MS/MS sequenced peptide. The complete peptidase C13 superfamily domain was included in this sequence. The PCR product had 990 bps (Figure 3.2.1) and encoded a protein of 330 amino acid residues (GenBank accession number: ACO24555) (Figure 3.2.2). All the seven MS/MS sequenced peptides could be matched on the peptide sequence of the PCR product (Figure 3.2.2). Theoretical molecular weight of this peptide sequence was 37.5 kD and pI value was 4.9 as calculated by the software Vector NTI. As with other legumains, the *Blastocystis* ortholog presumably codes for a precursor which is auto-cleaved at the C-terminal asparagine residue (Chen *et al.*, 2000), possibly at N285 to result in the mature form (30 kD protein). *Blastocystis* legumain contains a catalytic dyad with the motif His-Gly-spacer-Ala-Cys, which is also found in other legumains (Figure 3.2.3) and in caspases (Chen *et al.*, 1998). Multiple sequence alignment using ClustalW showed that *Blastocystis* legumain had a highly conserved catalytic domain of 40% to 60% sequence similarity to legumains from other species, but possessed unique N and C-terminus regions (Appendix II). Signal peptide prediction (http://rpsp.bioinfo.pl) showed that the first 15 amino acids (KFVSIALLRVLALAAA) comprised a putative secretary signal peptide.

```
  1  KFVSIALLRV LALAAADNWA VLVAGSDGFW NYRHQADVAH AYQIMRRGGI
                                                1
 51  PADHIVTMMY NDVASSSFNP FPGELYNHPG DESPDVYKGV VVDYEGEDVT
                                                    2
101  PENFMKVLLG DESTGKKVLK TNENDNIFMF FSDHGGPNVL CFPNGDLSKD

151  DFQATLKKMH EQKKYKHFVL YIEACYSGSM GVGFPEDLGI SIVTAANDSE
       3
201  SSWGWYCGEE AVVKGKDIGS CLGDEFSVFW MEDTDKGEQR TETLNEQWKR
                                              4
251  IHDGVTKSHA SRYGDVSFES DLIGEYVGYP EEKFNYDHQS SVAWDSRDAK
                                                  5
301  FLFLLYKYQH TTGSEKAKWE KLYLEEMSLR
                    6          7
```

Figure 3.2.1 Peptide sequence of PCR-amplified *Blastocystis* legumain (Genbank ACO24555). The seven sequenced peptides of MAb 1D5 target protein were marked in red and underlined.

```
                                  *                                   *
mouse        133 KVLKSGPRDHVFIY FTDHGATGILVFPND---DLHVKDLNKTIRYMYEHKMYQKMVFYIEACESGSMMN-HLPD 202
rat          133 KVLKSGPRDHVFVY FTDHGATGILVFPNE---DLHVKDLNKTIRYMYEHKMYQKMVFYIEACESGSMMN-HLPD 202
human        131 KVLKSGPQDHVFIY FTDHGSTGILVFPNE---DLHVKDLNETIHYMYKHKMYRKMVFYIEACESGSMMN-HLPD 200
bovine       131 KVLKSGPRDHVFVY FTDHGATGILVFPNE---DLHVKDLNETIRYMYEHKMYQKMVFYIEACESGSMMN-HLPP 200
frog         131 KVIHSGPNDHVFVY FTDHGAPGLLAFPND---DLHVMELNKTIQLMYEKKTYKKLVFYIEACESGSMMN-HLPN 200
zebra fish   133 KVLKSGPNDHVFVY FTDHGAPGLLAFPND---DLHVDDLMDTIKYMHSNNKYKKMVFYVEACESGSMMK-PLPV 202
Schistosoma  134 KVLKSGKNDDVFIY FTDHGAPGLIAFPDD---ELYAKQFMSTLKYLHSHKRYSKLVIYIEACESGSMFQRILPS 204
rice         163 KVIDSKPNDHIFIF YSDHGGPGVLGMPNLP--YLYAADFMKVLQEKHASNTYAKMVIYVEACESGSIFEGLMPE 234
tobacco      108 KVVNSGPNDHIFIY YTDHGGPGVVSMPSGE--DVYANDLIDVLKKKHASGTYDRLVFYLEACESGSMFDGLLPE 179
Blastocystis 118 KVLKTNENDNIFMF FSDHGGPNVLCFPNG---DLSKDDFQATLKKMHEQKKYKHFVLYIEACYSGSMGVG-FPE 187
Haemonchus   130 RVIHSTVNDRIFVY FSDHGGVGTISFPYE---RLTAKQLNSVLLDMHRKDKFGHLVFYLETCESGSMFHNILKK 200
Trichomonas  110 RALQSTAEDDVFVY YDDHGAPGLLCVPHNNGPEIYADNIASVISQMKKEKKFRNLFFVIEACYSGSVALN--IT 181
```

Figure 3.2.2 Multiple sequence alignment of the catalytic domain of the legumain family. The sequence segments containing known or putative catalytic residues in the legumain family were aligned by Vector NTI. Blocks of four predominantly hydrophobic residues (highlighted with a black background) are located 2 or 3 residues preceding each of the catalytic residues (asterisk). Other residues in the catalytic domains are highly conserved in legumain family. Sequences compared and their accession numbers were mouse (NP_035305), rat (NP_071562), human (AAH03061), bovine (NP_776526), frog (NP_001005720), zebra fish (NP_999924), *Schistosoma* (CAB71158), rice (BAC41386), tobacco (CAE84598), *Blastocystis* (ACO24555), *Haemonchus* (CAJ45481) and *Trichomonas* (AAQ93040).

Blastocystis legumain was overexpressed in *E. coli* with a glutathione S-transferase (GST) tag (Figure 3.2.3). The recombinant protein was purified and found to have the expected size of 65 kD. Western blot analysis using anti-human legumain IgG or MAb 1D5 confirmed that the purified recombinant protein was a *bona fide* target of

MAb 1D5. The variations in band intensities may be due to MAb 1D5 and anti-human legumain possessing different affinities for precursor and mature forms of legumain.

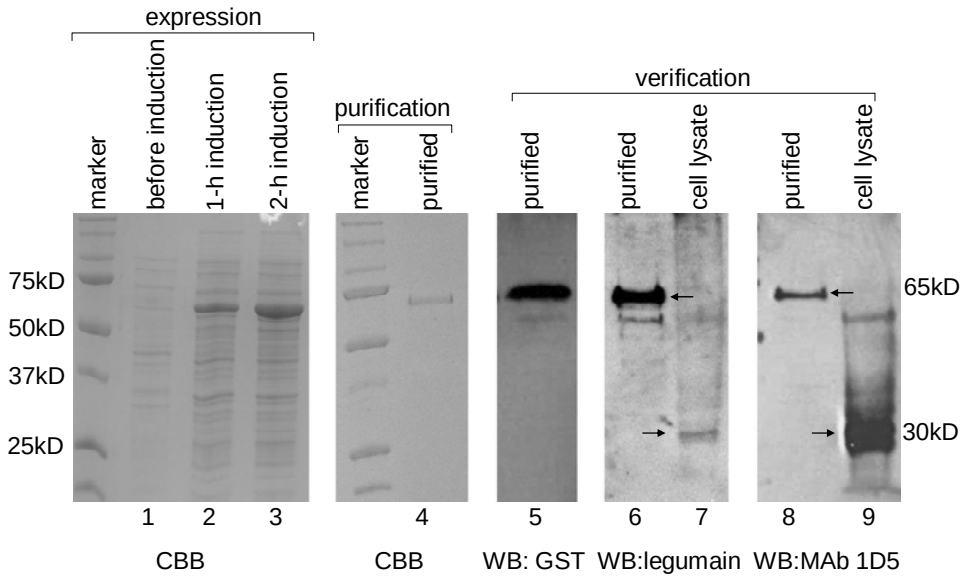

Figure 3.2.3 Expression, purification and verification of *Blastocystis* legumain. The *Blastocystis* legumain gene was inserted into pGEX-6p-1 and expressed in *E. coli* BL21(DE3) with induction of 0.5 mM IPTG at 16 °C (lanes 1-3). The expressed recombinant legumain was then purified by glutathione affinity column and purity assessed by SDS-PAGE (lane 4). Purified legumain was subjected to Western blotting and probed with anti-GST to confirm the purification (lane 5). Western blots of purified legumain and *Blastocystis* cell lysate were performed and probed with anti-human legumain and MAb 1D5, showing distinct bands at 65 kD (legumain with GST tag) and 30 kD (legumain). (Picture courtesy of Dr. Wu Binhui, Department of Microbiology, National University of Singapore, used with permission)

The purified recombinant legumain was incubated at 30 °C with the legumain specific substrate Z-Ala-Ala-Asn-NHMec to test its activity. Buffers with pH range from 3 to 8.8 were used (Figure 3.2.4). It was found that enzymatic activity of legumain peaked at two pH values, i.e. pH 4 and pH 7.4, the latter being the most optimal pH. Activity of *Blastocystis* legumain had a steep increase between pH 3 to 4 and a steep decrease from pH 4 to 5. From pH 5 to pH 7.4, the activity of legumain increased gradually. At pH higher than 7.4, the activity decreased sharply, which may result from lower stability of the active legumain. The reason for the unusual biphasic activity profile is

not known but may be related to the localization of *Blastocystis* legumain in intracellular compartments and on the parasite surface (see section 3.2.2).

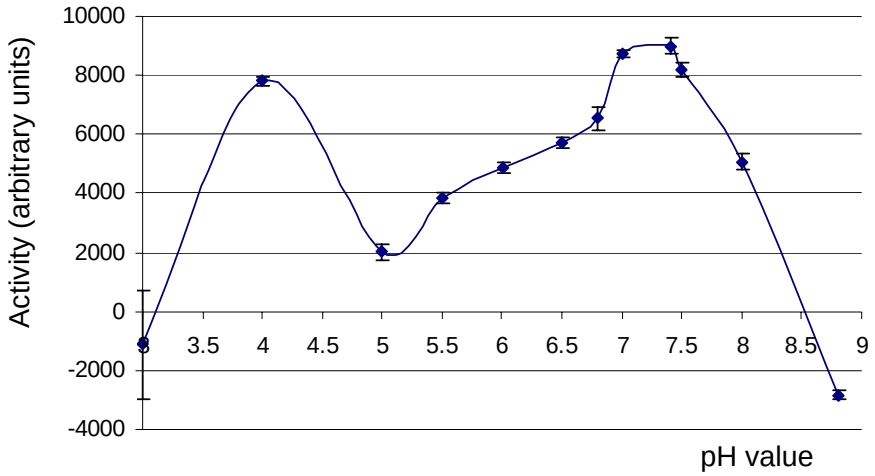

Figure 3.2.4 pH dependence of *Blastocystis* legumain. Purified recombinant legumain (r-legumain) and fluorogenic substrate (Z-Ala-Ala-Asn-NHMec) were incubated at 30 °C with pH buffers in the range from 3 to 8.8. Legumain activity (fluorescence arbitrary units) was plotted against pH values. Data shown were means ± stand deviations (error bar) from three independent experiments. (Picture courtesy of Dr. Wu Binhui, Department of Microbiology, National University of Singapore, used with permission)

3.2.2 MAb 1D5 targets legumain on the cell surface of Blastocystis

In order to investigate the subcellular localization of legumain in *Blastocystis* cells, immunofluorescence studies of non-permeabilized cells were carried out using MAb 1D5 or anti-human legumain as primary antibody and a secondary antibody conjugated to AlexaFluor 594 (red). DAPI (blue, staining nuclei) and FDA (green, staining cytoplasm and central vacuole) were also included as co-stains. It was observed that MAb 1D5 had the same staining pattern as anti-human legumain (Figure 3.2.5 and Figure 3.2.6). In healthy cells which were round and had strong stain of FDA (Breeuwer *et al.*, 1995), only the cell surface was stained, showing a red color ring around the cell (arrow pointed). In contrast, red stains could be observed in

the cytoplasm, central vacuole and on the cell surface (triangle indicated) of those cells with irregular cell shape and faint FDA staining, which might have become unhealthy during the staining procedure and the antibody could penetrate into cytoplasm due to the loss of cell membrane integrity. In fact, the same staining pattern was observed in permeabilized cells as with unhealthy cells. These results suggest that *Blastocystis* legumain localizes on the cell surface as well as in cytoplasm and central vacuole, and MAb 1D5 targets the cell surface legumain of healthy *Blastocystis* cells.

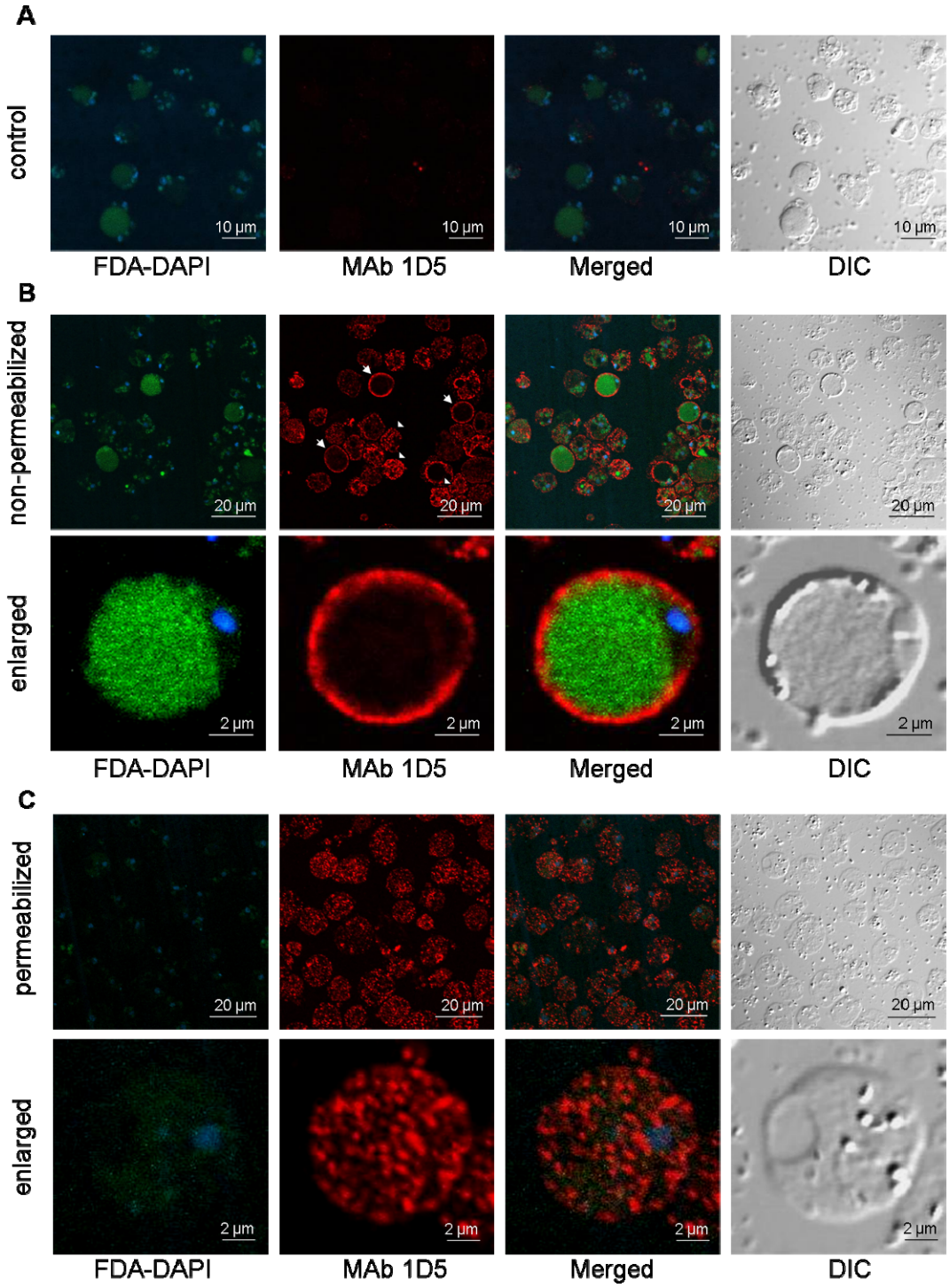

Figure 3.2.5 Cell surface localization of MAb 1D5. *Blastocystis* cells were incubated with MAb 1D5 followed by incubation with AlexaFluor 594-conjugated secondary antibody (red). Nuclei were stained with DAPI (blue). Cytoplasm and central vacuole were stained with FDA (green). **A**, control experiment was performed with a non-specific primary antibody. **B**, cells were not permeabilized prior to the addition of antibodies; arrow pointed were representative healthy cells showing cell surface staining while triangle indicated representative unhealthy cells showing staining of cell surface, cytoplasm as well as central vacuole. **C**, cells were permeabilized before antibody incubation.

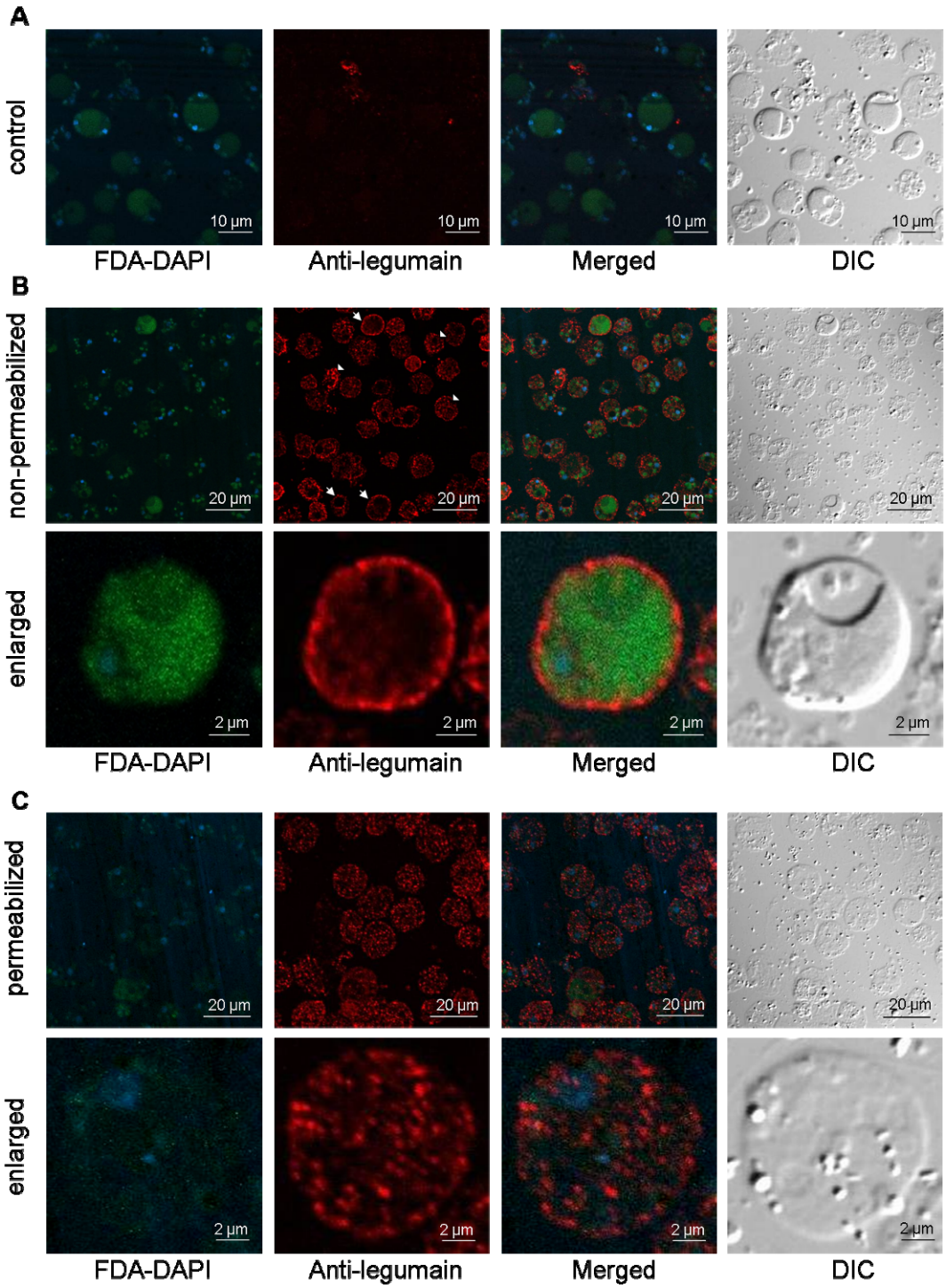

Figure 3.2.6 Cell surface localization of anti-legumain. *Blastocystis* cells were incubated with antibody against human legumain followed by incubation with AlexaFluor 594-conjugated secondary antibody (red). Nuclei were stained with DAPI (blue). Cytoplasm and central vacuole were stained with FDA (green). **A**, control experiment was performed without primary antibody. **B**, cells were not permeabilized prior to the addition of antibodies; arrow pointed were representative healthy cells showing cell surface staining while triangle indicated representative unhealthy cells showing staining of cell surface, cytoplasm as well as central vacuole. **C**, cells were permeabilized before antibody incubation.

3.2.3 Inhibition of legumain activity by MAb 1D5 and other protease inhibitors triggered apoptosis in Blastocystis

The protease activity of recombinant legumain was assessed using its fluorogenic substrate Z-Ala-Ala-Asn-NHMec in the presence of MAb 1D5, a non-specific IgM antibody, or different protease inhibitors (Figure 3.2.7). It was found that the legumain specific inhibitor Cbz-Ala-Ala-AAsn-RR-COOOEt (APE-RR) inhibited more than 90% of the legumain protease activity compared to MOCK control. Two other reported legumain inhibitors cystatin and Ac-YVAD-cmk (also known as the caspase-1 inhibitor) had about 45% and 15% inhibitory effect on the activity of recombinant legumain respectively. The cathepsin B inhibitor z-FA-fmk could not inhibit legumain activity even when the final concentration was increased to 5 folds. Interestingly, MAb 1D5 could also inhibit about 35% of legumain activity, whereas a non-specific mouse IgM monoclonal antibody had no inhibitory effect.

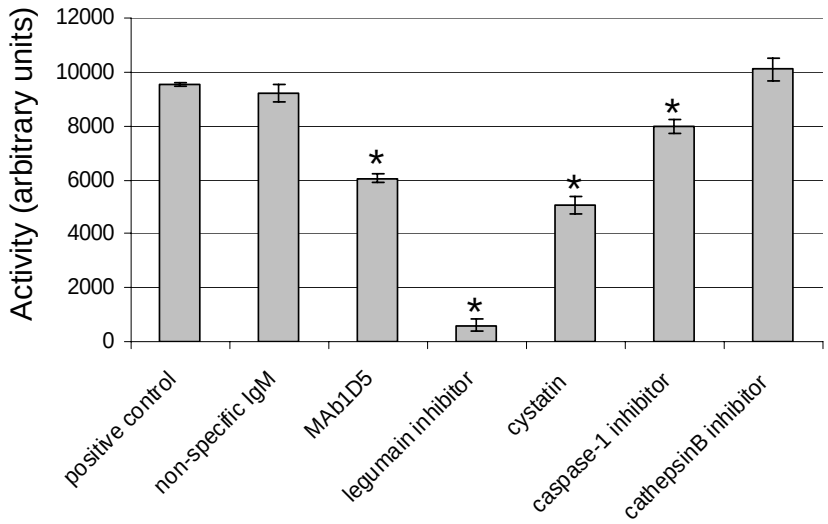

Figure 3.2.7 Regulation of legumain protease activity by antibody and inhibitors. Purified r-legumain and fluorogenic substrate were incubated at 30 °C in presence or absence of antibody or protease inhibitor in PBS. MOCK control was performed with same volume of solvent solution of antibody or inhibitors. Values are means ± standard deviations (error bar) from three independent sets of experiment. *, p <0.01 versus MOCK control. (Picture courtesy of Dr. Wu Binhui, Department of Microbiology, National University of Singapore, used with permission)

Since the cellular target of MAb 1D5 was found to be legumain and MAb 1D5 could inhibit legumain activity, it was hypothesized that inhibition of the surface legumain activity would trigger cell death in *Blastocystis*. To test this hypothesis, *Blastocystis* cells were incubated with MAb 1D5, non-specific IgM or various protease inhibitors for 4 h and assayed with Annexin V-FITC and PI staining to detect flipping of phosphatidylserine (PS) to the outer layer of cell membrane, an early marker of apoptosis. The flow cytometry scatterplots (Figure 3.2.8) showed that as compared to a baseline of less than 10% Annexin V-postive cells in MOCK control and non-specific IgM control, the treatment with MAb 1D5, cystatin and the legumain inhibitor APE-RR increased the percentage of Annexin V-positive cells to 18.29%, 49.53% and 47.04% respectively. To ensure reaction specificity, competitive inhibition assays were included. This involved the pre-incubation of MAb 1D5 or legumain inhibitor APE-RR with purified recombinant legumain protein (r-legumain) at a molecular ratio of 1:2 for 30 min before adding to cells. It was found that the extensive Annexin V-positive population seen in MAb 1D5 or legumain inhibitor treated cells was abrogated when MAb 1D5 or legumain inhibitor was pre-incubated with purified recombinant legumain protein (r-legumain). Caspase-1 inhibitor or cathepsin B inhibitor treatment did not alter the percentage of Annexin V positive cells. These results suggest that when legumain activity is inhibited, *Blastocystis* cells exhibited apoptotic features.

To confirm the correlation between legumain protease activity and *Blastocystis* cell death, TUNEL assay was performed to assess DNA fragmentation, a marker of late apoptosis. *Blastocystis* cells were subjected to treatments with MAb 1D5 and various

protease inhibitors for 24 h and flow cytometric analysis was employed to quantify cells displaying DNA fragmentation (Figure 3.2.9). It was observed that MAb 1D5-treated cells exhibited high TUNEL-positivity of 47.17%. Cystatin-treated cells showed 90.11% DNA fragementation, and cells exposed to the legumain inhibitor APE-RR had 80.25% DNA fragmentation. Percentages of TUNEL-positive cells for caspase-1 inhibitor treatment (2.5%) or cathespin B inhibitor (0.97%) treatment were close to that of MOCK control, similar to the observations with Annexin V assay. When MAb 1D5 was pre-incubated with r-legumain, the percentage of TUNEL positive cells decreased to 3.63%. Similarly, when legumain inhibitor APE-RR was pre-neutralized by r-legumain before adding to the cells, the percentage of TUNEL-positive cell population dropped to 9.64%.

The relation of legumain protease activity with cell death as indicated by Annexin V assay and TUNEL assay was summarized in Figure 3.2.10. It can be inferred that when legumain protease activity is blocked by MAb 1D5 or legumain inhibitors, *Blastocystis* cells were induced to undergo apoptotic PCD.

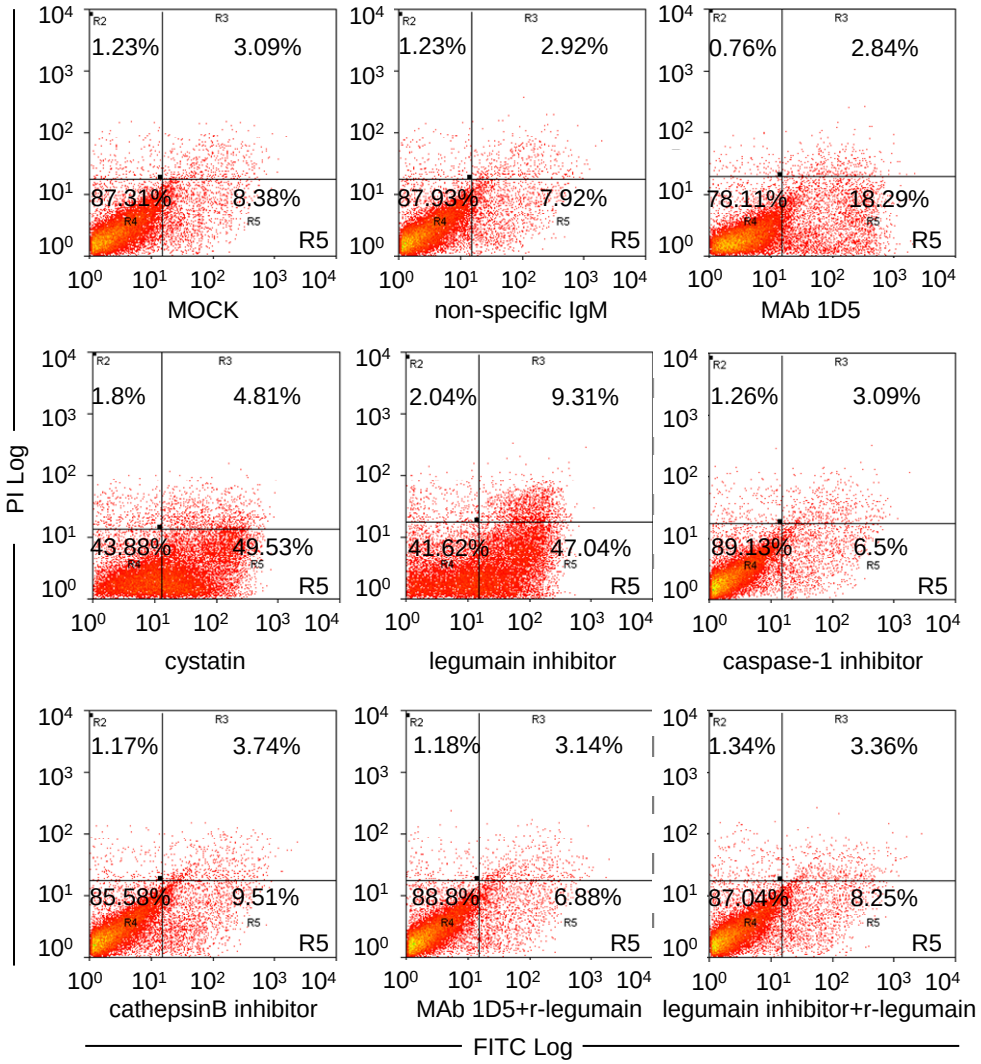

Figure 3.2.8 Annexin V apoptosis assay for inhibitor-pretreated cells. Cells were pretreated under different conditions (cultured with antibody, inhibitors, or neutralized antibody and inhibitor) for 4 h. Cells were stained with Annexin V-FITC to detect phosphatidylserine (PS) on cell surface and PI was used to stain cells with loss of plasma membrane integrity. 20000 cells were analyzed by a flow cytometer. The R5 quadrant represents the percentage of apoptotic cells (Annexin V-FITC positive/ PI negative cells) in the total cell population. MOCK control was performed with the same volume of antibody (PBS) or inhibitor (DMSO) diluent. Non-specific IgM was used as negative antibody control.

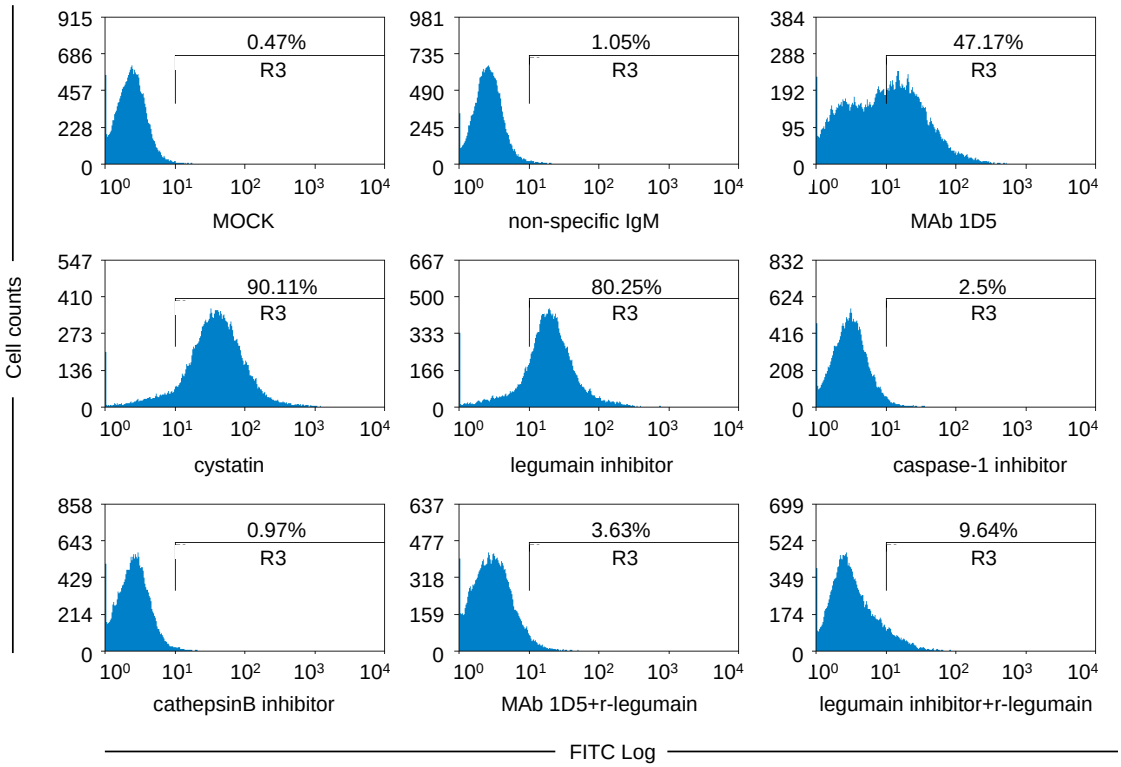

Figure 3.2.9 TUNEL apoptosis assays for inhibitor-pretreated cells. Cells were pretreated under different conditions (cultured with antibody, inhibitors, or neutralized antibody and inhibitor) for 24 h. Fragmented DNA was detected with BrdUTP and labeled with AlexaFluor 488 conjugated anti-BrdU antibody. 20000 cells were analyzed by a flow cytometer. R3 represents the percentage of apoptotic cells in the total cell population. MOCK control was performed with the same volume of antibody (PBS) or inhibitor (DMSO) diluent. Non-specific IgM was used as negative antibody control.

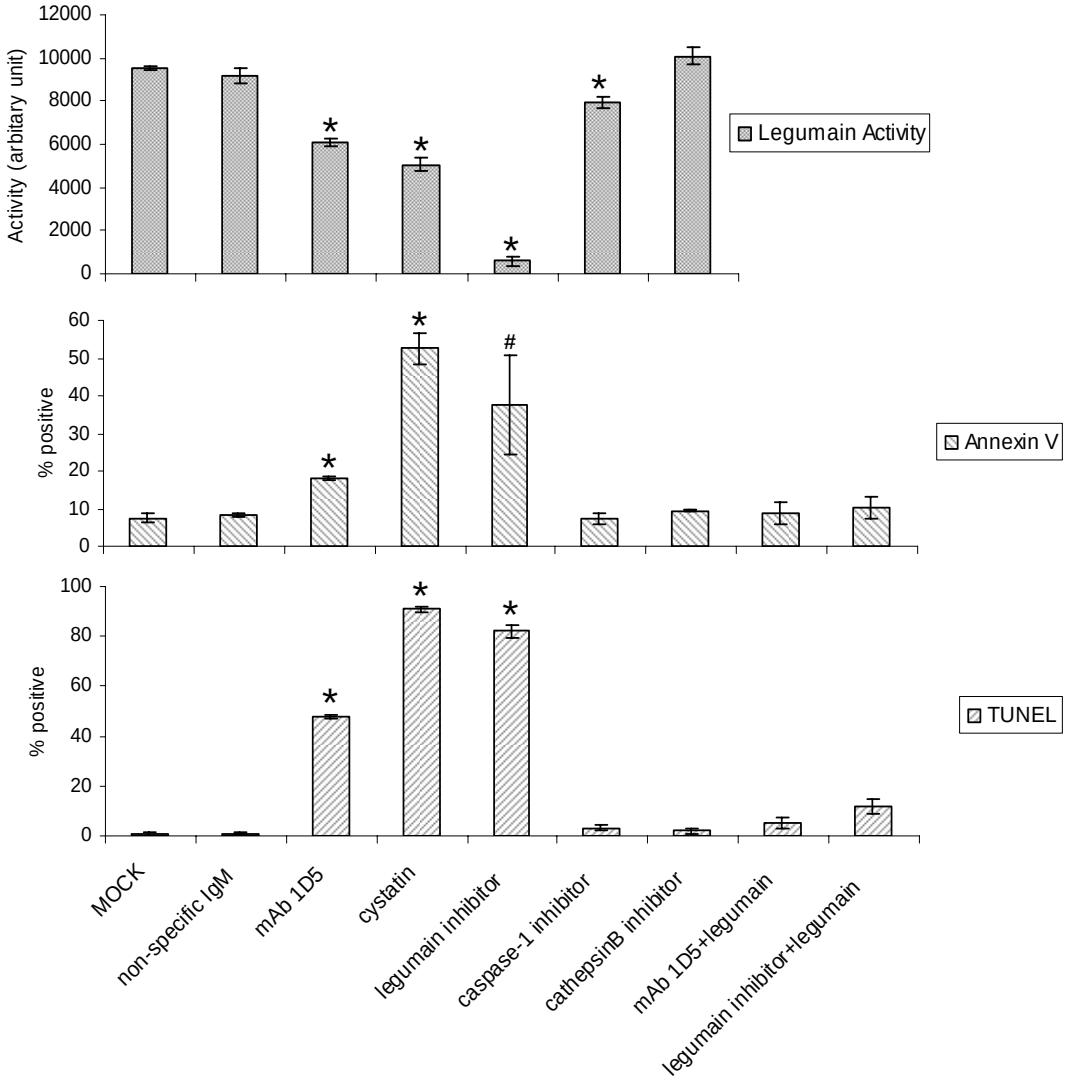

Figure 3.2.10 Relationship between *Blastocystis* legumain protease activity and cell death. Data of purified r-legumain protease activity in presence or absence of antibody or protease inhibitor was retrieved from Figure 3.2.7 and combined with data on cell death percentages by Annexin V and TUNEL apoptosis assays retrieved from Figure 3.2.8 and Figure 3.2.9, respectively. Values were means ± stand deviations (error bar) from two independent sets of experiments. *, p <0.01 versus MOCK control. #, p <0.05 versus MOCK control.

3.3 MAb 1D5 induces alternative cell death pathway through autophagy in *Blastocystis*

3.3.1 Autophagy induced by MAb 1D5 in Blastocystis

Previous studies demonstrated that apoptotic features induced by MAb 1D5 such as DNA fragmentation could be inhibited by the caspase inhibitor zVAD.fmk and mitochondrial outer membrane permeability (MOMP) inhibitor cyclosporine A; however, the cells could not be rescued from death (Nasirudeen and Tan, 2005). It was suggested that MAb 1D5 could elicit a PCD response in *Blastocystis* independent of caspases, mitochondria, or both, probably through an alternative pathway other than apoptosis (Nasirudeen and Tan, 2005; Tan and Nasirudeen, 2005). Since autophagic cell death has often been triggered as an alternative cell death pathway when apoptosis is blocked (Gozuacik and Kimchi, 2004), it is of interest to investigate whether MAb 1D5 can induce autophagic cell death in *Blastocystis*.

In order to evaluate the possibility of autophagic cell death in *Blastocystis* treated with MAb 1D5, alone or in the presence of zVAD.fmk and/or cyclosporine A, cells were labeled with monodansylcadaverine (MDC), an autofluorescent, autophagolysosome marker that specifically labels autophagic vacuoles in *in vivo* and *in vitro* conditions (Biederbick *et al.*, 1995; Munafo and Colombo, 2001; Niemann *et al.*, 2001). While a certain level of background staining was seen in all cells, the true MDC positive staining could still be identified by the prominent and punctuate fluorescence patterns. The cells in each treatment were visually scored for MDC positive staining by fluorescence microscopy (Figure 3.3.1 A and 3.3.2). Cells treated with growth media

or a non-specific IgM monoclonal antibody, alone or in the presence of zVAD.fmk and/or cyclosporine A showed a small percentage of MDC-positive cells (<15%). In contrast, MAb 1D5-treated cells had a higher percentage (18.9%) of MDC-positive population compared with control. In the presence of pan-caspase inhibitor zVAD.fmk, 37.9% of MAb 1D5-treated cells showed MDC-positivity. However, when cells were exposed to MAb 1D5 in the presence of cyclosporine A, the percentage of MDC-positive cells decreased to 11.6%. MAb 1D5-treated *Blastocystis* pre-exposed to zVAD.fmk and cyclosporine A showed 10.8% MDC-positive cells.

To evaluate if the incorporation of MDC was indeed via autophagy, cells were pre-treated with 3-methyladenine (3-MA), a specific inhibitor of autophagy. In the presence of 3-MA, an inhibitory effect on the incorporation of MDC was observed by fluorescence microscopy (Figure 3.3.1 B and 3.3.2). The percentage of MDC-positive cells observed in cells treated with MAb 1D5 alone or in the presence of zVAD.fmk, decreased to 11.4% and 14%, respectively. Hence, it is apparent that MDC incorporation was inhibited by 3-MA. These results indicated that the phenomenon of autophagy was triggered by MAb 1D5 treatment and was intensified in the presence of zVAD.fmk. In addition, the MAb 1D5-elicited autophagy might be associated with the induction of MOMP.

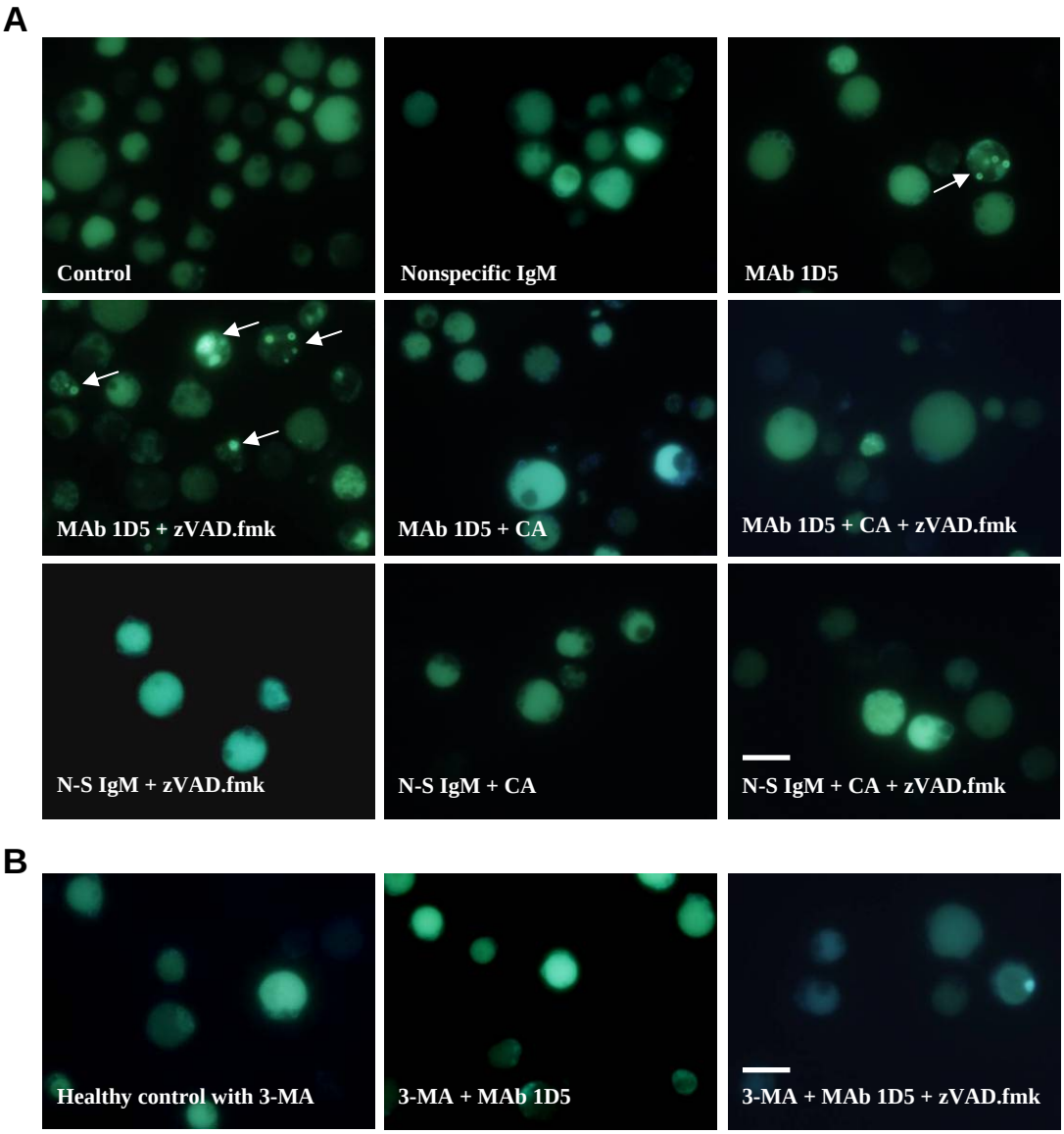

Figure 3.3.1 Exposure to MAb 1D5 increased MDC-positive staining in *Blastocystis*. **A**, fluorescent images of MDC staining of healthy and treated *Blastocytis* cells. **B**, MDC staining of healthy and MAb 1D5-treated *Blastocystis* cells in the presence of 3-MA. Bar = 10 μm.

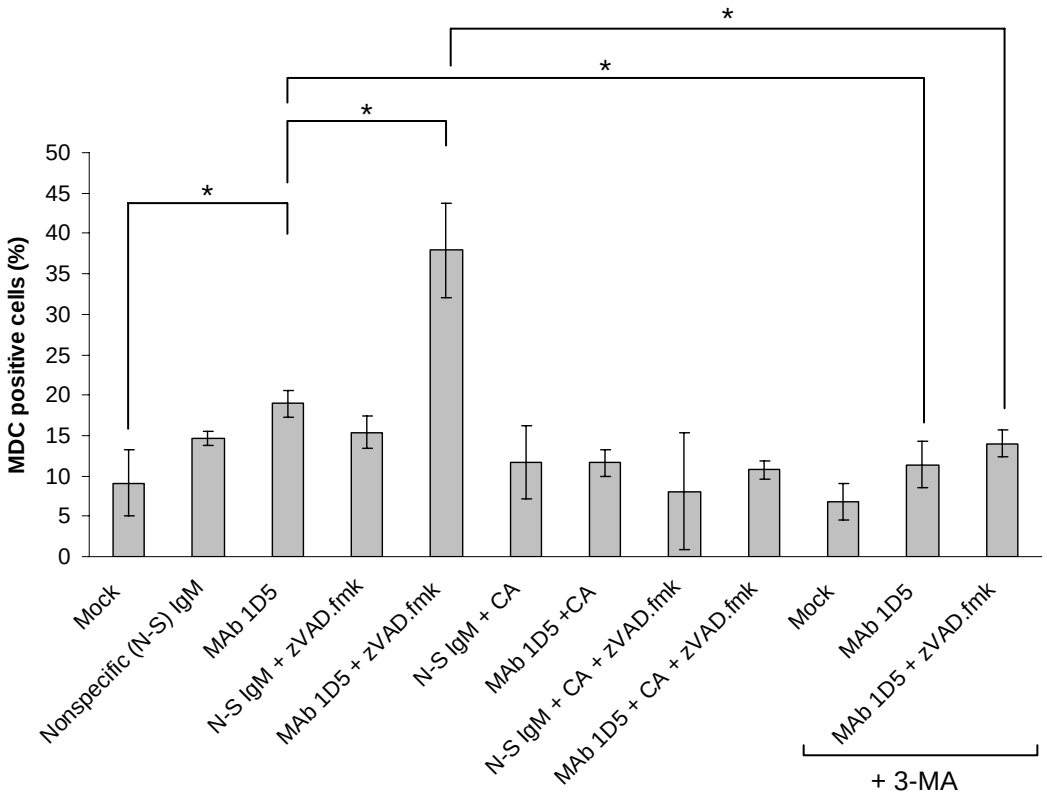

Figure 3.3.2 Bar chart comparing MDC-positive *Blastocystis* cells under different conditions. 500 cells were counted in each treatment. Error bars = SD of two separate experiments. *, $p<0.05$.

3.3.2 Occurrence of autophagy in Blastocystis colony

Autophagy of *Blastocystis* has not been described in literature so far. However, one study reporting the ultrastructural observations of *Blastocystis* grown as colonies showed the presence of membrane-bound vesicles containing lysosome-like organelles, small particulate inclusions and mitochondria within the central region of colonies (Tan *et al.*, 2001a), which implied the existence of autophagy in *Blastocystis* (Tan and Nasirudeen, 2005).

To further characterize the autophagy phenomenon in *Blastocystis* colonies, MDC was used to stain *Blastocystis* colonies. Discrete, buff-coloured opaque colonies could

be observed macroscopically in agar plate inoculated with *Blastocystis* cells on day 10. Using an inverted microscope, distinct biconvex disc-shaped colonies embedded in the soft agar were observed. Individual colonies were picked up by an inoculating loop and stained with MDC to examine the uptake of the stain by cells at the center and periphery of the colony (Figure 3.3.3). Cells located in the center of the colony showed a significant proportion of MDC-positive cells whereas cells located at the periphery of the colony had virtually no MDC positive staining. The data suggest that autophagy may indeed be triggered in cells located at the center of the colony.

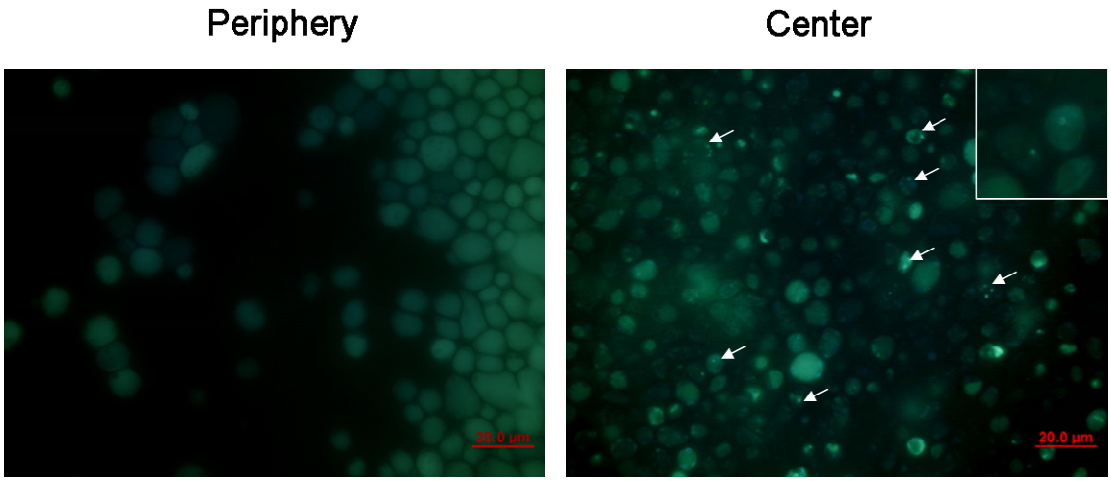

Figure 3.3.3 MDC staining of colony forms of *Blastocystis*. *Blastocystis* colonies embedded in the agar were removed by an inoculating loop and stained with MDC. Arrows point to representative MDC-positive cells.

3.3.3 Autophagy induced by nutritional stress in Blastocystis

Because it has been shown in other eukaryotic cells that autophagy is often rapidly up-regulated when cells are under nutritional stress (Levine and Klionsky, 2004b; Munafo and Colombo, 2001; Takeshige *et al.*, 1992), *Blastocystis* was deprived of amino acids supply to further study and ascertain the autophagy phenomenon in *Blastocystis*.

Blastocystis cells were incubated in normal IMDM medium (control) or in HBSS for one to three hours. After the treatments, cells were stained with MDC and the MDC positive cells were scored. As shown in Figure 3.3.4, the percentage of MDC-positive cells increased from 6.7±0.9% in cells incubated in normal growth medium to 19.7±2.2% after one hour amino acid starvation. There was also a time-dependent increase of MDC-positive cells as the starvation progressed to two hour (28.6±0.2%) and three hour (38.0±1.4%) periods. Hence, these results suggested that autophagy was rapidly triggered in *Blastocystis* cells in response to amino acid starvation.

Target of rapamycin (TOR) is a conserved Ser/Thr kinase and is a central controller of cell growth. It is a negative regulator of autophagy and inhibition of TOR leads to induction of autophagy (Meijer and Codogno, 2004). Nutrient starvation or absence of growth factors can inhibit TOR and triggers autophagy in yeast and mammalian cells (Lum *et al.*, 2005b; Wullschleger *et al.*, 2006). It is very likely that the TOR signaling pathway also exists and functions in *Blastocystis* and the accumulation of MDC staining observed in serum-starved *Blastocystis* cells was due to the inactivation of TOR. To verify the existence of TOR signaling network in *Blastocystis*, it was investigated whether rapamycin, the prototypical inhibitor of TOR, could induce autophagy in *Blastocystis*.

Blastocystis cells were treated with 100 nM, 500 nM or 1000 nM rapamycin for a period of three hours. MDC staining was visually scored using fluorescence microscopy (Figure 3.3.5). Similar to amino acid starvation, punctuate intensive staining by MDC could also be observed in rapamycin-treated cells. As compared to DMSO control (8.0±1.0%), cells which had been incubated with 1000 nM rapamycin

had a significantly higher percentage of MDC positive cells (45.5±12.4%). Rapamycin at the concentration of 100 nM or 500 nM did not induce significant change in MDC accumulation. These results indicated that rapamycin could induce autophagy in *Blastocystis* and thus the TOR signaling pathway was likely to be conserved in *Blastocystis*. Trypanosome TOR was reported to have an IC50 for rapamycin of 152 nM after 72 h treatment (Barquilla *et al.*, 2008). The fact that *Blastocystis* was insensitive to rapamycin concentration below 1000 nM may be due to the brief incubation period of 3 h.

To evaluate if the incorporation of MDC was indeed dependent on autophagy, cells were pre-treated with 3-MA or wortmannin, inhibitors of autophagic sequestration. 3-MA and wortmannin are phosphatidylinositol 3-kinase (PI3K) inhibitors and inhibit both class I and class III PI3K. Class I PI3K generates products to inhibit autophagic sequestration while class III PI3K products stimulate autophagic sequestration downstream of class I enzymes, so the overall effect of 3-MA and wortmannin is to block autophagy (Blommaart *et al.*, 1997; Petiot *et al.*, 2000). The addition of 3-MA to 3 h amino acid-starved cells decreased the percentage of MDC positive cells from 38.0±1.4% to 9.5±0.6% and the addition of wortmannin decreased the percentage to 5.5±3.1% (Figure 3.3.4). Similar inhibitory effect was seen in rapamycin treatment as the MDC uptake of cells treated with 1000 nM rapamycin dropped from 45.5±12.4% to 8.14±0.6% and 8.7±1.6% upon addition of 3-MA and wortmannin respectively (Figure 3.3.5). Therefore, in the presence of 3-MA or wortmannin, there was an inhibitory effect on the incorporation of MDC in both amino acid-starved and rapamycin-treated *Blastocystis* cells.

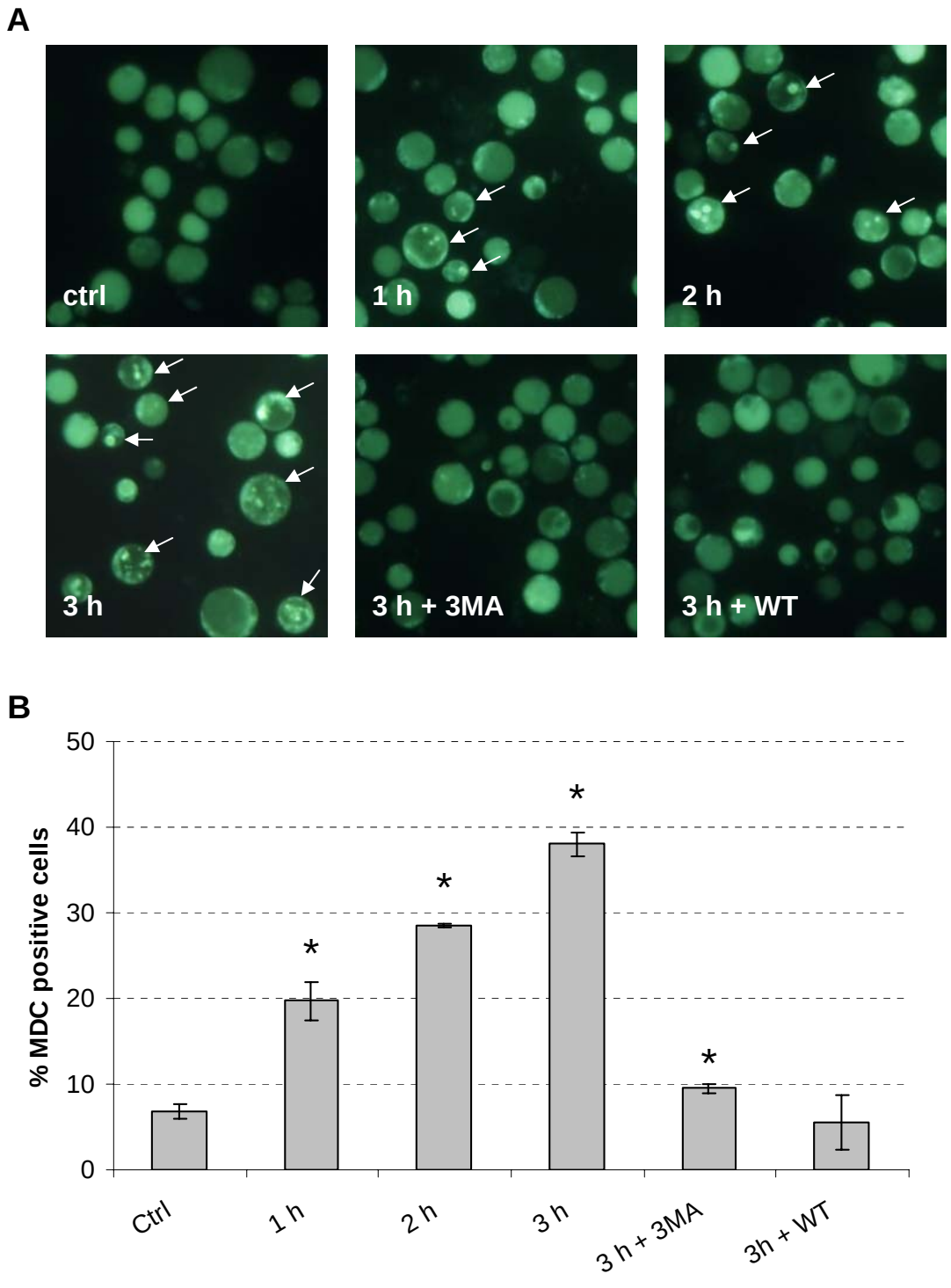

Figure 3.3.4 MDC staining of *Blastocystis* cells deprived of amino acids for 1 h, 2 h or 3 h. **A**, representative fluorescence images of MDC staining; arrows pointed to cells stained positive for MDC. **B**, percentages of MDC positive cells. Data were given as mean±SD of two independent experiments. *, $p<0.05$ versus control

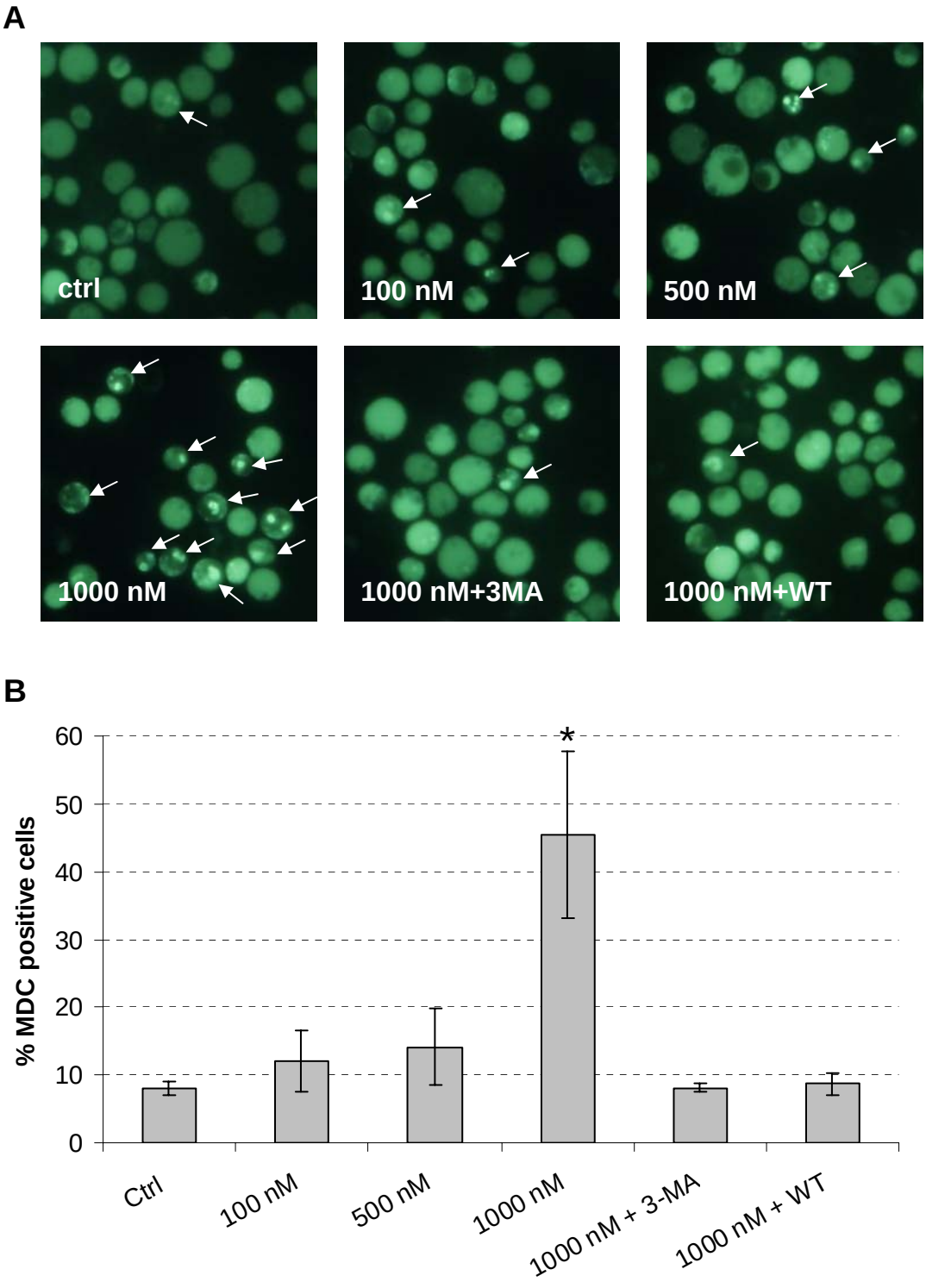

Figure 3.3.5 MDC staining of *Blastocystis* cells treated with 100 nM, 500 nM, or 1000 nM rapamycin for 3 h. **A**, representative fluorescence images of MDC staining; arrows pointed cells stained positive for MDC. **B**, percentages of MDC positive cells. Data were given as mean±SD of two independent experiments. *, $p<0.05$ versus control

It was observed that most of the MDC staining accumulated in the central vacuole. To elucidate the function of the *Blastocystis* central vacuole in autophagy, morphogical changes of amino acid-starved and rapamycin-treated cells was assessed via confocal microscopy after co-staining with MDC and Lysotracker. Lysotracker is a fluorophore which selectively accumulates in acidic compartments such as lysosomes whereas MDC was first described as a specific marker of autophagic vacuoles (Biederbick *et al.*, 1995). By double staining, the dynamics of autophagy process was anticipated because early autophagosomes should only be stained with MDC and after their fusion with lysosomes co-localization could be observed. However, Figure 3.3.6 showed that MDC staining and Lysotracker almost always co-localized. MDC or Lysotracker single-labeled controls were checked to ensure no cross-talk or bleed-through of the two fluorescent dyes (results not shown). This was not surprising since the specificity of MDC staining was cautioned by other workers previously and MDC was suggested to be like other acidotropic dyes (e.g. Lysotracker) and may preferentially label later stages in the degradation process of autophagy. Early autophagosomes may not be readily labeled by MDC because they are not acidic (Bampton *et al.*, 2005; Klionsky *et al.*, 2008; Mizushima, 2004). Nonetheless, these results suggest that in *Blastocystis* MDC and Lysotracker labeled the same autophagic compartments of acidic pH although the detailed nature of the structure awaits further investigation.

Examinations of the confocal microscopy images revealed unique MDC staining patterns in *Blastocystis*. Most of the extensive staining was seen inside the central vacuole as either individual circular specks or irregular shaped objects, which were likely to be clusters of several specks. The size of MDC-labeled individual specks was

0.5 - 1 μm, comparable to the autophagosomes in yeast (0.3 – 0.9 μm) (Yorimitsu and Klionsky, 2005). However, the size of the irregular shaped objects was 2 - 8 μm and has not be found in yeast or mammalian cells, except for the 5 – 10 μm autophagosomes containing bacteria or protozoan parasites (Andrade *et al.*, 2006; Nakagawa *et al.*, 2004). Interestingly, in another enteric protozoan parasite *Entamoeba invadens*, the sizes of autophagosome-like structure were very similar to the findings in *Blastocystis* (Picazarri *et al.*, 2008). In their study, the size of Atg8-associated structures varied from less than 1 μm to greater than 4 μm and the appearance of the large sized structures coincide with the initiation of encystation process.

A

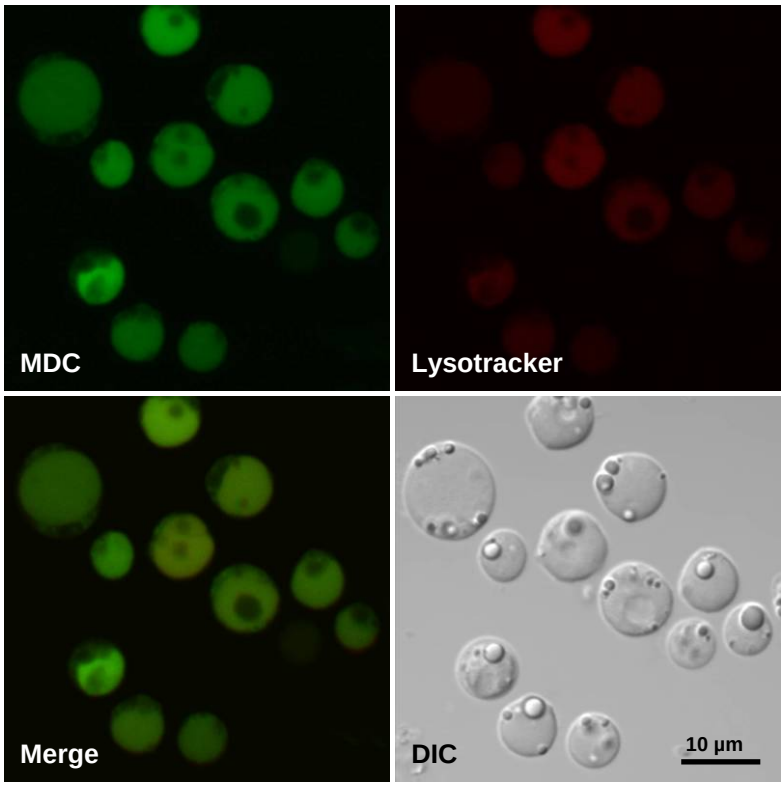

B

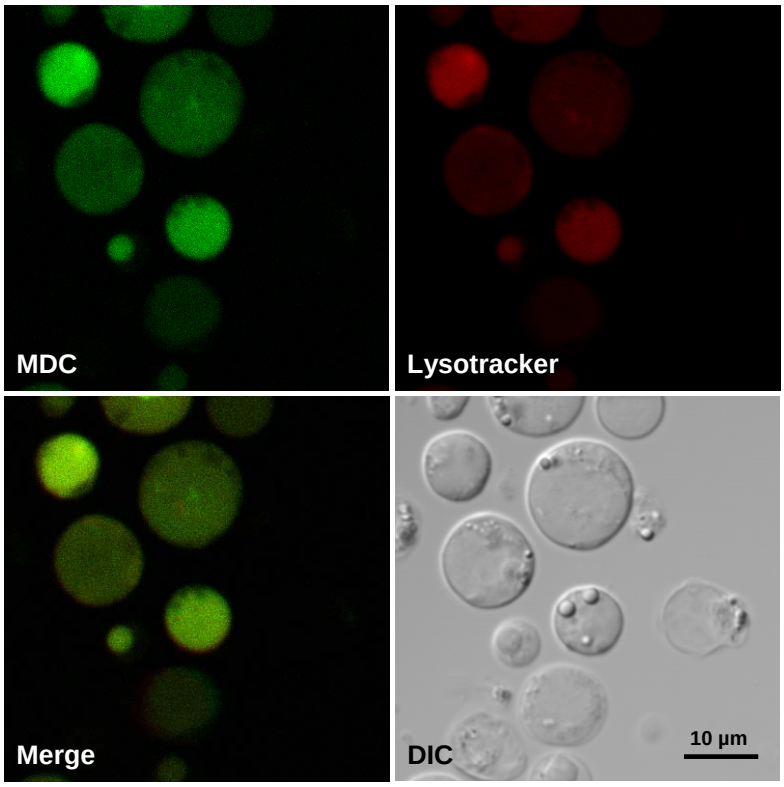

Figure 3.3.6 A, B Confocal microscopy images of healthy *Blastocystis* cells stained with MDC and Lysotracker.

C

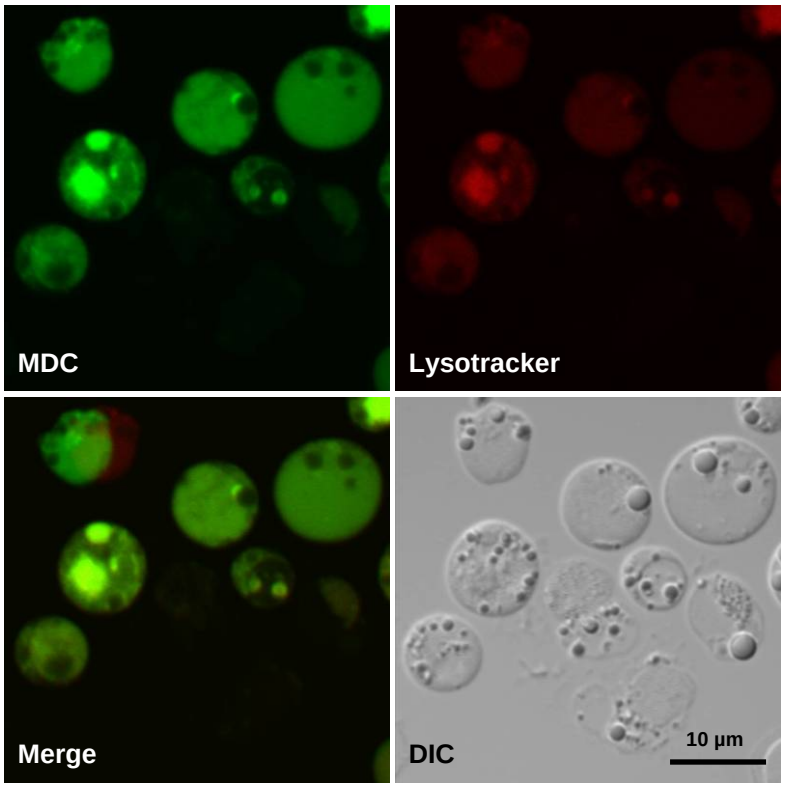

D

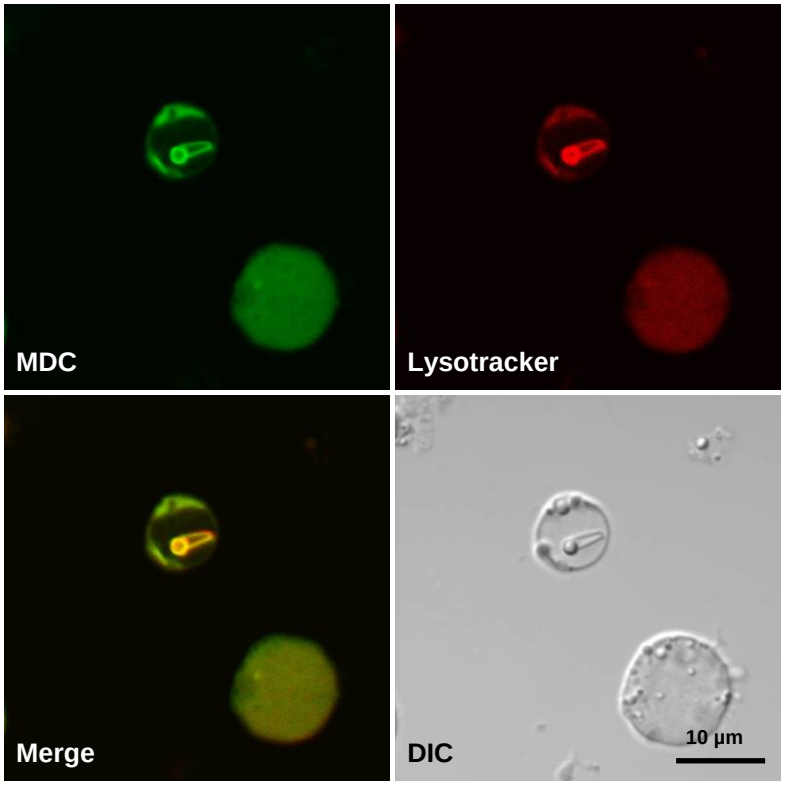

Figure 3.3.6 C, D Confocal microscopy images of *Blastocystis* incubated under amino acid starvation condition for 1 h and stained with MDC and Lysotracker.

E

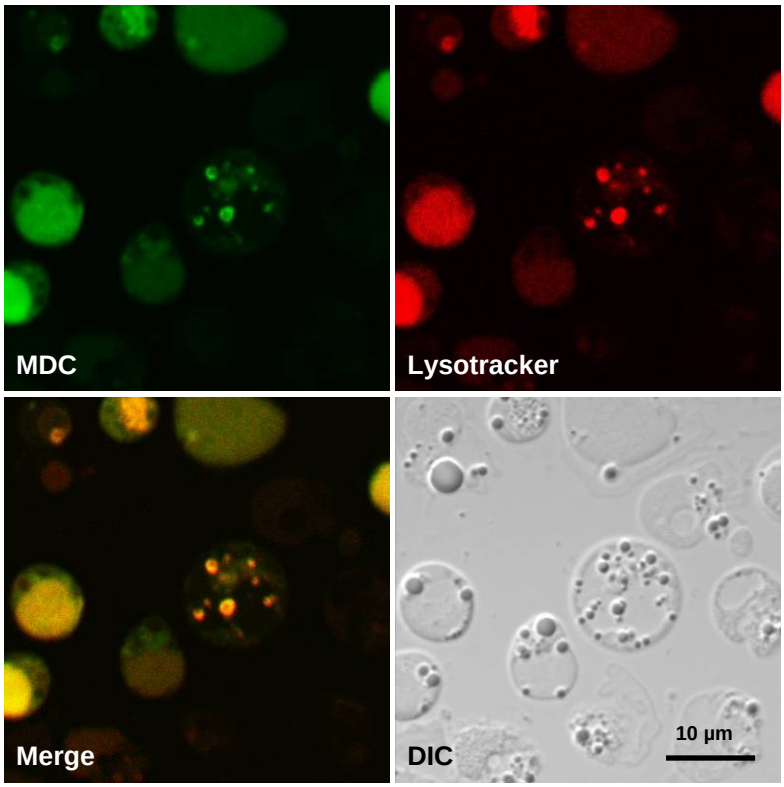

F

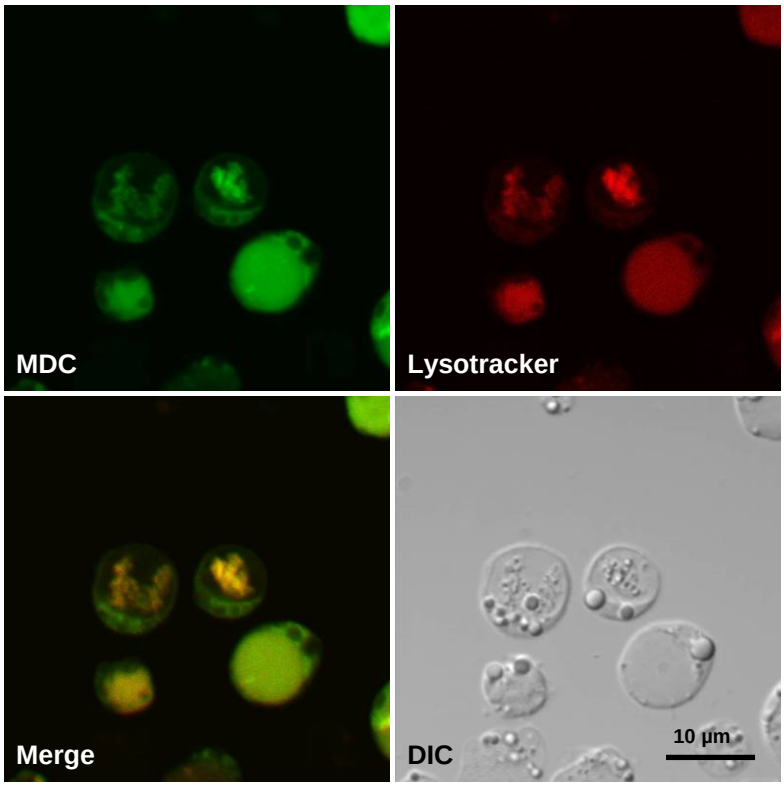

Figure 3.3.6 E, F Confocal microscopy images of *Blastocystis* incubated under amino acid starvation condition for 2 h and stained with MDC and Lysotracker.

G

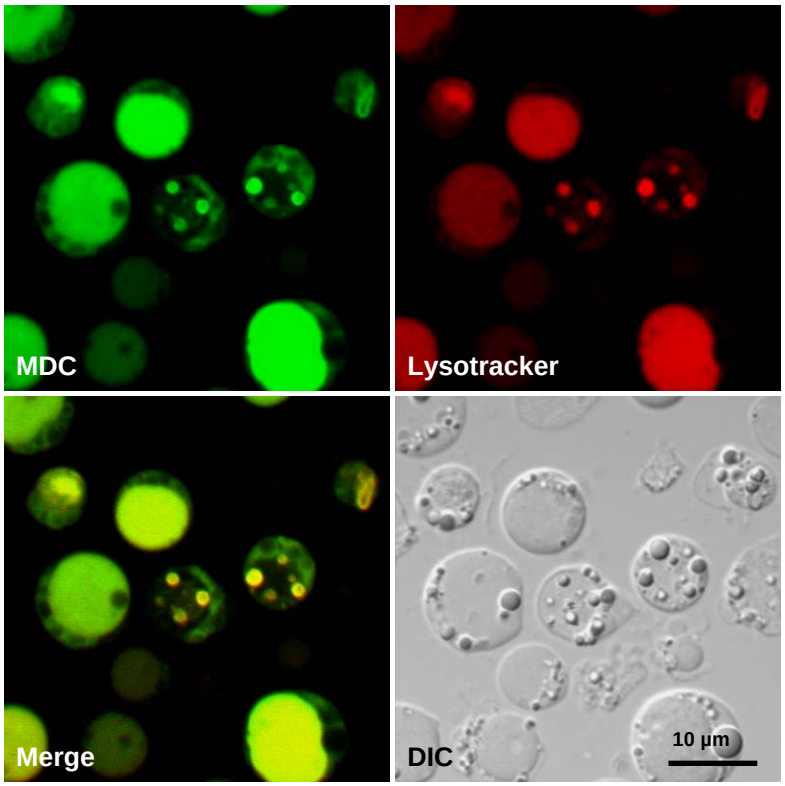

H

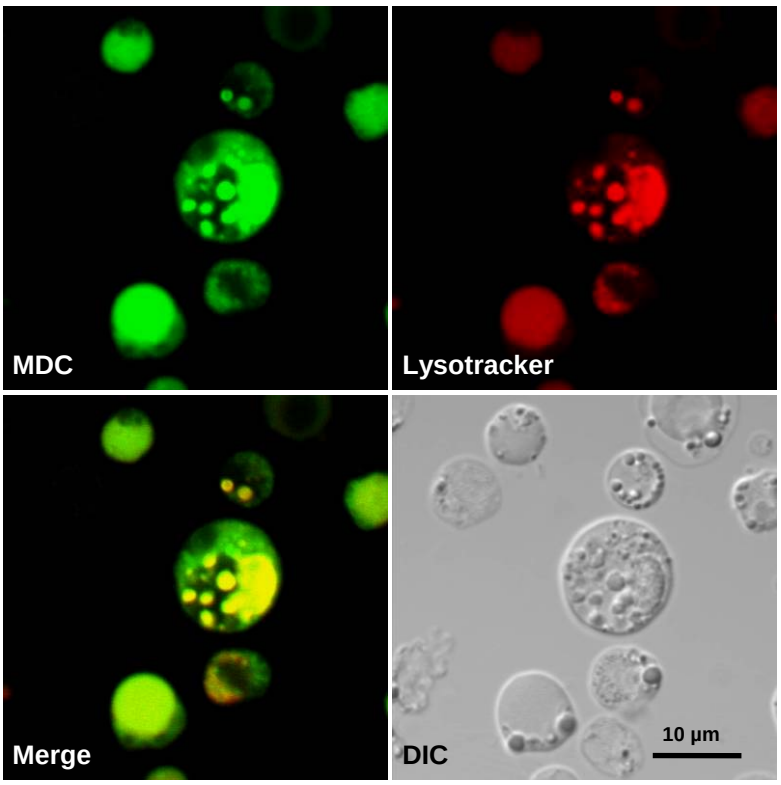

Figure 3.3.6 G, H Confocal microscopy images of *Blastocystis* incubated under amino acid starvation condition for 3 h and stained with MDC and Lysotracker.

I

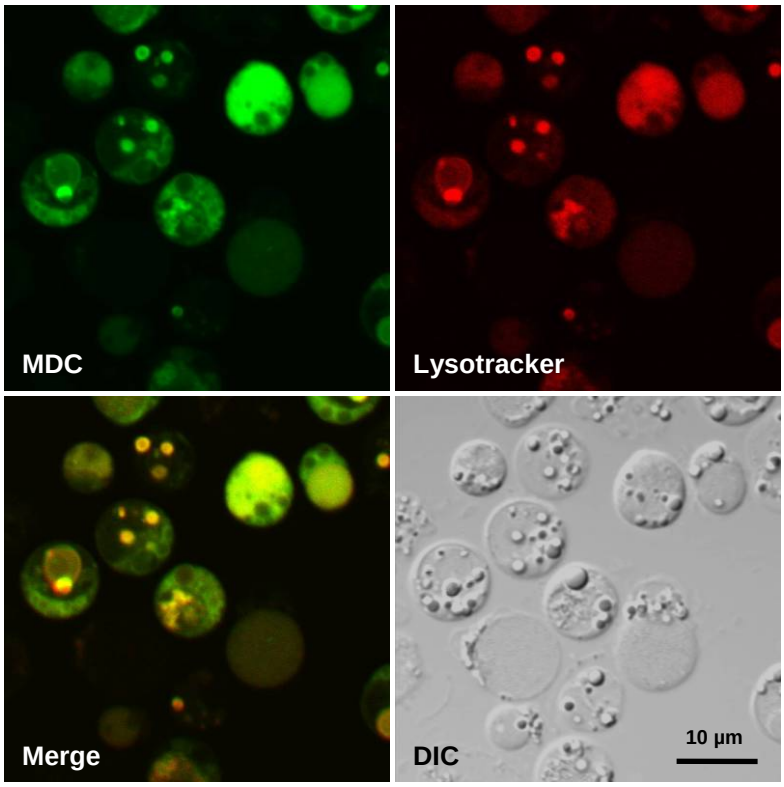

J

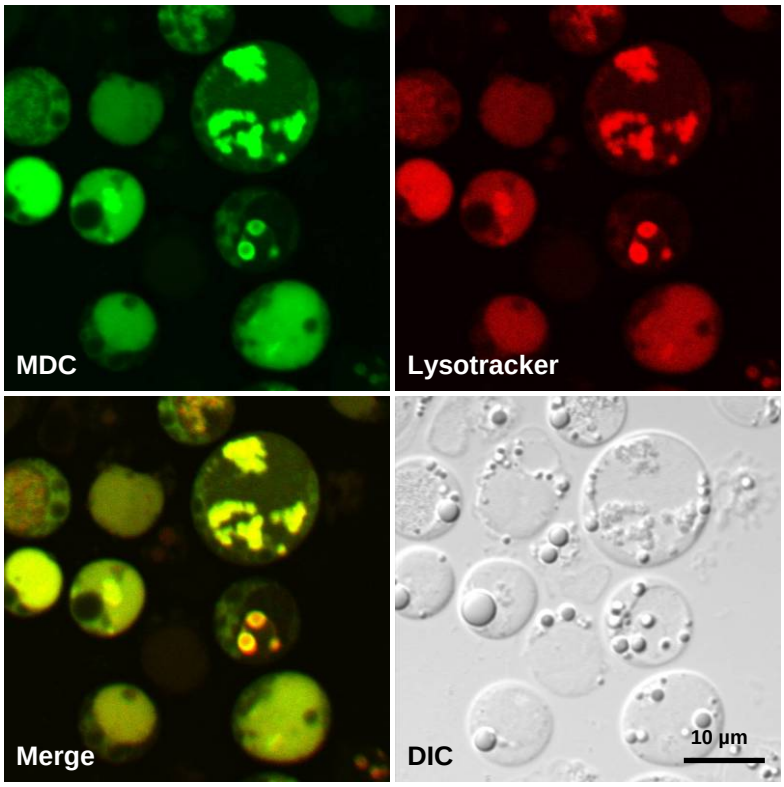

Figure 3.3.6 I, J Confocal microscopy images of *Blastocystis* incubated with 1000 nM rapamycin for 3 h and stained with MDC and Lysotracker.

Amino acid-starved or rapamycin-treated *Blastocystis* cells displayed ultrastructural features resembling those of autophagy (Figure 3.3.7). As compared to untreated control (Figure 3.3.7 A, B), most of the treated cells showed cytoplasmic vacuoles with membranous inclusions and numerous vacuoles were observed to be accumulating within the central vacuole. The content of the autophagic-like vacuoles included intact mitochondria, membrane whirls, and amorphous materials. The presence of vacuoles containing membranous inclusions or intact organelles is highly suggestive of autophagy. The size of most autophagic vacuoles observed in TEM was 0.5 – 1 μm, while some were 2 μm (Figure 3.3.7 I), 4 μm (Figure 3.3.8 A) and 6 μm (Figure 3.3.7 K arrow pointed) in size. This is consistent with the size of MDC-labeled structures observed by confocal microscopy. Less frequently, it was observed that cytoplasmic contents were invaginating through vesicle- or thin tube-like membrane structures into the central vacuole (Figure 3.3.8). Interestingly, there were vesicles budding at the end of the filament-like structures. We hypothesize that the autophagic vacuoles were formed in different ways: membrane expansion and sequestration of cytoplasmic material in the cytoplasm (Figure 3.3.7 L); extensive vacuolation in cytoplasmic regions near to the central vacuole and formation of vesicles which invaginate into the central vacuole (Figure 3.3.8 A-D); formation of a thin tube-like structure which extrudes into the central vacuole and budding off vesicles at the end of the tubular invagination into the central vacuole (Figure 3.3.8 E-G). All of the autophagic vacuoles end up in the central vacuole. It is likely that lysosomes are transferred from the cytoplasm into central vacuole in the meantime and fuse with newly formed autophagic vacuoles (Figure 3.3.7 C, D).

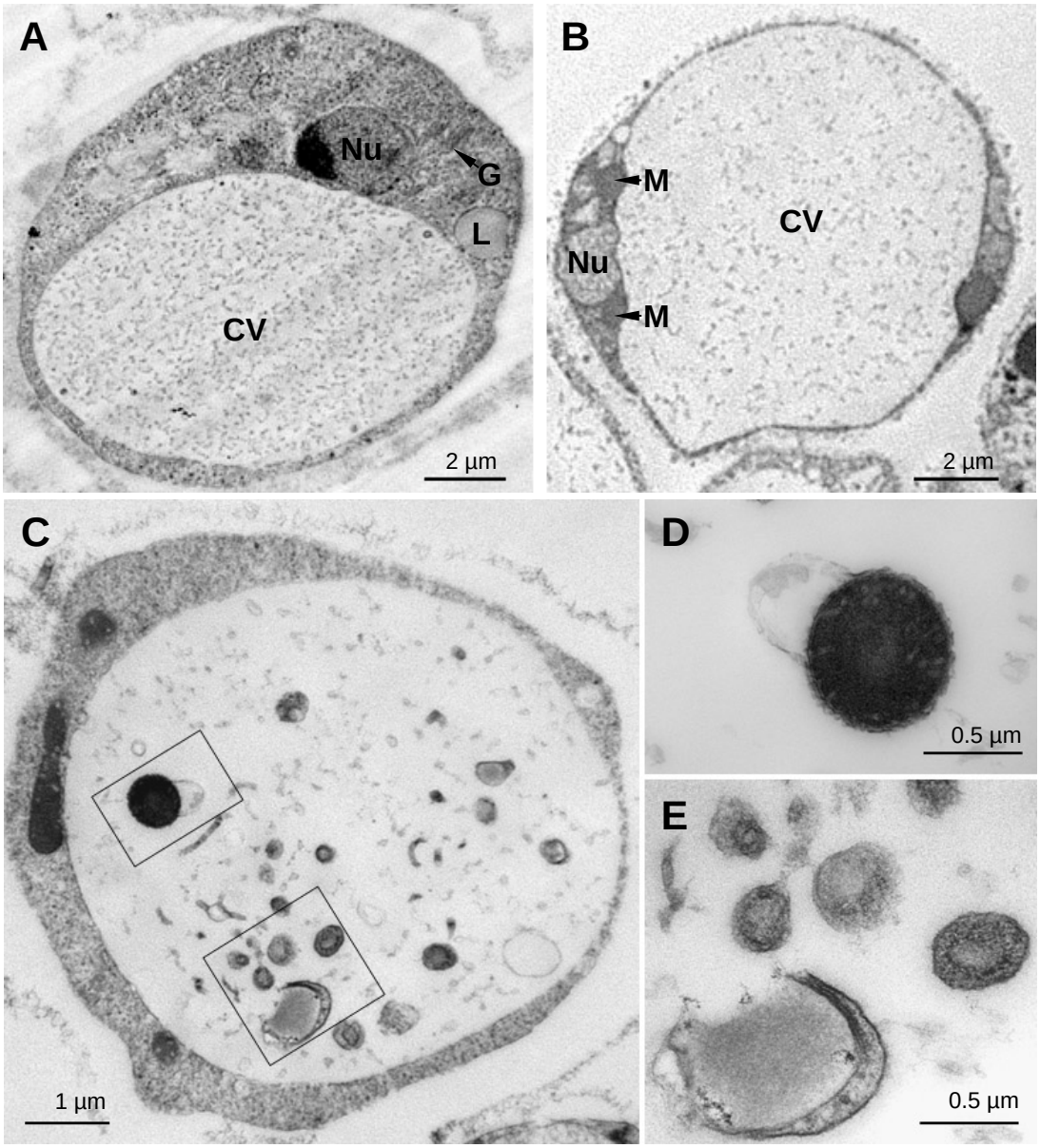

Figure 3.3.7 A-E Ultrastructural observations of autophagic vacuoles deposited in the central vacuole of *Blastocystis*. **A-B**, untreated controls displayed normal cell morphology. The central vacuole has flocculent contents. Nu, nucleus; M, mitochondrion; G, Golgi apparatus; L, lipid inclusion; CV, central vacuole. **C**, an amino acid-starved cell showing numerous autophagic-like vacuoles within the central vacuole. **D** is enlarged from boxed region in **C**, showing a mitochondrion appearing to be in the process of fusion with a lysosome. **E** is enlarged from another boxed region in **C**, showing several double-membrane vesicles with more disintegrated contents.

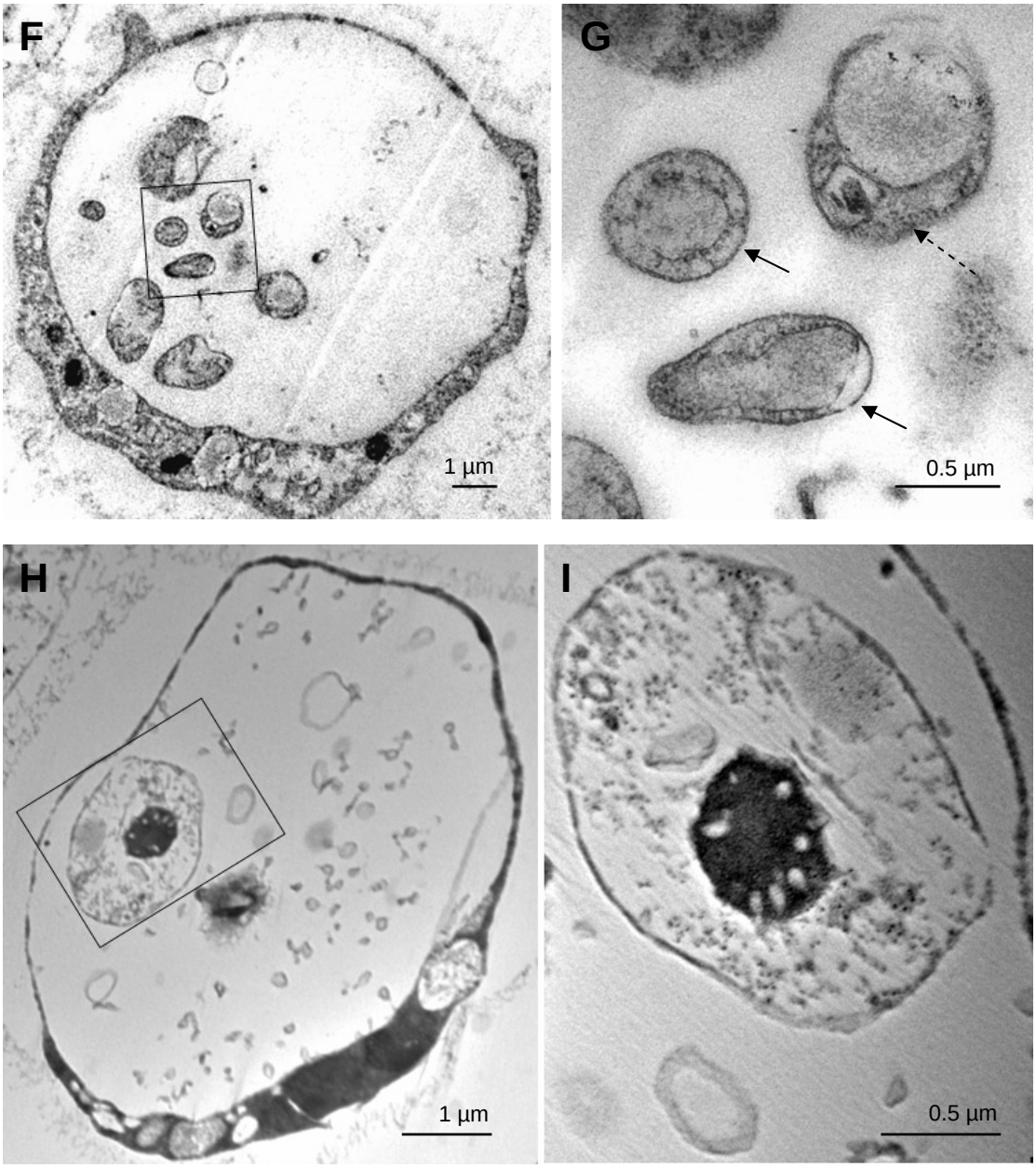

Figure 3.3.7 F-I Ultrastructural observations of autophagic vacuoles deposited in the central vacuole of *Blastocystis*. **F**, a rapamycin-treated cell harboring numerous vesicles in the central vacuole. **G**, enlarged from boxed region in **F**, showing two vesicles with an inner limiting membrane (arrow) and another vesicle containing enclosed membrane sacs and a lipid granule (dashed arrow). **H** and **I** (enlarged from **H**), a double membrane vacuole within the central vacuole of a rapamycin-treated cell, containing a mitochondrion and some cytoplasmic materials.

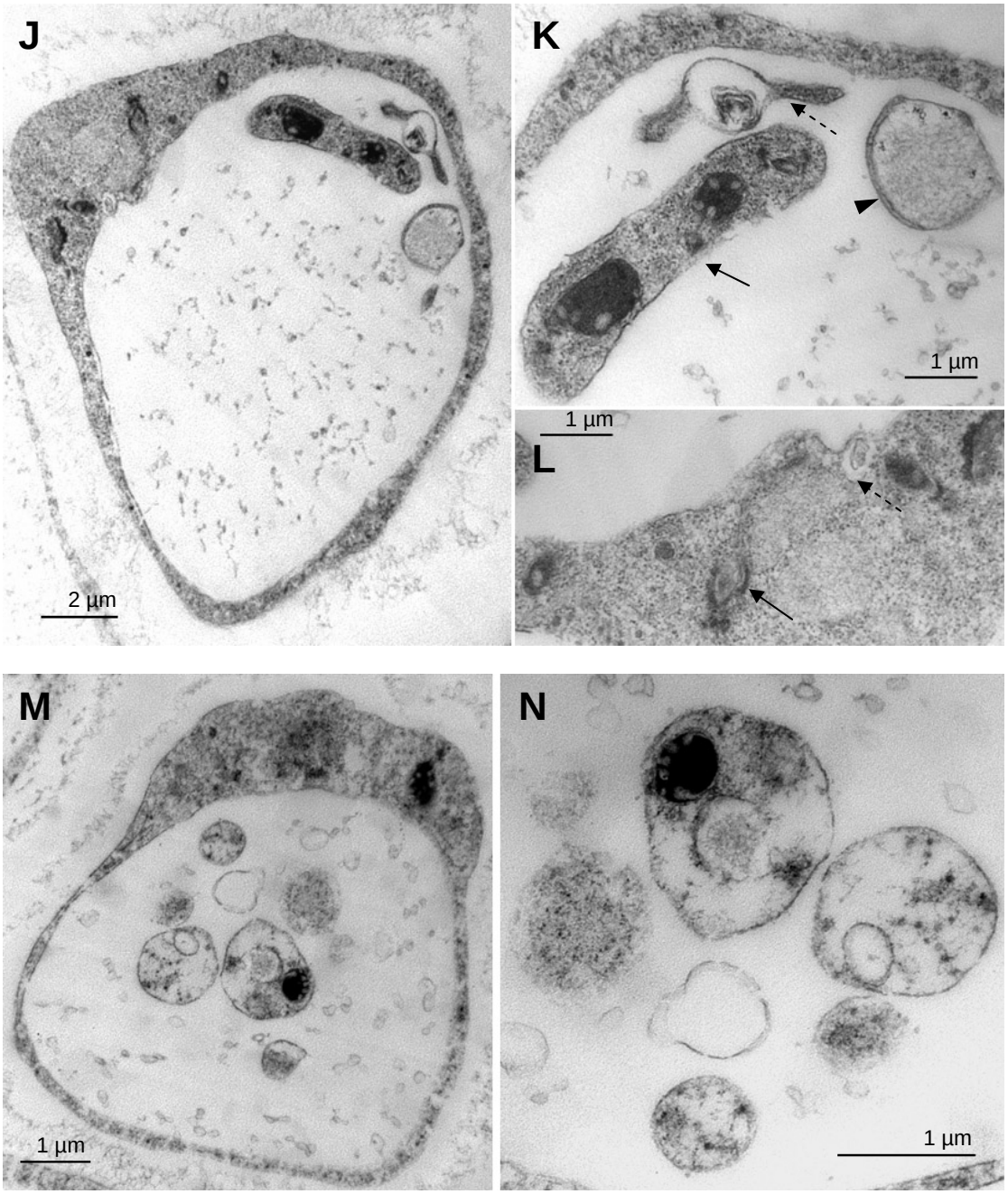

Figure 3.3.7 J-N Ultrastructural observations of autophagic vacuoles deposited in the central vacuole of *Blastocystis*. **J**, an amino acid-starved cell. **K** is enlarged from **J**, showing a vesicle containing two mitochondia and cytoplasm (arrow), a vacuole containing membranous whirls (dashed arrow), a vacuole containing membranous whirls (dashed arrow), and another double membrane vacuole (arrow head). **L** is enlarged from **J**, showing a double membrane formed in the cytoplasm (arrow) and a cytoplamic vacuole (dashed arrow). **M** and **N** (enlarged from **M**), an amino acid-starved cell.

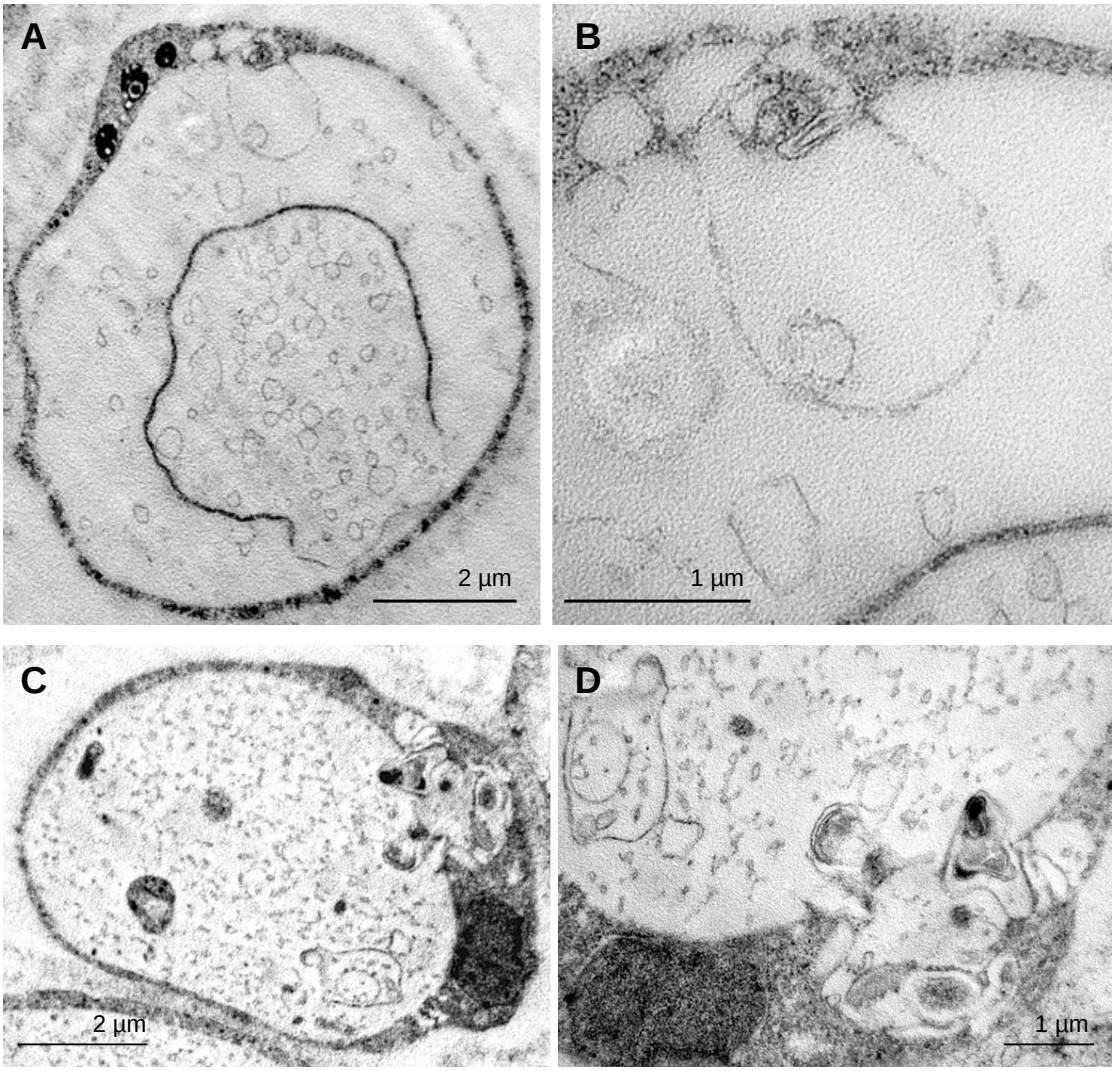

Figure 3.3.8 A-D Ultrastructural observations of cytoplasmic invagination into the central vacuole when cells were deprived of amino acids or treated with rapamycin. **A-D**, invagination of membrane bound vesicles into the central vacuole. Multiple vacuolations were seen in the cytoplasmic region near the central vacuole and some vesicles appeared to be in the process of invaginating into the central vacuole.

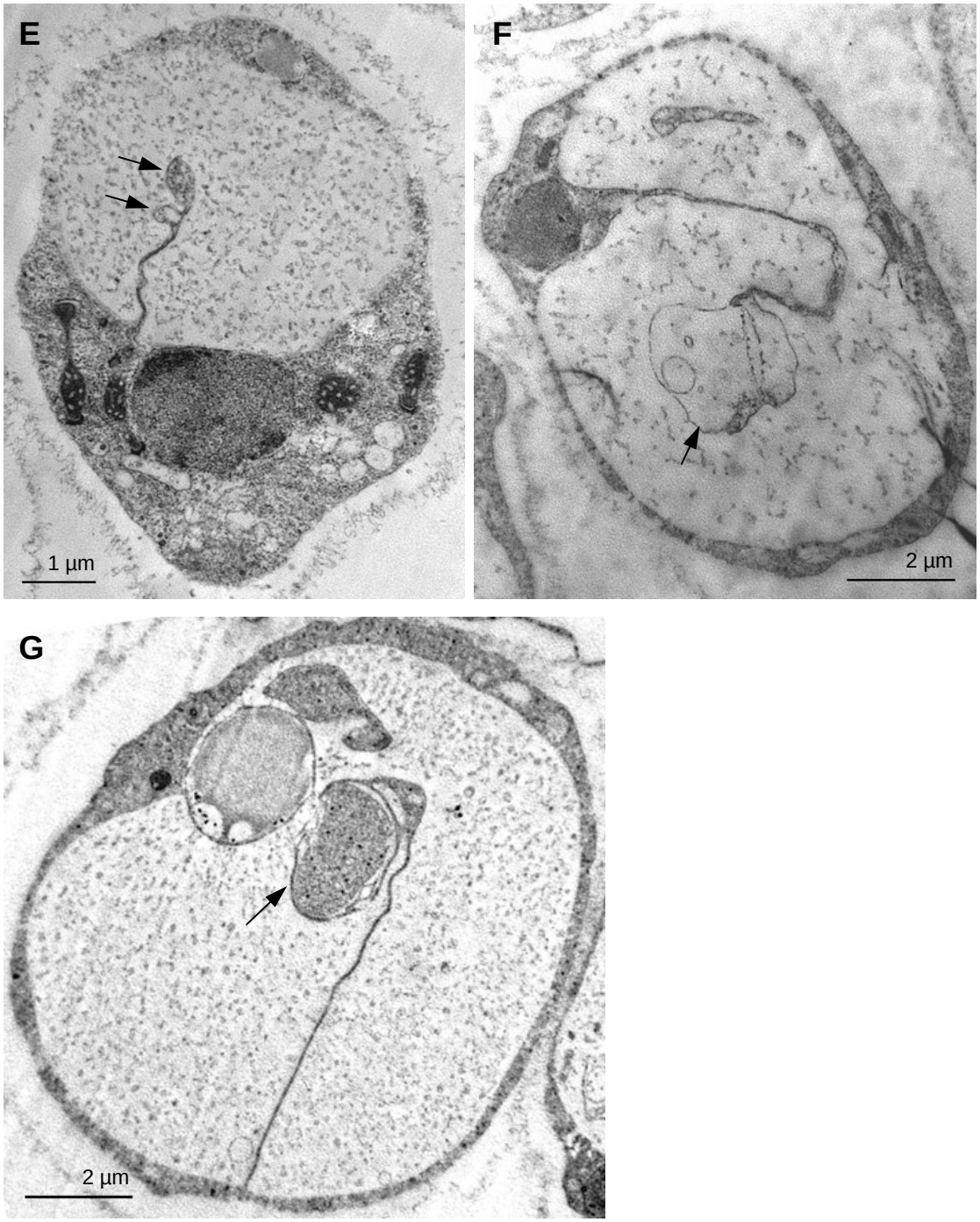

Figure 3.3.8 E-G Ultrastructural observations of cytoplasmic invagination into the central vacuole when cells were deprived of amino acids or treated with rapamycin. **E-G**, invagination of membrane bound filaments into central vacuole with vesicles budding from the tip of the filament (arrow).

3.4 Discussion

Previous studies showed that *Blastocystis* exhibited typical features of apoptosis when exposed to the surface reactive MAb 1D5 (Nasirudeen *et al.*, 2001a; Nasirudeen *et al.*, 2001b; Tan and Nasirudeen, 2005). However, the mechanism is still unknown. It was shown that MAb 1D5 targeted specifically at a 30 kD protein on the plasma membrane (Tan *et al.*, 2001b; Tan *et al.*, 1996a; Tan *et al.*, 1997). The MAb 1D5 reactive protein is functionally important and identifying this protein will be a key initial step to delineate cell death pathways in *Blastocystis*.

Two-dimensional gel based proteomics is very useful in resolving individual proteins in complex protein mixtures followed by identifying the protein of interest through mass spectrometry. The present study aimed to establish a 2-D proteome map of *Blastocystis* and to detect and identify the MAb 1D5 targeted protein from the 2-D proteome map. Sample preparation is a crucial step in 2-D electrophoresis but there is no single method that can be applied universally for all kinds of samples (Gorg *et al.*, 2004). The sample preparation procedures have to be determined empirically while conform to the rules of being as simple as possible and minimizing any protein modifications. Direct extraction with sample solubilization buffer after cell disruption is easy to manipulate and also minimize protein loss or modifications from additional sample preparation steps. However, when applied on *Blastocystis*, this method failed to generate good separation of proteins on 2-D gel. This may be due to the presence of interfering compounds in the sample such as salts, nucleic acids, lipids and polysaccharides. *Blastocystis* was reported to store many lipid granules in the central vacuole as well as cytoplasm (Yoshikawa *et al.*, 1995b). One study showed that

Blastocystis isolates had 1.19 mg to 4.3 mg total lipid per 10^8 cells (Keenan *et al.*, 1992) while only 1 to 2 mg protein can be isolated from 10^8 cells (unpublished observation). Lipids may interact with membrane proteins and consume detergent (Gorg *et al.*, 2004). *Blastocystis* also has a lot of carbohydrates at various cellular locations (Yoshikawa *et al.*, 1995a) and carbohydrates may interact with carrier ampholytes and proteins (Gorg *et al.*, 2004). Carbohydrates and other unknown components in the slimy surface coat of *Blastocystis* increase the viscosity of the sample and can obstruct gel pores. It is thus desirable to remove these interfering compounds. Precipitation is a common method to separate proteins from contaminants in the sample and to concentrate proteins. After evaluation of four precipitation methods, it was found that the coupling of TCA with acetone yielded most satisfactory result in terms of protein resolution and spot intensity. As protein loss (less than 30%) in the precipitation and resolubilization processes is at an acceptable range, TCA/acetone method should be an efficient method for 2-D analysis of *Blastocystis* proteins. However, it should be noted that a different set of proteins may be obtained using the precipitation method compared to extracting with sample solubilization buffer directly (Weiss and Gorg, 2008).

Based on the optimized sample preparation method, the proteome map was constructed for *Blastocystis* and over 1000 protein spots were well resolved on the pH 4-7 gel and around 900 spots were detected on the pH 3-10 gel. The narrow range of pH 4-7 yielded higher number of protein spots due to the better resolution of proteins in this range where most of proteins have their isoelectric points. The full resolving potential of 2-D gel analysis can be even greater using a combination of several micro-range IPG strips with single pH unit such as pH 3.9–5.1, 4.7–5.9, and 5.5–6.7.

In the present study, *Blastocystis* proteins in the alkaline range also showed good isoelectric focusing and were well separated. This is in line with the fact that TCA/acetone precipitation is good for enrichment and visualization of alkaline proteins (Gorg *et al.*, 2004). Future studies can use the current sample preparation method with narrow range gel of pH 7-10 if the proteins of interest are basic proteins. It is currently not clear how many proteins are expected in the *Blastocystis* proteome. A recently released *Blastocystis* EST database contains 3330 EST clusters (O'Brien *et al.*, 2007). Because EST databases are likely to exclude many lowly or transiently expressed genes, the number of genes should be higher. Five protein species are estimated for each gene in human cells due to alternative splicing and posttranslational modifications (Jungblut *et al.*, 1996). In other protozoans such as *Toxoplasma gondii*, one gene also encodes more than one protein. Therefore, the number of proteins in *Blastocystis* is definitely higher than the number of EST clusters. Despite the considerable resolution power of the 2-D analyses, it is important to note that the protein gels in this study represent only a fraction of all *Blastocystis* proteins and there are some inherent technical limitations with 2-D gel electrophoresis. Membrane proteins are usually underrepresented in 2-D gels due to their low solubility and are still a challenge in proteomic studies (Rabilloud, 2009). Proteins of low abundance are also difficult to detect and prefractionation of cell extract such as separating by cell organelles can enrich these proteins.

MALDI-TOF mass spectrometry is a rapid and efficient method for protein identification. The protein of interest is digested by an enzyme such as trypsin, and then analyzed by MALDI-TOF mass spectrometry. The generated peptide mass fingerprint data are compared with theoretical fingerprint profiles derived from *in*

silico digestion of a database of known proteins (Henzel *et al.*, 1993). However, there is no available protein database for *Blastocystis*. Searching NCBI nonredundant and Swissprot protein database using the peptide mass fingerprinting data of selected *Blastocystis* protein spots from 2-D gel failed to generate any significant matches. The feasibility of scanning the peptide mass fingerprint against the theoretical translation and proteolytic digest of an unpublished in-house draft genome was then investigated. The draft genome was not annotated yet and consisted of contigs of varied lengths. The contigs were *in silico* translated in all six frames for MASCOT searching. For the 16 selected landmark proteins analyzed, it was demonstrated that statistically significant match to a certain genome contig could be produced by this method (Table 3.1.1). The matched genome contig sequence was also found to cover the major peaks of the mass spectra. Subsequent bioinformatic analyses such as similarity search by BLAST and conserved domain prediction helped to preliminarily annotate the identified protein. Therefore, until any annotated genome database becomes available, this strategy can be used to identify *Blastocystis* proteins in future proteomic study and to facilitate downstream functional analysis. Very recently, a *Blastocystis* EST sequence database with automatic annotation was published (O'Brien *et al.*, 2007). BLAST analysis of the 16 proteins identified through use of the draft genome translated database showed corresponding matches in the EST database, which also confirmed the robustness of the genome approach.

This study aimed to identify the MAb 1D5 targeted protein. Using 2-D gel followed by immunolabeling with the MAb, the immunoreactive spots were precisely located. In-gel digestion of the targeted spots followed by MALDI-TOF MS analysis enabled the identification of genomic origin of the protein recognized by the MAb. After

MALDI-TOF MS, the protein of interest was further subjected to tandem MS analysis. In tandem MS, selected peptide ions are introduced to a collision chamber and a collision gas will cause stepwise fragmentation along the peptide backbone. The series of fragments differ in mass by a single amino acid and the amino acid sequence of the peptide can be deduced (Kuster *et al.*, 2001). Tandem MS is believed to provide authoritative identifications of the partical amino acid sequences and combining the peptides mass fingerprint with the partial amino acid sequences obtained from MS/MS produces high confidence identification of proteins (Barrett *et al.*, 2005). The application of tandem MS in the MAb 1D5 reactive protein spot was successful as seven tryptic peptides were sequenced in total. This facilitated the unambiguous identification of the genomic origin of the MAb 1D5 reactive protein. The current approach to identify the target of MAb is based on 2-D gel immunoblotting. An alternative and often used approach is through immunoprecipitation. However, the isotype of MAb 1D5 is IgM and the pentameric structure of IgM makes it difficult to use in immunoprecipitation. IgM antibodies also do not bind well to protein A or protein G. Therefore, this study demonstrates that 2-D gel immunoblotting is an effective method for identifying the target of IgM antibodies.

Most of sequenced peptides were localized on a putative gene predicted by the program GENSCAN. Bioinformatic analysis of the translated protein sequence showed that the putative gene encoded a protein containing a complete peptidase C13 domain and an incomplete NIF (NLI interacting factor-like phosphatase) superfamily domain. All of the sequenced peptides were within the peptidase C13 domain, and none fell within the NIF superfamily domain at C-terminus. Out of the four exons predicted in the putative gene by GENSCAN, the score for the predicted exon

containing the peptidase C13 domain was very high, whereas score for other exons were very low. Therefore, the real gene should definitely contain the regions covering the C13 domain, while other predicted exons may not be included. A 5' and 3' RACE (Rapid amplification of cDNA end) PCR will define the start and end of the coding sequence.

The peptidase C13 domain characterizes a family of asparaginyl endopeptidases, also known as legumains (Chen *et al.*, 1997). Legumain (EC3.4.22.34) is a novel class of cysteine protease and was originally identified from the plant legume, hence the name legumain (Abe *et al.*, 1993; Ishii, 1994). It was first identified in animals in the blood fluke parasite *Schistosoma mansoni* (Dalton *et al.*, 1995), and has since been found in mammals, helminth worms and the protozoan *Trichomonas vaginalis* (Beck *et al.*, 2001; Chen *et al.*, 2001; Maehr *et al.*, 2005; Manoury *et al.*, 1998; Shirahama-Noda *et al.*, 2003). Legumains have specificity for the hydrolysis of bonds on the carboxyl side of asparagines (Li *et al.*, 2003) and legumains from different species have been shown to function in the processing of other proteins, such as processing food storage proteins in plants(Muntz and Shutov, 2002), processing bacterial and endogenous peptides for MHC class II presentation in mammals (Manoury *et al.*, 1998), and processing and activating cathepsin B zymogens in *S. mansoni* (Sajid *et al.*, 2003).

The present study is the first to describe the presence of a legumain in *Blastocystis*, a second protozoan legumain besides *T. vaginalis* legumain. Comparison of *Blastocystis* legumain protein sequence with other legumain sequences showed that *Blastocystis* legumain was 30.1% identical to human, 28.4% identical to blood fluke, and 22.8% identical to *T. vaginalis* legumains. Key conserved features include the

catalytic His-Cys dyad, 4 predominantly hydrophobic amino acids closely preceding each of the catalytic residues, putative N-terminal prodomain and C-terminal extension, activity against legumain substrates and inhibition by legumain-specific inhibitors. From the multiple sequence alignment, *Blastocystis* legumain possesses unique N and C terminal regions, suggesting downstream substrates, localization and other properties distinct from reported legumains.

Regarding pH dependence of stability and activity, mammalian and plant legumains have been found to be unstable at neutral pH (Rotari *et al.*, 2001), and exhibit optimal activity at low pH, with the pH optimum of human legumain at pH 4.0 (Li *et al.*, 2003), pig legumain at pH 5.8 (Rotari *et al.*, 2001) and kidney bean legumain at pH 5.4 (Rotari *et al.*, 2001). Legumains from parasite origins, in contrast, have pH optimum near neutral pH, e.g., *T. vaginalis* legumain at pH 7.0 (Leon-Felix *et al.*, 2004) and the helminth *Haemonchus contortus* and *Schistosoma mansoni* legumains at pH 7.0 (Oliver *et al.*, 2006) and 6.8 (Dalton *et al.*, 1995) respectively. *Blastocystis* legumain is active over the wide range of pH 4 to 8 with the optimum pH at 7.4, similar to what has been reported in *T. vaginalis* (Leon-Felix *et al.*, 2004). It has been shown that parasitic cysteine proteases have a broad pH profile and serve various extra-lysosomal functions as opposed to the narrow pH range of mammalian lysosomal cysteine proteases which primarily exert their activity in the lysosome (Sajid and McKerrow, 2002). Interestingly, *Blastocystis* legumain has biphasic pH dependence, with peaks at pH 4.0 and 7.4, a property that has not been seen in legumains from all other origins. It is presently unclear why *Blastocystis* legumain exhibits two peaks of enzyme activity. The localization of the enzyme on the cell surface and in intracellular compartments is consistent with activity peaks at neutral

and acidic pH values. It is postulated that *Blastocystis* legumain possesses multiple functions and plays important roles at the cell surface and within acidic compartments. Legumains are generally located within lysosomes of mammalian cells and vacuoles of plant cells but have been reported to localize to the cell surface of metastatic tumors (Liu *et al.*, 2003) and on the microvillar surfaces of helminth intestinal cells (Oliver *et al.*, 2006). Surface legumains were suggested to activate local zymogens which may aid tumor invasion or participate in helminth alimentary digestion of host proteins. *Blastocystis* cysteine proteases are able to cleave human immunoglobulin A (Puthia *et al.*, 2005) and also induce pro-inflammatory responses in host cells (Puthia *et al.*, 2008). The presence of legumain on the parasite surface may similarly function to activate these proteases. The localization of *Blastocystis* legumain to the cell surface is probably promoted by its uncommon secretory signal peptide. Such signal peptide has only been explicitly described in the legumain of the Chinese liver fluke *Clonorchis sinensis* (Ju *et al.*, 2009), which was found in the excretory-secretory products as a serological antigen.

Blastocystis legumain activity was abolished by legumain specific inhibitor APE-RR, an aza-Asn derivative that does not cross react with caspases, papain and cathepsin (Asgian *et al.*, 2002). It is moderately inhibited by cystatin and MAb 1D5 and weakly inhibited by caspase-1 inhibitor Ac-YVAD-CMK. Cystatins are potent inhibitors of the papain-like cysteine peptidases in the unrelated family C1 but also inhibit legumain, due to a separate site on the cystatin molecule (Alvarez-Fernandez *et al.*, 1999), while plant and mammalian legumains have been shown to cleave caspase-1 substrates (Hatsugai *et al.*, 2004; Rotari *et al.*, 2001). Hence, *Blastocystis* legumain shares a number of characteristics with legumains of other origins.

In plants, legumain is essential for hypersensitive response cell death (Hatsugai *et al.*, 2004) and is also involved in fungal toxin FB1-induced plant cell death (Kuroyanagi *et al.*, 2005). Virus-induced gene silencing of VPE revealed loss of VPE and caspase-1 cleavage activities concomitant with loss of PCD features upon TMV-induction, resulting in increased virus proliferation. Hence, VPE-mediated cell death is important for resistance to pathogen infection. VPE targets that mediate HR cell death are currently unknown (Lam, 2005). In contrast to the plant model, the present studies suggest that *Blastocystis* legumain mediates pro-survival functions. This is evidenced by the significant PS-externalization and *in situ* DNA fragmentation upon incubation with legumain inhibitors. There was a positive correlation between the extents of these PCD features with the degree of legumain inhibition (Figure 3.2.10), with legumain-specific inhibitor and cystatin inducing the greatest amount of PS flipping and DNA fragmentation. The data indicates that PCD in *Blastocystis* is regulated by surface legumain activity and suggests a pro-survival role for the surface molecule. However, although cystatin only caused 45% inhibition of *Blastocystis* legumain activity as compared to 90% inhibitory effect by legumain-specific inhibitor, the extent of cell death induced by cystatin was even higher than that induced by legumain specific inhibitor. Since cystatin is also a high affinity inhibitor of family C1 cysteine proteases, it is possible that there is a papain-like cysteine protease downstream of legumain whose inhibition triggers PCD and by inhibiting both legumain and this hypothetical substrate protease cystatin causes massive cell death in *Blastocystis*. Because cystatin is a cell impermeable inhibitor (Claveau *et al.*, 2000), it is thus unlikely that PCD induction was due to inhibition of some other intracellular enzyme. It is speculated that *Blastocystis* cell surface legumain may be responsible for processing and activating a downstream cysteine protease which also localizes at the

cell surface and has important function in nutrition uptake. Alternatively, cystatin may independently trigger PCD by inactivating papain-like proteases on the parasite surface. Previous studies showed that MAb 1D5 exposure induces PCD features rapidly, evidenced by PS-externalization and caspase-like activity by 2 h post induction (Nasirudeen *et al.*, 2001a; Nasirudeen and Tan, 2004), suggesting a direct role for legumain in *Blastocystis* PCD. In this study, it was demonstrated that MAb 1D5 was able to inhibit *Blastocystis* legumain. It is known that enzymes can be inhibited by some of their specific antibodies through mechanisms such as steric hindrance and conformational changes (Gelboin and Krausz, 2006). MAbs of different Ig subtypes have been used to study the role of individual cytochrome P450 isoforms. Because of their high specificity and high inhibitory activity, carefully selected MAbs were suggested to be superior to chemical inhibitors to target specific cytochrome P450 enzymes (Gelboin and Krausz, 2006). MAb 1D5 is the first reported legumain-specific antibody which has an inhibitory effect on this enzyme. The mechanism by which *Blastocystis* legumain modulates PCD is presently unclear. Human embryonic kidney (HEK) 293 cells overexpressing legumain appear more resistant to apoptosis compared to cells that have basal levels, and is associated with tumor invasion and metastasis *in vivo* (Liu *et al.*, 2003). More work needs to be done to unravel the pro-survival mechanism of *Blastocystis* legumain and to determine if it is similar to that of tumor cells. Identification of the substrates of legumain will take us one step further in delineating the legumain-mediated PCD pathway.

It was reported that MAb 1D5-treated *Blastocytis* pre-exposed to zVAD.fmk and/or cyclosporine A was not rescued from cell death (Nasirudeen and Tan, 2004, 2005). In the presence of either inhibitor, there seemed to be a compensatory mechanism as the

cells were able to trigger the mitochondrial-dependent death pathway in the absence of caspase-like activity, and vice versa. However, even though both caspase-like activity and MOMP were inhibited and DNA fragmentation was abolished completely, the cells continued to die. Therefore, besides apoptosis, other cell death pathways might exist in *Blastocystis* and be triggered upon MAb 1D5 induction.

Autophagy has been suggested to play a role in alternative cell death pathway (Berry and Baehrecke, 2008; Kourtis and Tavernarakis, 2009). In order to investigate if caspase-independent PCD in MAb 1D5-treated *Blastocystis* occurred through autophagy, a specific autophagic marker monodansylcadaverine (MDC) was used. Autophagy is often characterized by the presence of vacuoles containing sequestered cytoplasmic components and organelles and MDC can accumulate in these vacuoles due to ion trapping mechanism and interaction with membrane lipid, functioning as a solvent polarity probe (Niemann *et al.*, 2000).

MDC-labeled vesicles were observed in MAb 1D5-treated *Blastocystis* and 18.9% of cells showed MDC positive staining, suggesting that autophagy was triggered by MAb 1D5. The interplay between apoptosis and autophagy is complex and not fully understood yet. Similar stimuli can induce either apoptosis or autophagy concomitantly, sequentially, or in a mutually exclusive manner (Maiuri *et al.*, 2007). It appeared that MAb 1D5 could trigger both apoptosis and autophagy, although apoptosis was still the major mode of cell death. However, when *Blastocystis* was pre-exposed to zVAD.fmk before incubation with MAb 1D5, the percentage of MDC-positive cells increased to 37.9%, indicating an up-regulation of autophagy when caspase-like activity was blocked. This is consistent with many metazoan cell lines

which were sensitized to autophagic cell death in the absence of caspase activation (Vandenabeele *et al.*, 2006; Yu *et al.*, 2004). The current study also demonstrated the importance of mitochondrial outer membrane permeabilization (MOMP) in MAb 1D5-initiated autophagy as when MOMP was inhibited by cyclosporine A, MDC positive staining was abolished in MAb 1D5 treated cells, even with pre-treatment of zVAD.fmk. Mitochondrial damage has been reported to be a signal for autophagy in mammalian cells. Overexpression of mitochondrial calpain 10 was found to cause mitochondrial swelling and increased autophagy, which was blocked by cyclosporine A (Arrington *et al.*, 2006). It is likely that autophagy was triggered in *Blastocystis* via MAb 1D5-mediated mitochondrial dysfunction.

This study is the first to report the occurrence of autophagy in *Blastocystis* through induction by a cytotoxic antibody. Further analysis of *Blastocystis* colony forms revealed that autophagy also occurs naturally in this organism. Strong and punctate MDC staining was observed in cells located in the center of a *Blastocystis* colony. Within a colony, cells in the center have less access to nutrients and hence, they are mostly like to undergo starvation as compared to cells at the periphery of the colony. Cells grown in liquid culture but deprived of amino acids also had a high percentage of MDC-positive staining. In addition, time-dependent increase of MDC staining was observed during the first three hours of amino acid starvation. These results suggest a strong correlation between MDC staining and the nutritional state of the cell. Since MDC was reported to stain autophagic vacuoles and autophagy is rapidly up-regulated in response to nutrient-deficient conditions in other organisms (Takeshige *et al.*, 1992; Yorimitsu and Klionsky, 2005), the intensive MDC staining should be a good reflection of the autophagic activity in *Blastocystis* and can be used in future

investigation of autophagy in *Blastocystis*. The results also demonstrated that autophagy occurs naturally when cells have limited access to nutrients or can be rapidly induced by removing nutrients from culture media.

Cells induce autophagy in response to nutrient scarcity and generate recycled metabolic substrates to maintain energy homeostasis (Meijer and Codogno, 2004; Tsukada and Ohsumi, 1993). However, when nutrient supply via autophagy becomes ultimately depleted in prolonged starvation, massive autophagy may contribute to cell death (Eskelinen, 2005; Galluzzi *et al.*, 2008). *Blastocystis* grown in liquid culture also responded to starvation by initiating autophagy when the cells were deprived of amino acids.

Results of the current study suggest that the some of the autophagy machinery is conserved in *Blastocystis*. Target of rapamycin (TOR) is a conserved Ser/Thr kinase and a negative regulator of autophagy. Rapamycin induces autophagy through inhibition of TOR (Meijer and Codogno, 2004). It was found that in *Blastocystis*, treatment with rapamycin elicited similar response to that of amino acid starvation. Rapamycin treatment was effective in intensifying MDC-labeled vesicles; hence *Blastocystis* is likely to have a homolog of TOR and the TOR signaling pathway should also exist and function in *Blastocystis*. The phosphatidylinositol 3-kinase (PI3K) inhibitors 3-MA and wortmannin was shown to inhibit the incorporation of MDC effectively. Both class I and class III PI3K have been reported to regulate autophagy in yeast and mammalian cells. Class I PI3K generates products to inhibit autophagic sequestration while class III PI3K products stimulate autophagic sequestration downstream of class I enzymes, so the overall effect of 3-MA and

wortmannin is to block autophagy (Blommaart *et al.*, 1997; Petiot *et al.*, 2000). Inhibition of MDC incorporation by 3-MA and wortmannin suggested similar regulation pathway existed in *Blastocystis* and also confirmed the autophagic nature of MDC-labeled vesicles. The concentration of 3-MA used to effectively inhibit MDC incorporation in *Blastocystis* is comparable to that in mammalian cells and many other cells (Munafo and Colombo, 2001). However, the concentration of wortmannin needed to inhibit MDC incorporation was higher in *Blastocystis* (in the micromolar range) than in mammalian cells (in the nanomolar range), but is comparable to plants (μM) (Takatsuka *et al.*, 2004). The different sensitivity range of wortmannin in *Blastocystis*, plants and mammalian cells may be due to the difference in the structure of PI3K subunit which wortmannin binds to. It was reported that wortmannin binds to the catalytic subunit of PI3K, while 3-MA interacts with the regulatory subunit of PI3K (Walker *et al.*, 2000).

Morphological examinations by confocal microscopy and transmission electron microscopy (TEM) revealed several unique features of autophagy in *Blastocystis*. Most of the extensive MDC staining was observed inside the central vacuole, suggesting a role of this organelle in the autophagy process. MDC stained structures either appeared as individual circular vesicles of size 0.5 - 1 μm or big clusters of several specks of size 2 - 8 μm. Similar big sized structures in autophagy was only described in another intestinal protozoan parasite *E. invadens* and their appearance was found to coincide with the initiation of encystation process (Picazarri *et al.*, 2008). Since starvation was known to induce encystation in protozoan parasites such as *Giardia lamblia* and *E. invadens* (Avron *et al.*, 1986; Lujan *et al.*, 1996), it is possible that starvation has triggered some *Blastocystis* cells to transit into granular or cyst

forms and autophagy may promote the morphological changes through massive clusters of autophagic vacuoles. TEM is the most reliable method for monitoring autophagy (Mizushima, 2004). Highly polymorphic autophagic vacuoles were observed in amino acid-starved and rapamycin-treatecd cells. Based on these randomly observed profiles, it is postulated that the process of autophagy in *Blastocystis* starts from cytoplasmic membrane expansion to enclose organelles and other materials, or transfer of cytoplasmic components through vesicle- or tubular invagination and subsequent budding of vesicles into the central vacuole. Morphologically, the first scenario resembles that of macroautophagy, while the latter scenario is similar to microautophagy in the yeast. Regardless of the origin, all of the autophagic vacuoles appeared to be deposited into the central vacuole. The central vacuole is the largest organelle in *Blastocystis* vacuolar forms and takes up approximately 90% of the cell's volume. It is speculated to be an important organelle of this organism. However, the function of central vacuole is still largely unknown (Tan, 2008). Through amino acid starvation and rapamycin treatment, the current study has clearly demonstrated a role of the central vacuole in autophagy. Previous studies using biochemical staining for carbohydrates or lipids showed that some cells accumulated these two substances in the central vacuole while some cells did not show any positive reactions to the stainings (Yoshikawa *et al.*, 1995a; Yoshikawa *et al.*, 1995b). It is likely that the lipids and carbohydrates are actually released from degraded autophagic vacuoles as autophagy serves to maintain homeostasis in healthy cells. The current study could also shed light to numerous unexplained observations with the central vacuole in previous studies. Cytoplasmic inclusions within the central vacuole reported in previously (Dunn *et al.*, 1989b; Pakandl, 1999), which may be due to baseline autophagy in the parasites. The cytoplasmic projections into the

central vacuole was shown to increase during unfavorable culture conditions such as in the presence of high concentrations of antibiotics (Boreham and Stenzel, 1993). It is possible that the cells up-regulated autophagy in face of environmental stress.

In this study, autophagy was found to be involved in the response to nutritional stress and in cytotoxic antibody mediated cell death. Triggering autophagy in response to nutrient scarcity may represent an adaptive response by generating recycled metabolic substrates to maintain energy homeostasis (Meijer and Codogno, 2004; Tsukada and Ohsumi, 1993). However, when nutrient supply via autophagy becomes ultimately depleted in prolonged starvation, massive autophagy may contribute to cell death (Eskelinen, 2005; Galluzzi *et al.*, 2008). Autophagy may also serve as an alternative pathway to die when cells are stressed, such as with exposure to the cytotoxic antibody MAb 1D5, and may become the main pathway of cell death when classical apoptosis is inhibited. The cellular target of MAb 1D5 has been identified to be a cell surface legumain, an asparagine endopeptidase which was suggested to participate in helminth alimentary digestion of host proteins (Oliver *et al.*, 2006). It is postulated that inhibition of legumain activity by MAb 1D5 hinders the nutritional uptake of *Blastocystis* and thus elicits a starvation response in the parasite.

Figure 3.4.1 shows a proposed model of MAb 1D5-mediated PCD based on the present study and previous reports. The data in this chapter suggest that MAb 1D5 targets at cell surface legumain to induce cell death in *Blastocystis*. Inhibition of legumain activity was also found to trigger apoptotic cell death in this organism. Since MAb 1D5 can inhibit legumain activity to some extent, the cytotoxicity of this antibody might be due to the inhibition of legumain. Besides apoptosis, autophagy

was also induced by MAb 1D5 in *Blastocystis*, which augment in the presence of caspase inhibitor. Since legumain as been suggested in the nutrient uptake of helminths, it is possible that autophagy triggered through legumain inhibition by MAb 1D5 is similar to the starvation response. When cells are starved or treated with rapamycin, the target of rapamycin (TOR) is inhibited and autophagy is triggered. Autophagy may initially help the cells to survive by recycling its cytoplasmic constituents while eventually when cells fail to cope with stress it serve as alternative cell death pathway. However, this still requires further investigations.

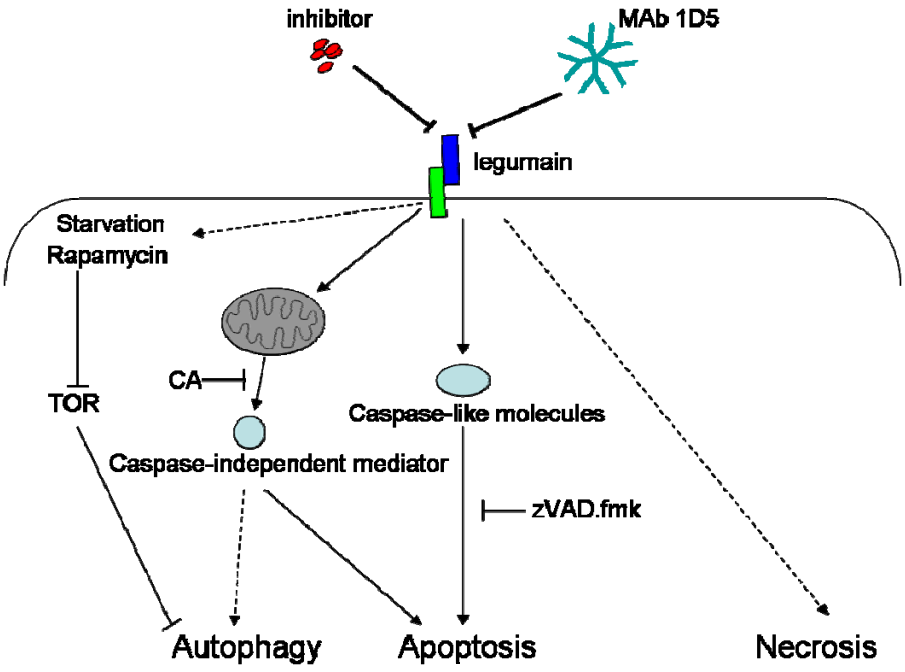

Figure 3.4.1 Proposed model of MAb 1D5 induced cell death in *Blastocystis*. CA, cyclosporine A. TOR, target of rapamycin. The binding of MAb 1D5 to legumain on the surface of *Blastocystis* leads to caspase-like proteases activation and MOMP, resulting in mainly apoptotic cell death and autophagic cell death to a less extent. In the presence of zVAD.fmk, the phenotype of cell death shifts more to autophagy. In addition, the presence of both zVAD.fmk and CA may trigger other death pathways which may be necrosis.

Chapter 4

Mechanisms of Staurosporine-Induced PCD in *Blastocystis*

4.1 Staurosprine triggers apoptotic features in *Blastocystis*

Staurosporine, a protein kinase inhibitor, has been shown to induce PCD in all mammalian cells studied so far (Weil *et al.*, 1996; Zhang *et al.*, 2004) and is a valuable tool in PCD studies. Staurosporine at a concentration of 1 μM induced in *Blastocystis* a rapid cell death process with apoptotic features. As shown in Figure 4.1.1, flow cytometry analysis of staurosporine-treated cells showed reduction in cell size at 3 h. Dot plot of control cells displayed two distinct populations of cells. The population on the right represented larger cells (healthy cells and some early apoptotic cells) while the population on the left were necrotic cells, cellular debris and late apoptotic cells. When treated with staurosporine, there was a shift of the population to the left, indicating cell shrinkage. The histogram of forward size scatter (Figure 4.1.1 B) also showed that staurosporine-treated cells were smaller than controls. The decrease in cell volume is an important early event of apoptosis that distinguishes it from necrosis (Maeno *et al.*, 2000).

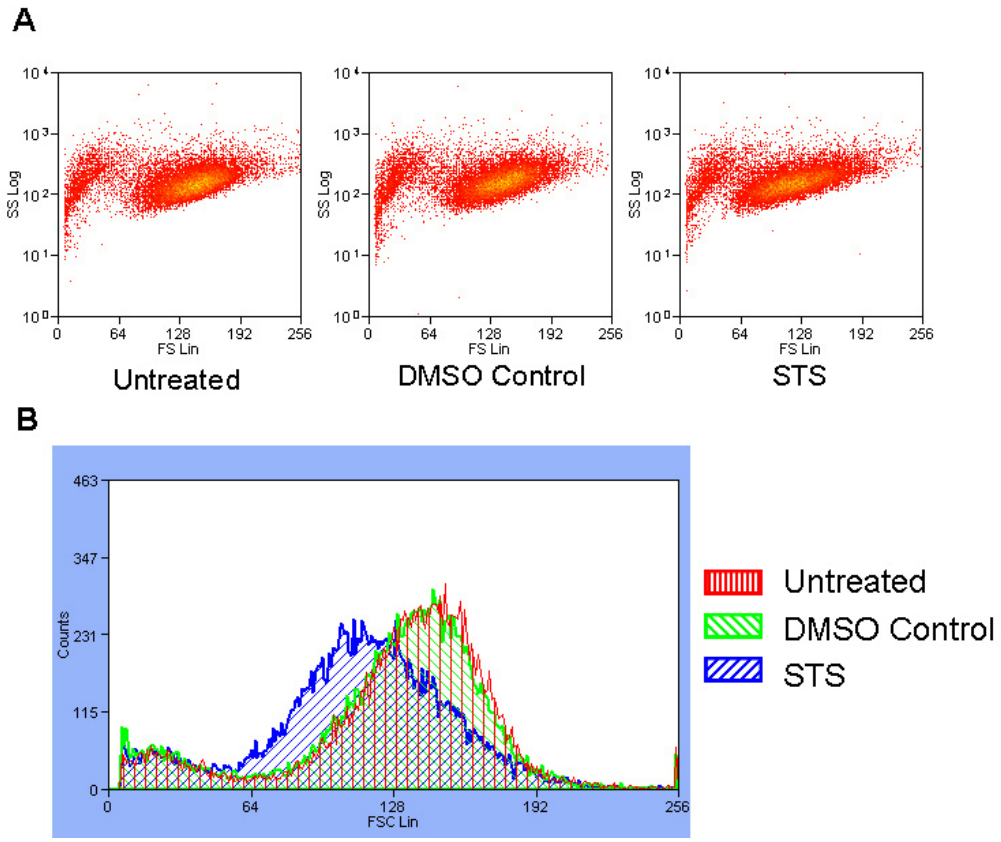

Figure 4.1.1 Effect of staurosporine on *Blastocystis* cell size as analyzed by flow cytometry. *Blastocystis* cells were incubated in the absence (Untreated) or presence (STS) of staurosporine (1 µM) for 3 h. DMSO control is the vehicle control. **A**, dot plot of forward (size) versus side (granularity) light-scatter. **B**, histogram representation of cell size.

Blastocystis cells exposed to staurosporine maintained membrane integrity while exhibited phosphatidylserine (PS) externalization, another two characteristics of apoptotic cells (Figure 4.1.2). Propidium iodide (PI), when used in the absence of cell permeant, can only enters cells with damaged plasma membrane and stains the nucleic acid. Exclusion of PI demonstrates the preservation of membrane integrity. Combined use of PI and Annexin V, which binds to PS exposed on the outer layer of plasma membrane during apoptosis, can differentiate apoptotic, necrotic and healthy cells. As shown by flow cytometry analysis in Figure 4.1.2, staurosporine-treated cells had a very low percentage of cells with PI-positive staining, similar to that of

untreated and vehicle control. In contrast, heat-induced necrotic cells showed a very high percentage (86.31%) of PI-positive cells. While maintaining membrane integrity, staurosporine-treated cells had 33.17% subpopulation with Annexin V-positive and PI-negative staining, much higher than that of untreated and DMSO control. The response was rapid as *Blastocystis* was treated with staurosporine for only three hours.

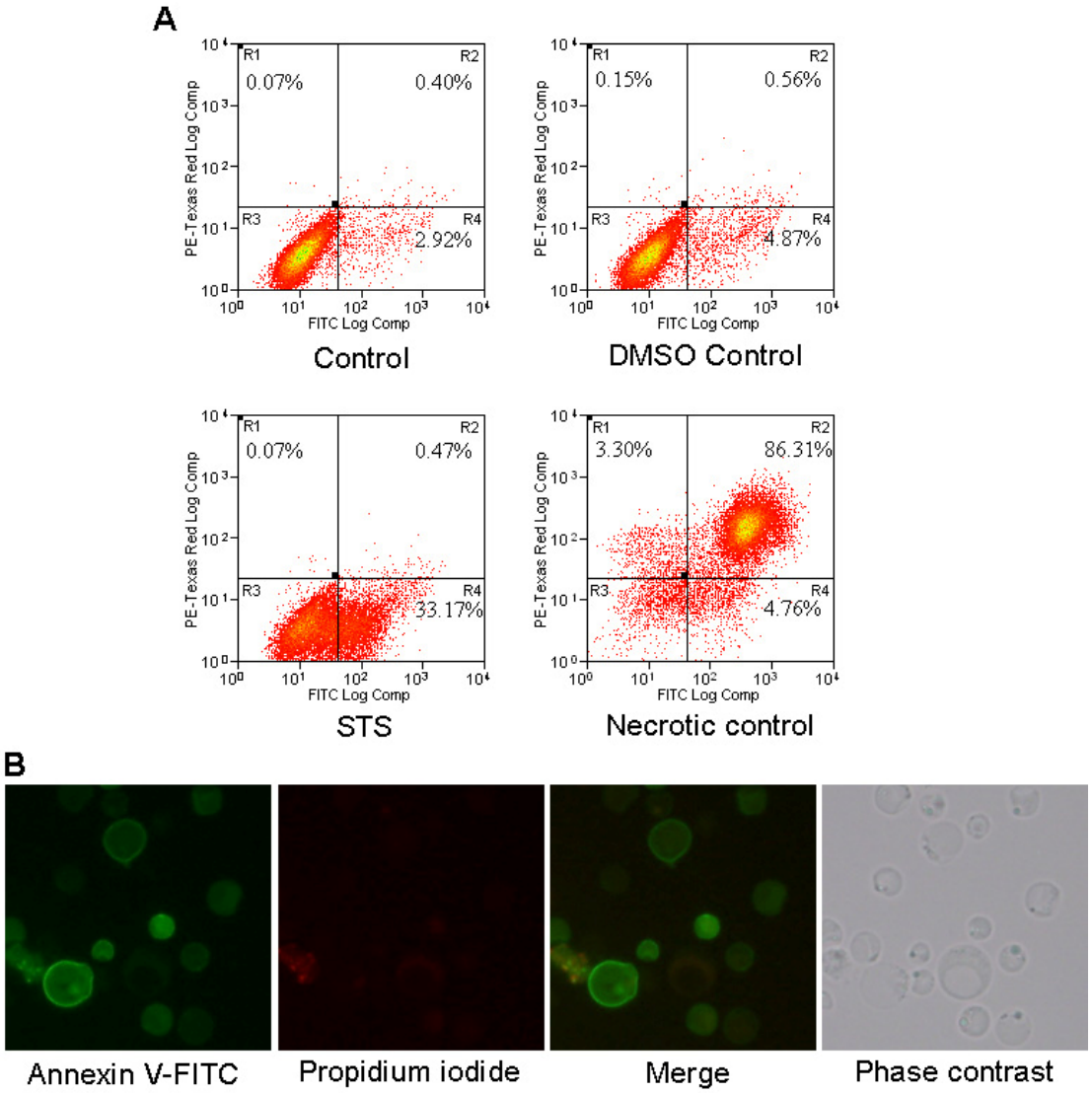

Figure 4.1.2 Preservation of membrane integrity and externalization of PS in cells treated with staurosporine. *Blastocystis* cells were incubated in the absence (Untreated) or presence (STS) of staurosporine (1 µM) for 3 h. DMSO control is the vehicle control. Necrosis was induced by heating the cells in an 80 ºC water bath for 15 min. **A**, representative dot plots of Annexin V-FITC and PI staining assay. **B**, fluorescent microscopy image of staurosporine-treated cells stained by Annexin V-FITC and PI.

DNA fragmentation is a hallmark of apoptosis and usually a late event in apoptosis (Collins *et al.*, 1997). TUNEL assay relies on the specific binding of terminal deoxynucleotidyl transferase (TdT) to exposed 3'-OH end of DNA followed by the synthesis of a labeled deoxyuridine molecule. Hence formation of DNA strand breaks as a consequence of endonuclease activity can be detected by flow cytometry analysis and expressed as a percentage of TUNEL-positive cells. As shown in Fig. 3, cells treated with staurosporine for 12 h exhibited 56.09% TUNEL-positivity, whereas untreated cells or vehicle control had a very low percentage of TUNEL-positive cells. Therefore, these results demonstrate that as in mammalian cells, staurosporine is also a strong apoptosis inducer for *Blastocystis*.

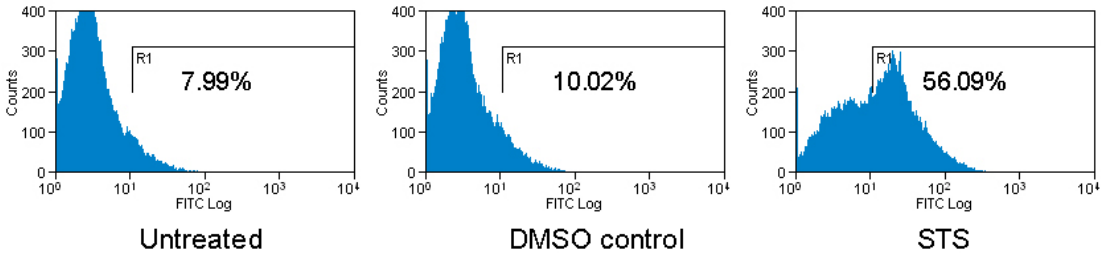

Figure 4.1.3 Representative histograms showing *in situ* DNA fragmentation analysis (TUNEL) of *Blastocystis* cells by flow cytometry. Cells treated with staurosporine for 12 h had a significant increase in fluorescence intensity compared to untreated control or vehicle control.

Transmission electron micrographs of staurosporine-treated cells also exhibited apoptotic features. As compared to the healthy control, cells exposed to staurosporine showed massive cytoplasmic vacuolation (Figure 4.1.4 A, D) and margination and segregation of nuclear chromatin (Figure 4.1.4 C, F). Condensed cells with collapsed central vacuoles were also observed (Figure 4.1.4 E).

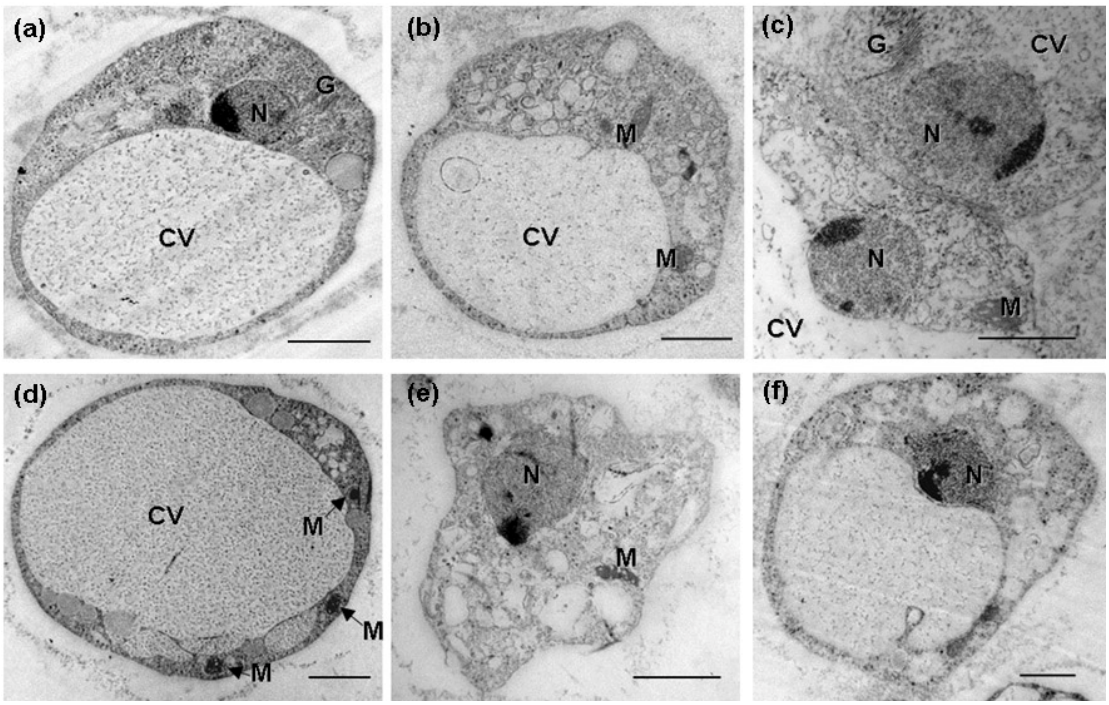

Figure 4.1.4 Transmission electron microscopy of *Blastocystis* cells exposed to staurosporine for 3 h or 12 h. **A**, Healthy *Blastocystis* cell with normal morphology and DNA chromatin seen as a crescentic mass. **B**, massive cytoplasmic vacuolation in a cell treated with staurosporine for 3 h. **C** and **F**, condensed and segregated chromatin in cells treated with staurosporine for 12 h. **D**, coalescing of large cytoplasmic vacuoles with central vacuole in cell treated with staurosporine for 12 h. **E**, cell displaying collapsed central vacuole, severe shrinkage and multiple vacuoles. N, nucleus; CV, central vacuole; M, mitochondria. Bars, 2 µm.

4.2 Regulation of staurosporine-induced apoptosis by mitochondria and cysteine proteases

Since staurosporine was found to be a strong and robust inducer of apoptotic cell death in *Blastocystis*, it was used to screen potential regulators of *Blastocystis* PCD. The mitochondrion and cysteine proteases are the key regulators of apoptosis in higher eukaryotes. Therefore, the mitochondrial transition pore blocker cyclosporine A and inhibitors of a range of cysteine proteases was used to pre-treat the cells before their exposure to staurosporine. Staurosporine-treated *Blastocystis* showed 55.3±3% cells with PS exposure at 3 h and 51.3±1.7% cells with *in situ* DNA fragmentation at

12 h (Figure 4.2.3). Cyclosporine A completely abolished staurosporine-induced PS exposure and DNA fragmentation (Figures 4.2.1 and 4.2.2). The general cysteine protease inhibitor IA in the concentration range of 10 μM to 100μM could inhibit the two apoptotic features in a dose-dependent manner. However, even with the highest concentration 100 μM, IA could only reduce the percentage of Annexin V-positive cells and TUNEL positive cells to 25.6±3.8% and 22.7±3.1% respectively, and was thus not as effective as cyclosporine A. The effects of more specific inhibitors of different families of cysteine proteases were also investigated. The caspase inhibitor z-VAD.fmk and cathepsin B and L inhibitors z-FF.fmk, z-FA-fmk, CA-074-Me could not inhibit staurosporine-induced changes in PS exposure and DNA fragmentation. Interestingly, two calpain inhibitors z-LLL.fmk and ALLN could promote staurosporine-induced apoptotic responses, evidenced by the increased PS exposure to 65.3±2.6% (z-LLL.fmk) and 64.6±2.2% (ALLN), and increased DNA fragmentation to 64.0±2.9% (z-LLL.fmk) and 62.7±2.0% (ALLN). However, because it was reported that the calpain inhibitor ALLN may also inhibit the proteosome (McDonald *et al.*, 2001), the effect of the proteosome inhibitor epoxomicin was also tested. No inhibition of staurosporine-induced apoptotic features could be observed with pre-treatment of epoxomicin (Figures 4.2.1, 4.2.2 and 4.2.3), indicating that the apoptosis-promoting effect of calpain inhibitors should be due specifically to the inhibition of calpain activity.

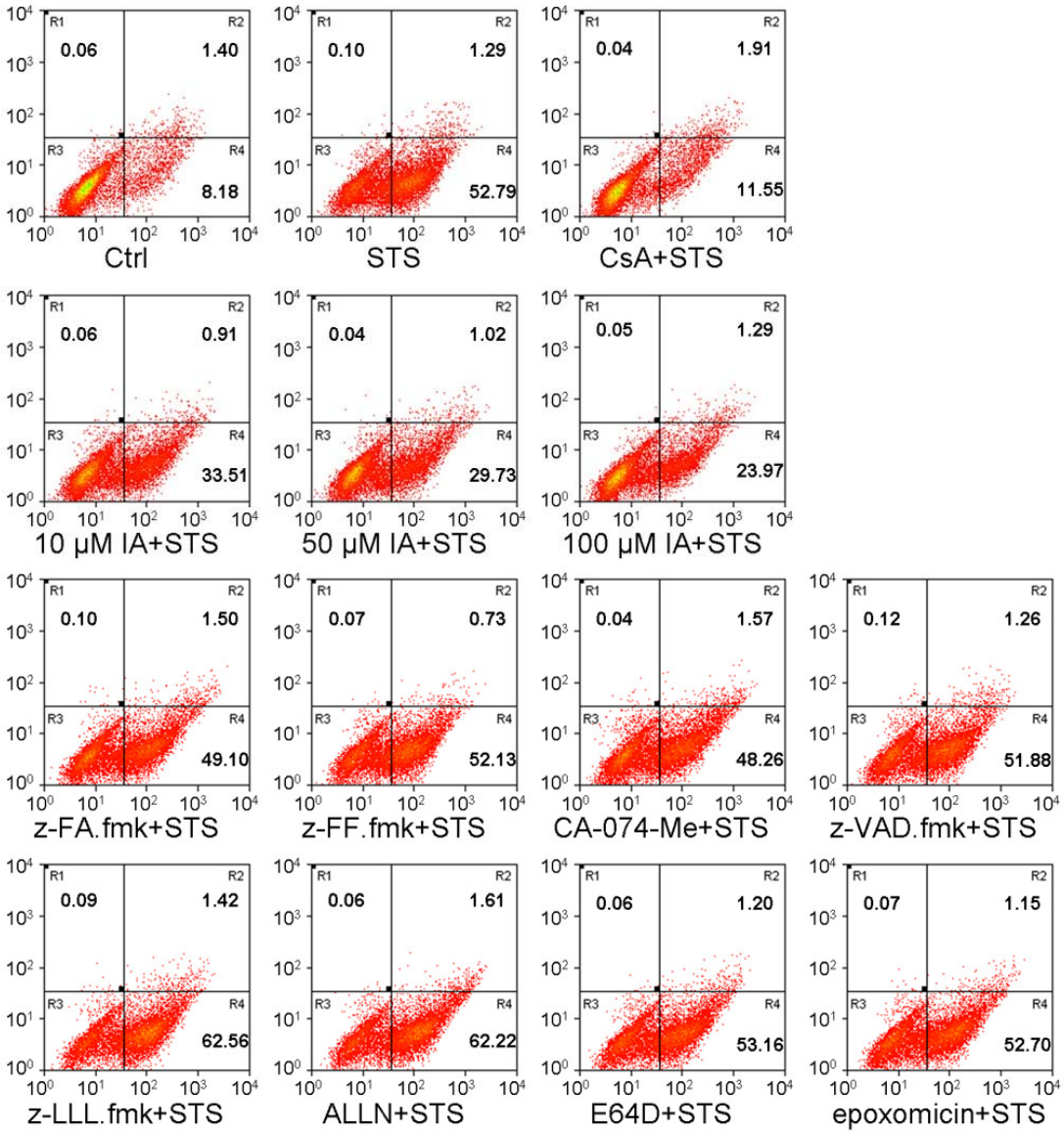

Figure 4.2.1 Annexin V assay of inhibitor-pretreated cells. Cells were pretreated with protease inhibitors or CsA for 30 min before incubation with staurosporine for 3 h. The R4 quadrant represents the percentage of apoptotic cells (Annexin V-FITC positive/ PI negative cells) in the total cell population. Control was performed with the same volume of inhibitor diluent (DMSO).

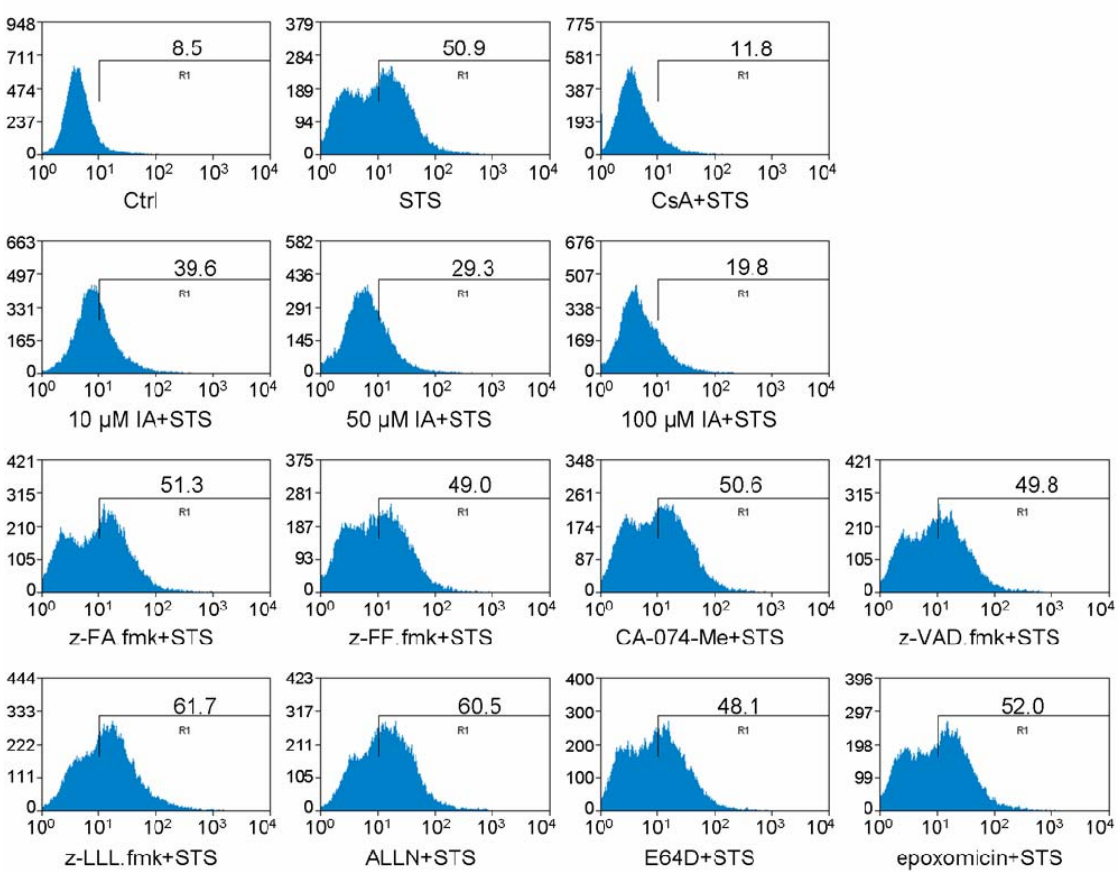

Figure 4.2.2 TUNEL assay of inhibitor-pretreated cells. Cells were pretreated with protease inhibitors or CsA for 30 min before incubation with staurosporine for 12 h. The gated population represents the percentage of apoptotic cells (TUNEL positive) in the total cell population. Control was performed with the same volume of inhibitor diluent (DMSO).

Since calpain inhibitors were found to be augmenting staurosporine-induced apoptotic responses, the activity of calpain was assessed to see if there are any correlation between calpain activity and the apoptotic responses. As shown in Figure 4.2.3, calpain is constitutively active in healthy cells. However, exposure to staurosporine potently increased calpain activity to double that of the control. As expected, the calpain inhibitor z-LLL.fmk and ALLN completely inhibited the enzymatic activity of this protease. Therefore, the data suggests that *Blastocystis* calpain becomes more active upon exposure of cells to staurosporine and exerts a protective effect to the staurosporine challenge. The general cysteine protease inhibitors IA could inhibit some extent of the staurosporine-induced apoptotic responses whereas E64D, a broad-range inhibitor of cathepsins and calpains had no inhibitory effect. The different inhibitory profile of these two protease inhibitors on calpain activity might provide an explanation to their opposing effects on apoptotic responses. Figure 4.2.3 showed that E64D was a potent inhibitor of calpain while IA only inhibited calpain activity moderately. It is likely that the two inhibitors could exert a protective effect on the cells by inhibiting an unknown protease which is responsible for mediating the staurosporine-induced apoptosis; however, the cytoprotective effect of E64D was neutralized by its apoptosis-promoting effect through inhibition of calpain.

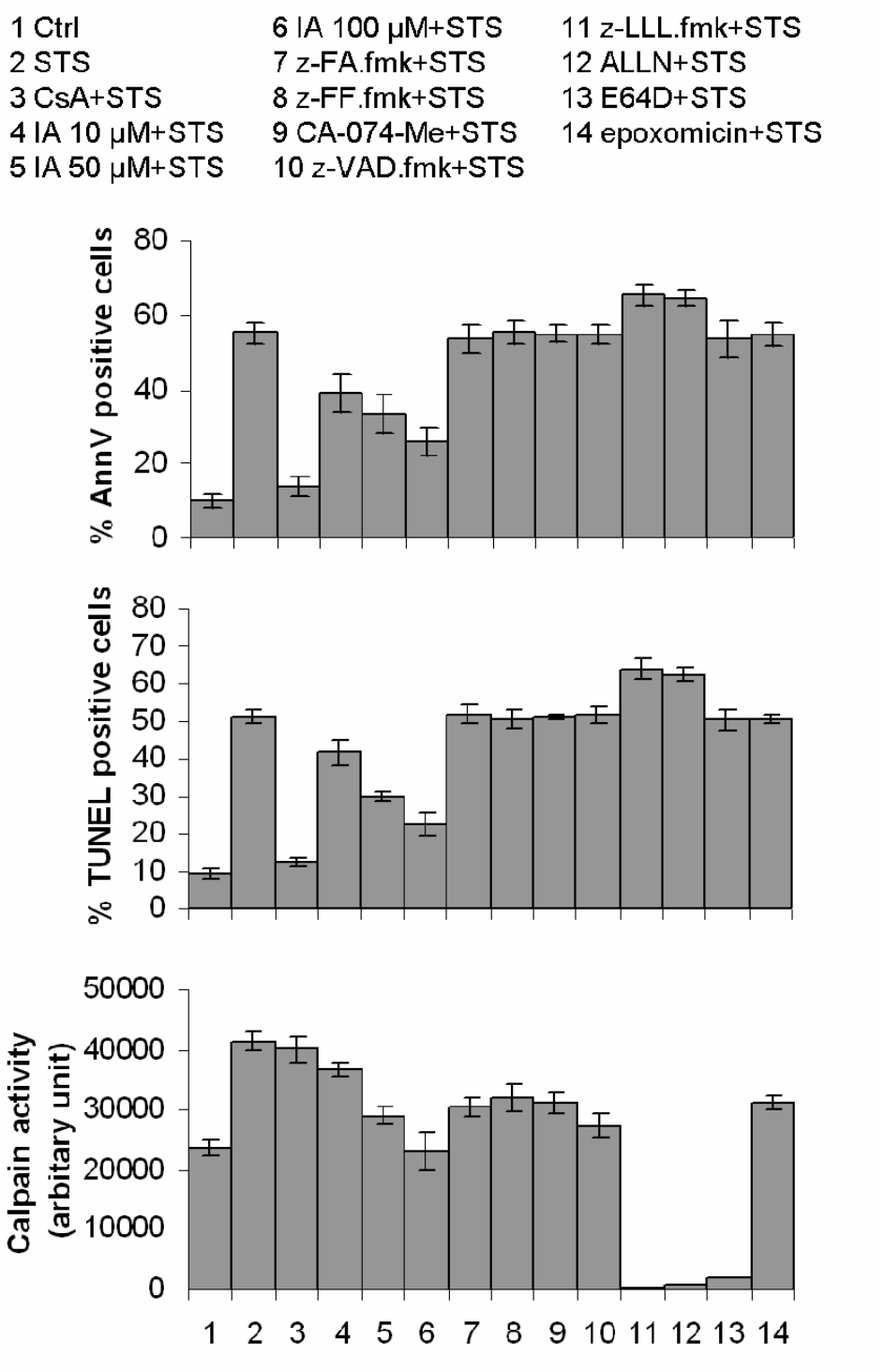

Figure 4.2.3 Relationship between *Blastocystis* calpain protease activity and staurosporine-induced apoptosis. Data of Annexin V and TUNEL assays were retrieved from Figure 4.2.1 and Figure 4.2.2. Calpain activity assay was done by incubating cell lysates with fluorogenic substrate Ac-LLY-AFC. Values were means ± standard deviation from three independent experiments.

4.3 Discussion

In the present study, the PCD-inducing potential of staurosporine in *Blastocystis* was investigated and the staurosporine-induced apoptotic signaling pathway was analyzed. The results demonstrated that the protein kinase inhibitor staurosporine can induce an apoptotic cell death process with several cytoplasmic and nuclear features of mammalian apoptosis, including cell shrinkage, exposure of PS molecules, maintenance of plasma membrane integrity, extensive cytoplasmic vacuolation, nuclear condensation and DNA fragmentation.

Apoptosis in mammalian cells is mediated primarily by the activation of a family of cysteine proteases called caspases which cleave substrates critical for cell survival (Taylor *et al.*, 2008). Another major executionary pathway is through mitochondrial outer membrane permeabilization and subsequent release of cytochrome c and other pro-apoptotic molecules (Kroemer *et al.*, 2007). Using the mitochondrial transition pore blocker cyclosporine A, we showed that mitchondria also play important roles in the execution of apoptosis induced by staurosporine because cyclosporine A could effectively abolish staurosporine-induced PS exposure and DNA fragmentation. In Hela cells, mitochondria were found to have a central role in staurosporine-induced apoptosis and inhibition of the mitochondrial permeability transition prevented apoptosis (Tafani *et al.*, 2001) Mitochondrial dysfunction has also been frenquently observed among protozoan parasites which are induced to undergo apoptosis (Deponte, 2008). The involvement of mitochondria in programmed cell death was suggested to be of very ancient evolutionary origin (Arnoult *et al.*, 2002). However, the pro-apoptotic molecules released by mitochondria in *Blastocystis* may be very different from that of mammalian cells and other protozoan parasites, since this

organism has unusual mitochondria that has been reported to lack cytochromes (Lantsman *et al.*, 2008).

Despite the indispensable role of caspases in mammalian apoptosis, no orthologous sequences have been found in protozoan parasites. Nonetheless, a lot of studies showed caspase-like activity by the cleavage of synthetic peptide substrates during cell death of protozoa, including *Blastocystis* (Nasirudeen *et al.*, 2001a). It was found that caspase-3-like activity was triggered with a cytotoxic antibody and inhibition of the caspase-like molecule by z-VAD.fmk could inhibit the apoptotic features to some extent (Nasirudeen and Tan, 2004, 2005). In contrast to the involvement of caspase-like molecule in the previous studies, the present data suggest that staurosporine-induced apoptosis is independent of caspase-like molecules, as pre-treatment with z-VAD.fmk did not alter the PS exposure or DNA fragmentation induced by staurosporine. However, the general cysteine protease inhibitor IA could reduce the apoptotic responses in a dose-dependent manner, suggesting the involvement of a cysteine protease in the execution of staurosporine-induced apoptosis. As cysteine cathepsins have been suggested to regulate cell death in mammalian cells (Turk and Stoka, 2007), the effect of inhibitors of cathepsins was examined. Three different inhibitors of cathepsins, namely z-FF.fmk (cathepsins B and L), z-FA.fmk (cathepsins B and L) and CA-074-Me (cathepsin B), were used to pre-treat *Blastocystis* cells before exposure to staurosporine; however, Annexin V and TUNEL assays revealed that the cathepsin inhibitors did not have any inhibitory effect on staurosporine-induced apoptosis.

Interestingly, calpain inhibitors z-LLL.fmk and ALLN were shown to enhance staurosporine-induced apoptosis while these potently inhibited calpain protease activity. Calpains are non-lysosomal calcium-dependent cysteine proteases and have been implicated in cell death signaling (Broker *et al.*, 2005). Calpain was reported to facilitate caspase-3 activation by initial cleavage of the pro-enzyme (Blomgren *et al.*, 2001). Cleavage of Bax to its proapoptotic Bax/p18 was found to be mediated by calpain and mediate cytochrome c release and execution of apoptosis (Gao and Dou, 2000). On the other hand, anti-apoptotic roles of calpains have also been suggested. For example, proteolytic cleavage of p53 protected cells from apoptosis induced by DNA damage (Kubbutat and Vousden, 1997). Capn4-/- MEFs lacked calpain activities and were more susceptible to staurosporine- and TNFα-induced apoptosis. The anti-apoptotic function of calpain might be related to activation of the PI3-kinase/Akt survival pathway (Tan *et al.*, 2006). It seems that calpains also play a protective role in staurosporine-mediated apoptosis in *Blastocystis*. Identifying its substrates may help to further dissect signaling networks regulating cell death in *Blastocystis*. It is worth noticing that the pre-treatment with cyclosporin A blocked apoptotic features induced by staurosporine but calpain activity was still up-regulated. Previous studies showed that apoptotic features induced by a cytotoxic antibody in *Blastocystis* could be inhibited by the combined use of z-VAD.fmk and cyclosporine A, but the cells could not be rescued from death, suggesting the existence of alternative cell death pathways in this parasite (Nasirudeen and Tan, 2005). It is likely that despite rescue of staurosporine-induced apoptosis by pre-treatment with cyclosporine A, the cells still die through alternative cell death pathways and thus calpain activity was up-regulated as a survival response.

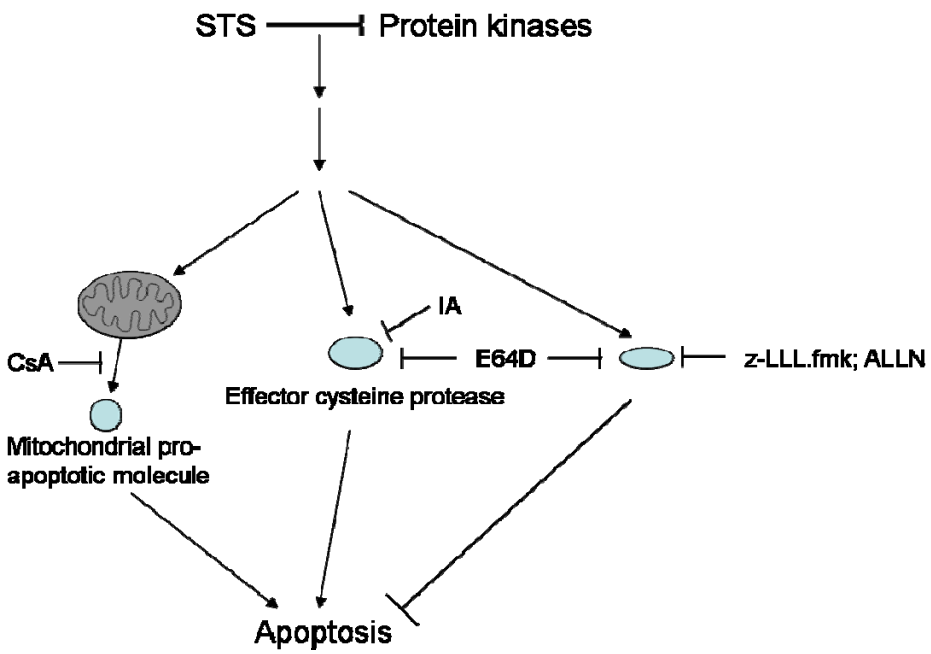

Figure 4.3.1 Proposed model of staurosporine-induced apoptosis in *Blastocystis*.

A model on the mechanism of staurosporine-induced apoptosis was proposed based on the results in this chapter (Figure 4.3.1). In summary, the present study has shown that staurosporine can induce apoptotic features in *Blastocystis*, which is mediated by mitochondria and an as yet unidentified cysteine protease; furthermore, calpain activity is up-regulated to protect the cells from apoptosis induced by staurosporine.

Chapter 5

Conclusion

5.1 Conclusions

1. This study, being the first proteomic study of *Blastocystis*, has established a reliable method for two-dimensional gel electrophoresis and constructed a reference proteome map for this organism.

2. Through proteomic analysis, this study has identified the cellular target of the cytotoxic antibody MAb 1D5 as legumain, with a conserved asparagines-specific cysteine protease C13 family domain. This is the key initial step in elucidating the mechanism of MAb 1D5-induced programmed cell death in *Blastocystis*. The present study is the first to describe the presence of a legumain in *Blastocystis*, a second protozoan legumain besides *T. vaginalis* legumain.

3. While legumains of other organisms are usually found in lysosomal/acidic compartments, this study has demonstrated a cell surface localization of legumain in addition to cytosolic localization. Thus MAb 1D5 can assess the legumain on the cell surface.

4. Inhibition of legumain activity by a legumain specific inhibitor induced apoptosis-like PCD in *Blastocystis*. MAb 1D5 was also found to inhibit legumain activity. Therefore, this study strongly suggests that legumain has a key role in the regulation

of *Blastocystis* PCD and legumain is the first PCD mediator characterized in this organism.

5. By using the autophagic marker monodansylcadaverine (MDC) and autophagic inhibitors 3-methyladenine and wortmannin, this study has shown the existence of autophagy in *Blastocystis* colony culture, or through exposure to MAb 1D5, amino acid starvation and treatment with rapamycin. This is the first report of autophagy in *Blastocystis*.

6. MAb 1D5-induced autophagy was found to up-regulate in the presence of caspase inhibitor and appeared to be mediated through mitochondrial outer membrane permeabilization. Hence this study demonstrated the interplay between apoptosis and autophagy in *Blastocystis*.

7. This study has presented unique features of autophagy in *Blastocystis*. The autophagic compartments was found to have unusually large size and appeared to be deposited into the parasite central vacuole. The central vacuole was postulated to be a repository for autophagic vacuoles.

8. This study showed that *Blastocystis* exhibited apoptotic features in response to a common apoptosis inducer staurosporine. The apoptosis appeared to be mediated by mitochondria and an as yet unidentified cysteine protease, but not caspases or cathepsins B and L. Calpain was found to play a protective role. This study demonstrated that *Blastocystis* PCD has multiple regulators.

5.2 Future studies

This study suggests that the seemingly simple protozoon possesses complex cell death machinery. Further studies are required for more insights into its cell death mechanism. Future studies can be conducted to identify the downstream substrates of legumain and further dissect the signaling network of MAb 1D5-induced PCD. A possible role of legumain in nutrient uptake and autophagy can also be investigated since MAb 1D5 was shown to induce autophagy and legumain in helminths was suggested to be involved in alimentary digestion of host proteins. It can be examined whether staurosporine can trigger autophagy, because mitochodria were found to mediate staurosporine-induced apoptosis as well as MAb 1D5-induced apoptosis and autophagy. Mitochondria may be an important switch between apoptosis and autophagy in *Blastocystis*. When a high quality and annotated genome database becomes available, bioinformatic analysis can be performed to search for the orthologs of proteins involved in apoptosis and autophagy. Proteomic studies of differentially expressed proteins of healthy cells and cells undergoing PCD can also help to identify the potential regulators of PCD. Further research in the mechanism of protozoan PCD may facilitate the development of novel therapeutics targeting novel modulators of the protozoan cell death pathway.

References

Abe, Y., Shirane, K., Yokosawa, H., Matsushita, H., Mitta, M., Kato, I., and Ishii, S. (1993). Asparaginyl endopeptidase of jack bean seeds. Purification, characterization, and high utility in protein sequence analysis. J Biol Chem *268*, 3525-3529.

Abou El Naga, I.F., and Negm, A.Y. (2001). Morphology, histochemistry and infectivity of *Blastocystis hominis* cyst. J Egypt Soc Parasitol *31*, 627-635.

Abraham, M.C., and Shaham, S. (2004). Death without caspases, caspases without death. Trends Cell Biol *14*, 184-193.

Abudugupur, A., Mitsui, K., Yokota, S., and Tsurugi, K. (2002). An ARL1 mutation affected autophagic cell death in yeast, causing a defect in central vacuole formation. Cell Death Differ *9*, 158-168.

Al-Olayan, E.M., Williams, G.T., and Hurd, H. (2002). Apoptosis in the malaria protozoan, *Plasmodium berghei*: a possible mechanism for limiting intensity of infection in the mosquito. Int J Parasitol *32*, 1133-1143.

Alexeieff, A. (1911). Sur la nature des formations dites kystes de *Trichomonas intestinalis*. C R Soc Biol *71*, 296-298.

Alvarez-Fernandez, M., Barrett, A.J., Gerhartz, B., Dando, P.M., Ni, J., and Abrahamson, M. (1999). Inhibition of mammalian legumain by some cystatins is due to a novel second reactive site. J Biol Chem *274*, 19195-19203.

Alvarez, V.E., Kosec, G., Sant Anna, C., Turk, V., Cazzulo, J.J., and Turk, B. (2008). Blocking autophagy to prevent parasite differentiation: a possible new strategy for fighting parasitic infections? Autophagy *4*, 361-363.

Alzate, J.F., Alvarez-Barrientos, A., Gonzalez, V.M., and Jimenez-Ruiz, A. (2006). Heat-induced programmed cell death in *Leishmania infantum* is reverted by Bcl-X(L) expression. Apoptosis *11*, 161-171.

Alzate, J.F., Arias, A.A., Moreno-Mateos, D., Alvarez-Barrientos, A., and Jimenez-Ruiz, A. (2007). Mitochondrial superoxide mediates heat-induced apoptotic-like death in *Leishmania infantum*. Mol Biochem Parasitol *152*, 192-202.

Ameisen, J.C. (2002). On the origin, evolution, and nature of programmed cell death: a timeline of four billion years. Cell Death Differ *9*, 367-393.

Ameisen, J.C., Idziorek, T., Billaut-Mulot, O., Loyens, M., Tissier, J.P., Potentier, A., and Ouaissi, A. (1995). Apoptosis in a unicellular eukaryote (*Trypanosoma cruzi*): implications for the evolutionary origin and role of programmed cell death in the control of cell proliferation, differentiation and survival. Cell Death Differ *2*, 285-300.

Anderson, N.L., and Anderson, N.G. (1998). Proteome and proteomics: new technologies, new concepts, and new words. Electrophoresis *19*, 1853-1861.

Andrade, R.M., Wessendarp, M., Gubbels, M.J., Striepen, B., and Subauste, C.S. (2006). CD40 induces macrophage anti-*Toxoplasma gondii* activity by triggering autophagy-dependent fusion of pathogen-containing vacuoles and lysosomes. J Clin Invest *116*, 2366-2377.

Arisue, N., Hashimoto, T., Yoshikawa, H., Nakamura, Y., Nakamura, G., Nakamura, F., Yano, T.A., and Hasegawa, M. (2002). Phylogenetic position of *Blastocystis hominis* and of stramenopiles inferred from multiple molecular sequence data. J Eukaryot Microbiol *49*, 42-53.

Arnoult, D., Akarid, K., Grodet, A., Petit, P.X., Estaquier, J., and Ameisen, J.C. (2002). On the evolution of programmed cell death: apoptosis of the unicellular eukaryote *Leishmania major* involves cysteine proteinase activation and mitochondrion permeabilization. Cell Death Differ *9*, 65-81.

Arnoult, D., Tatischeff, I., Estaquier, J., Girard, M., Sureau, F., Tissier, J.P., Grodet, A., Dellinger, M., Traincard, F., Kahn, A.*, et al.* (2001). On the evolutionary conservation of the cell death pathway: mitochondrial release of an apoptosis-inducing factor during *Dictyostelium discoideum* cell death. Mol Biol Cell *12*, 3016-3030.

Arrington, D.D., Van Vleet, T.R., and Schnellmann, R.G. (2006). Calpain 10: a mitochondrial calpain and its role in calcium-induced mitochondrial dysfunction. Am J Physiol Cell Physiol *291*, C1159-1171.

Asgian, J.L., James, K.E., Li, Z.Z., Carter, W., Barrett, A.J., Mikolajczyk, J., Salvesen, G.S., and Powers, J.C. (2002). Aza-peptide epoxides: a new class of inhibitors selective for clan CD cysteine proteases. J Med Chem *45*, 4958-4960.

Avron, B., Stolarsky, T., Chayen, A., and Mirelman, D. (1986). Encystation of *Entamoeba invadens* IP-1 is induced by lowering the osmotic pressure and depletion of nutrients from the medium. J Protozool *33*, 522-525.

Baehrecke, E.H. (2005). Autophagy: Dual roles in life and death? Nat Rev Mol Cell Biol *6*, 505-510.

Bampton, E.T., Goemans, C.G., Niranjan, D., Mizushima, N., and Tolkovsky, A.M. (2005). The dynamics of autophagy visualized in live cells: from autophagosome formation to fusion with endo/lysosomes. Autophagy *1*, 23-36.

Barquilla, A., Crespo, J. L., and Navarro, M. (2008). Rapamycin inhibits trypanosome cell growth by preventing TOR complex 2 formation. Proc Natl Acad Sci U S A *105*, 14579–14584.

Barrett, J., Brophy, P.M., and Hamilton, J.V. (2005). Analysing proteomic data. Int J Parasitol *35*, 543-553.

Barry, M., Heibein, J.A., Pinkoski, M.J., Lee, S.F., Moyer, R.W., Green, D.R., and Bleackley, R.C. (2000). Granzyme B short-circuits the need for caspase 8 activity during granule-mediated cytotoxic T-lymphocyte killing by directly cleaving bid. Mol Biol Cell *20*, 3781-3794.

Beck, H., Schwarz, G., Schroter, C.J., Deeg, M., Baier, D., Stevanovic, S., Weber, E., Driessen, C., and Kalbacher, H. (2001). Cathepsin S and an asparagine-specific endoprotease dominate the proteolytic processing of human myelin basic protein in vitro. Eur J Immunol *31*, 3726-3736.

Bera, A., Singh, S., Nagaraj, R., and Vaidya, T. (2003). Induction of autophagic cell death in *Leishmania donovani* by antimicrobial peptides. Mol Biochem Parasitol *127*, 23-35.

Berry, D.L., and Baehrecke, E.H. (2007). Growth arrest and autophagy are required for salivary gland cell degradation in Drosophila. Cell *131*, 1137-1148.

Berry, D.L., and Baehrecke, E.H. (2008). Autophagy functions in programmed cell death. Autophagy *4*, 359-360.

Bidere, N., Lorenzo, H.K., Carmona, S., Laforge, M., Harper, F., Dumont, C., and Senik, A. (2003). Cathepsin D triggers bax activation, resulting in selective apoptosis-inducing factor (AIF) relocation in T lymphocytes entering the early commitment phase to apoptosis. J Biol Chem *278*, 31401-31411.

Biederbick, A., Kern, H.F., and Elsasser, H.P. (1995). Monodansylcadaverine (MDC) is a specific in vivo marker for autophagic vacuoles. Eur J Cell Biol *66*, 3-14.

Blomgren, K., Zhu, C.L., Wang, X.Y., Karlsson, J.O., Leverin, A.L., Bahr, B.A., Mallard, C., and Hagberg, H. (2001). Synergistic activation of caspase-3 by m-calpain after neonatal hypoxia-ischemia - A mechanism of "pathological apoptosis"? J Biol Chem *276*, 10191-10198.

Blommaart, E.F., Krause, U., Schellens, J.P., Vreeling-Sindelarova, H., and Meijer, A.J. (1997). The phosphatidylinositol 3-kinase inhibitors wortmannin and LY294002 inhibit autophagy in isolated rat hepatocytes. Eur J Biochem *243*, 240-246.

Boreham, P.F., and Stenzel, D.J. (1993). *Blastocystis* in humans and animals: morphology, biology, and epizootiology. Adv Parasitol *32*, 1-70.

Breeuwer, P., Drocourt, J.L., Bunschoten, N., Zwietering, M.H., Rombouts, F.M., and Abee, T. (1995). Characterization of uptake and hydrolysis of fluorescein diacetate and carboxyfluorescein diacetate by intracellular esterases in *Saccharomyces cerevisiae*, which result in accumulation of fluorescent product. Appl Environ Microbiol *61*, 1614-1619.

Broker, L.E., Huisman, C., Span, S.W., Rodriguez, J.A., Kruyt, F.A., and Giaccone, G. (2004). Cathepsin B mediates caspase-independent cell death induced by microtubule stabilizing agents in non-small cell lung cancer cells. Cancer Res *64*, 27-30.

Broker, L.E., Kruyt, F.A.E., and Giaccone, G. (2005). Cell death independent of caspases: A review. Clin Cancer Res *11*, 3155-3162.

Bruchhaus, I., Roeder, T., Rennenberg, A., and Heussler, V.T. (2007). Protozoan parasites: programmed cell death as a mechanism of parasitism. Trends Parasitol *23*, 376-383.

Brumpt, E. (1912). *Blastocystis hominis* n sp. et formes voisines. Bull Soc Pathol Exot *5*, 725-730.

Bursch, W., Hochegger, K., Torok, L., Marian, B., Ellinger, A., and Hermann, R.S. (2000). Autophagic and apoptotic types of programmed cell death exhibit different fates of cytoskeletal filaments. J Cell Sci *113*, 1189-1198.

Buttner, S., Eisenberg, T., Herker, E., Carmona-Gutierrez, D., Kroemer, G., and Madeo, F. (2006). Why yeast cells can undergo apoptosis: death in times of peace, love, and war. J Cell Biol *175*, 521-525.

Cande, C., Cecconi, F., Dessen, P., and Kroemer, G. (2002). Apoptosis-inducing factor (AIF): key to the conserved caspase-independent pathways of cell death? J Cell Sci *115*, 4727-4734.

Chen, J.M., Dando, P.M., Rawlings, N.D., Brown, M.A., Young, N.E., Stevens, R.A., Hewitt, E., Watts, C., and Barrett, A.J. (1997). Cloning, isolation, and characterization of mammalian legumain, an asparaginyl endopeptidase. J Biol Chem *272*, 8090-8098.

Chen, J.M., Fortunato, M., and Barrett, A.J. (2000). Activation of human prolegumain by cleavage at a C-terminal asparagine residue. Biochem J *352 Pt 2*, 327-334.

Chen, J.M., Fortunato, M., Stevens, R.A., and Barrett, A.J. (2001). Activation of progelatinase A by mammalian legumain, a recently discovered cysteine proteinase. Biol Chem *382*, 777-783.

Chen, J.M., Rawlings, N.D., Stevens, R.A., and Barrett, A.J. (1998). Identification of the active site of legumain links it to caspases, clostripain and gingipains in a new clan of cysteine endopeptidases. FEBS Lett *441*, 361-365.

Chose, O., Noel, C., Gerbod, D., Brenner, C., Viscogliosi, E., and Roseto, A. (2002). A form of cell death with some features resembling apoptosis in the amitochondrial unicellular organism *Trichomonas vaginalis*. Exp Cell Res *276*, 32-39.

Chose, O., Sarde, C.O., Noel, C., Gerbod, D., Jimenez, J.C., Brenner, C., Capron, M., Viscogliosi, E., and Roseto, A. (2003). Cell death in protists without mitochondria. Ann N Y Acad Sci *1010*, 121-125.

Christensen, S.T., Chemnitz, J., Straarup, E.M., Kristiansen, K., Wheatley, D.N., and Rasmussen, L. (1998). Staurosporine-induced cell death in *Tetrahymena thermophila* has mixed characteristics of both apoptotic and autophagic degeneration. Cell Biol Int *22*, 591-598.

Cirioni, O., Giacometti, A., Drenaggi, D., Ancarani, F., and Scalise, G. (1999). Prevalence and clinical relevance of *Blastocystis hominis* in diverse patient cohorts. Eur J Epidemiol *15*, 389-393.

Clark, C.G. (1997). Extensive genetic diversity in *Blastocystis hominis*. Mol Biochem Parasitol *87*, 79-83.

Clarke, P.G. (1990). Developmental cell death: morphological diversity and multiple mechanisms. Anat Embryol (Berl) *181*, 195-213.

Claveau, D., Riendeau, D., and Mancini, J.A. (2000). Expression, maturation, and rhodamine-based fluorescence assay of human cathepsin K expressed in CHO cells. Biochem Pharmacol *60*, 759-769.

Collins, J.A., Schandi, C.A., Young, K.K., Vesely, J., and Willingham, M.C. (1997). Major DNA fragmentation is a late event in apoptosis. J Histochem Cytochem *45*, 923-934.

Cornillon, S., Foa, C., Davoust, J., Buonavista, N., Gross, J.D., and Golstein, P. (1994). Programmed cell death in *Dictyostelium*. J Cell Sci *107 (Pt 10)*, 2691-2704.

Croft, S.L., Sundar, S., and Fairlamb, A.H. (2006). Drug resistance in leishmaniasis. Clin Microbiol Rev *19*, 111-126.

Dalton, J.P., Hola-Jamriska, L., and Brindley, P.J. (1995). Asparaginyl endopeptidase activity in adult *Schistosoma mansoni*. Parasitology *111 (Pt 5)*, 575-580.

Das, M., Mukherjee, S.B., and Shaha, C. (2001). Hydrogen peroxide induces apoptosis-like death in *Leishmania donovani* promastigotes. J Cell Sci *114*, 2461-2469.

Debrabant, A., Lee, N., Bertholet, S., Duncan, R., and Nakhasi, H.L. (2003). Programmed cell death in trypanosomatids and other unicellular organisms. Int J Parasitol *33*, 257-267.

Deponte, M. (2008). Programmed cell death in protists. Biochimica Et Biophysica Acta-Molecular Cell Research *1783*, 1396-1405.

Deponte, M., and Becker, K. (2004). *Plasmodium falciparum* - do killers commit suicide? Trends Parasitol *20*, 165-169.

DosReis, G.A., and Barcinski, M.A. (2001). Apoptosis and parasitism: from the parasite to the host immune response. Adv Parasitol *49*, 133-161.

Dunn, L.A., Boreham, P.F., and Stenzel, D.J. (1989a). Ultrastructural variation of *Blastocystis hominis* stocks in culture. Int J Parasitol *19*, 43-56.

Dunn, L.A., Boreham, P.F.L., and Stenzel, D.J. (1989b). Ultrastructural variation of *Blastocystis hominis* stocks in culture. Int J Parasitol *19*, 43-56.

Edinger, A.L., and Thompson, C.B. (2004). Death by design: apoptosis, necrosis and autophagy. Curr Opin Cell Biol *16*, 663-669.

Eskelinen, E.L. (2005). Doctor Jekyll and Mister Hyde: autophagy can promote both cell survival and cell death. Cell Death Differ *12 Suppl 2*, 1468-1472.

Festjens, N., Vanden Berghe, T., and Vandenabeele, P. (2006). Necrosis, a well-orchestrated form of cell demise: signalling cascades, important mediators and concomitant immune response. Biochim Biophys Acta *1757*, 1371-1387.

Fidock, D.A., Eastman, R.T., Ward, S.A., and Meshnick, S.R. (2008). Recent highlights in antimalarial drug resistance and chemotherapy research. Trends Parasitol *24*, 537-544.

Figarella, K., Rawer, M., Uzcategui, N.L., Kubata, B.K., Lauber, K., Madeo, F., Wesselborg, S., and Duszenko, M. (2005). Prostaglandin D2 induces programmed cell death in *Trypanosoma brucei* bloodstream form. Cell Death Differ *12*, 335-346.

Figarella, K., Uzcategui, N.L., Beck, A., Schoenfeld, C., Kubata, B.K., Lang, F., and Duszenko, M. (2006). Prostaglandin-induced programmed cell death in *Trypanosoma brucei* involves oxidative stress. Cell Death Differ *13*, 1802-1814.

Foghsgaard, L., Wissing, D., Mauch, D., Lademann, U., Bastholm, L., Boes, M., Elling, F., Leist, M., and Jaattela, M. (2001). Cathepsin B acts as a dominant execution protease in tumor cell apoptosis induced by tumor necrosis factor. J Cell Biol *153*, 999-1010.

Frohlich, K.U., Fussi, H., and Ruckenstuhl, C. (2007). Yeast apoptosis--from genes to pathways. Semin Cancer Biol *17*, 112-121.

Galluzzi, L., Vicencio, J.M., Kepp, O., Tasdemir, E., Maiuri, M.C., and Kroemer, G. (2008). To die or not to die: that is the autophagic question. Curr Mol Med *8*, 78-91.

Gao, G., and Dou, Q.P. (2000). N-terminal cleavage of Bax by calpain generates a potent proapoptotic 18-kDa fragment that promotes Bcl-2-independent cytochrome c release and apoptotic cell death. J Cell Biochem *80*, 53-72.

Gelboin, H.V., and Krausz, K. (2006). Monoclonal antibodies and multifunctional cytochrome P450: drug metabolism as paradigm. J Clin Pharmacol *46*, 353-372.

Gorg, A., Weiss, W., and Dunn, M.J. (2004). Current two-dimensional electrophoresis technology for proteomics. Proteomics *4*, 3665-3685.

Gozuacik, D., and Kimchi, A. (2004). Autophagy as a cell death and tumor suppressor mechanism. Oncogene *23*, 2891-2906.

Gutierrez, M.G., Master, S.S., Singh, S.B., Taylor, G.A., Colombo, M.I., and Deretic, V. (2004). Autophagy is a defense mechanism inhibiting BCG and *Mycobacterium tuberculosis* survival in infected macrophages. Cell *119*, 753-766.

Hatsugai, N., Kuroyanagi, M., Nishimura, M., and Hara-Nishimura, I. (2006). A cellular suicide strategy of plants: vacuole-mediated cell death. Apoptosis *11*, 905-911.

Hatsugai, N., Kuroyanagi, M., Yamada, K., Meshi, T., Tsuda, S., Kondo, M., Nishimura, M., and Hara-Nishimura, I. (2004). A plant vacuolar protease, VPE, mediates virus-induced hypersensitive cell death. Science *305*, 855-858.

Haughwout, F.G. (1918). The tissue-invasive powers of the flagellated and ciliated protozoa with especial reference to *Trichomonas intesitialis*. A critical review. Philipp J Sci *8*, 217-258.

Hegde, R., Srinivasula, S.M., Zhang, Z.J., Wassell, R., Mukattash, R., Cilenti, L., DuBois, G., Lazebnik, Y., Zervos, A.S., Fernandes-Alnemri, T.*, et al.* (2002). Identification of Omi/HtrA-2 as a mitochondrial apoptotic serine protease that disrupts inhibitor of apoptosis protein-caspase interaction. J Biol Chem *277*, 432-438.

Heinrich, M., Neumeyer, J., Jakob, M., Hallas, C., Tchikov, V., Winoto-Morbach, S., Wickel, M., Schneider-Brachert, W., Trauzold, A., Hethke, A.*, et al.* (2004). Cathepsin D links TNF-induced acid sphingomyelinase to Bid-mediated caspase-9 and -3 activation. Cell Death Differ *11*, 550-563.

Henson, P.M., Bratton, D.L., and Fadok, V.A. (2001). Apoptotic cell removal. Curr Biol *11*, R795-R805.

Henzel, W.J., Billeci, T.M., Stults, J.T., Wong, S.C., Grimley, C., and Watanabe, C. (1993). Identifying proteins from two-dimensional gels by molecular mass searching of peptide fragments in protein sequence databases. Proc Natl Acad Sci U S A *90*, 5011-5015.

Ho, L.C., Armiugam, A., Jeyaseelan, K., Yap, E.H., and Singh, M. (2000). *Blastocystis* elongation factor-1alpha: genomic organization, taxonomy and phylogenetic relationships. Parasitology *121 (Pt 2)*, 135-144.

Ho, L.C., Singh, M., Suresh, G., Ng, G.C., and Yap, E.H. (1993). Axenic culture of *Blastocystis hominis* in Iscove's modified Dulbecco's medium. Parasitol Res *79*, 614-616.

Hoevers, J.D., and Snowden, K.F. (2005). Analysis of the ITS region and partial ssu and lsu rRNA genes of *Blastocystis* and *Proteromonas lacertae*. Parasitology *131*, 187-196.

Irigoin, F., Inada, N.M., Fernandes, M.P., Piacenza, L., Gadelha, F.R., Vercesi, A.E., and Radi, R. (2009). Mitochondrial calcium overload triggers complement-dependent superoxide-mediated programmed cell death in *Trypanosoma cruzi*. Biochem J *418*, 595-604.

Ishii, S. (1994). Legumain: asparaginyl endopeptidase. Methods Enzymol *244*, 604-615.

Johnson, A.M., Thanou, A., Boreham, P.F., and Baverstock, P.R. (1989). *Blastocystis hominis*: phylogenetic affinities determined by rRNA sequence comparison. Exp Parasitol *68*, 283-288.

Johnson, D.E. (2000). Noncaspase proteases in apoptosis. Leukemia *14*, 1695-1703.

Ju, J.W., Joo, H.N., Lee, M.R., Cho, S.H., Cheun, H.I., Kim, J.Y., Lee, Y.H., Lee, K.J., Sohn, W.M., Kim, D.M., *et al.* (2009). Identification of a serodiagnostic antigen, legumain, by immunoproteomic analysis of excretory-secretory products of *Clonorchis sinensis* adult worms. Proteomics *9*, 3066-3078.

Jungblut, P., Thiede, B., Zimny-Arndt, U., Muller, E.C., Scheler, C., Wittmann-Liebold, B., and Otto, A. (1996). Resolution power of two-dimensional electrophoresis and identification of proteins from gels. Electrophoresis *17*, 839-847.

Kamada, Y., Funakoshi, T., Shintani, T., Nagano, K., Ohsumi, M., and Ohsumi, Y. (2000). Tor-mediated induction of autophagy via an Apg1 protein kinase complex. J Cell Biol *150*, 1507-1513.

Kanki, T., Wang, K., Cao, Y., Baba, M., Klionsky, D.J., Okamoto, K., Kondo-Okamoto, N., and Ohsumi, Y. (2009). Atg32 is a mitochondrial protein that confers selectivity during mitophagy. Dev Cell *17*, 98-109.

Keenan, T.W., Huang, C.M., and Zierdt, C.H. (1992). Comparative analysis of lipid composition in axenic strains of *Blastocystis hominis*. Comp Biochem Physiol B *102*, 611-615.

Kerr, J.F., Wyllie, A.H., and Currie, A.R. (1972). Apoptosis: a basic biological phenomenon with wide-ranging implications in tissue kinetics. Br J Cancer *26*, 239-257.

Klionsky, D.J. (2007). Autophagy: from phenomenology to molecular understanding in less than a decade. Nat Rev Mol Cell Biol *8*, 931-937.

Klionsky, D.J., Abeliovich, H., Agostinis, P., Agrawal, D.K., Aliev, G., Askew, D.S., Baba, M., Baehrecke, E.H., Bahr, B.A., Ballabio, A.*, et al.* (2008). Guidelines for the use and interpretation of assays for monitoring autophagy in higher eukaryotes. Autophagy *4*, 151-175.

Klionsky, D.J., Cregg, J.M., Dunn, W.A., Jr., Emr, S.D., Sakai, Y., Sandoval, I.V., Sibirny, A., Subramani, S., Thumm, M., Veenhuis, M.*, et al.* (2003). A unified nomenclature for yeast autophagy-related genes. Dev Cell *5*, 539-545.

Klionsky, D.J., and Emr, S.D. (2000). Autophagy as a Regulated Pathway of Cellular Degradation. Science *290*, 1717-1721.

Kobayashi, T., and Endoh, H. (2005). A possible role of mitochondria in the apoptotic-like programmed nuclear death of Tetrahymena thermophila. Febs Journal *272*, 5378-5387.

Kosta, A., Roisin-Bouffay, C., Luciani, M.F., Otto, G.P., Kessin, R.H., and Golstein, P. (2004). Autophagy gene disruption reveals a non-vacuolar cell death pathway in *Dictyostelium*. J Biol Chem *279*, 48404-48409.

Kourtis, N., and Tavernarakis, N. (2009). Autophagy and cell death in model organisms. Cell Death Differ *16*, 21-30.

Kroemer, G., El-Deiry, W., Golstein, P., Peter, M.E., Vaux, D., Vandenabeele, P., Zhivotovsky, B., Blagosklonny, M.V., Malorni, W., Knight, R.A., *et al.* (2005). Classification of cell death: recommendations of the Nomenclature Committee on Cell Death. Cell Death and Differ *12*, 1463-1467.

Kroemer, G., Galluzzi, L., and Brenner, C. (2007). Mitochondrial membrane permeabilization in cell death. Physiol Rev *87*, 99-163.

Kroemer, G., and Levine, B. (2008). Autophagic cell death: the story of a misnomer. Nat Rev Mol Cell Biol *9*, 1004-1010.

Kroemer, G., and Martin, S.J. (2005). Caspase-independent cell death. Nat Med *11*, 725-730.

Kroemer, G., and Reed, J.C. (2000). Mitochondrial control of cell death. Nat Med *6*, 513-519.

Kubbutat, M.H., and Vousden, K.H. (1997). Proteolytic cleavage of human p53 by calpain: a potential regulator of protein stability. Mol Cell Biol *17*, 460-468.

Kuma, A., Hatano, M., Matsui, M., Yamamoto, A., Nakaya, H., Yoshimori, T., Ohsumi, Y., Tokuhisa, T., and Mizushima, N. (2004). The role of autophagy during the early neonatal starvation period. Nature *432*, 1032-1036.

Kuroyanagi, M., Yamada, K., Hatsugai, N., Kondo, M., Nishimura, M., and Hara-Nishimura, I. (2005). Vacuolar processing enzyme is essential for mycotoxin-induced cell death in Arabidopsis thaliana. J Biol Chem *280*, 32914-32920.

Kuster, B., Mortensen, P., Andersen, J.S., and Mann, M. (2001). Mass spectrometry allows direct identification of proteins in large genomes. Proteomics *1*, 641-650.

Lam, E. (2005). Vacuolar proteases livening up programmed cell death. Trends Cell Biol *15*, 124-127.

Lantsman, Y., Tan, K.S., Morada, M., and Yarlett, N. (2008). Biochemical characterization of a mitochondrial-like organelle from *Blastocystis* sp. subtype 7. Microbiology *154*, 2757-2766.

Leder, K., Hellard, M.E., Sinclair, M.I., Fairley, C.K., and Wolfe, R. (2005). No correlation between clinical symptoms and *Blastocystis hominis* in immunocompetent individuals. J Gastroenterol Hepatol *20*, 1390-1394.

Lee, C.Y., and Baehrecke, E.H. (2001). Steroid regulation of autophagic programmed cell death during development. Development *128*, 1443-1455.

Lee, N., Bertholet, S., Debrabant, A., Muller, J., Duncan, R., and Nakhasi, H.L. (2002). Programmed cell death in the unicellular protozoan parasite *Leishmania*. Cell Death and Differ *9*, 53-64.

Leist, M., and Jaattela, M. (2001). Four deaths and a funeral: From caspases to alternative mechanisms. Nat Rev Mol Cell Biol *2*, 589-598.

Lenardo, M., Chan, F.K.M., Hornung, F., McFarland, H., Siegel, R., Wang, J., and Zheng, L.X. (1999). Mature T lymphocyte apoptosis - Immune regulation in a dynamic and unpredictable antigenic environment. Annu Rev Immunol *17*, 221-253.

Leon-Felix, J., Ortega-Lopez, J., Orozco-Solis, R., and Arroyo, R. (2004). Two novel asparaginyl endopeptidase-like cysteine proteinases from the protist *Trichomonas vaginalis*: their evolutionary relationship within the clan CD cysteine proteinases. Gene *335*, 25-35.

Levine, B., and Klionsky, D.J. (2004a). Development by Self-Digestion: Molecular Mechanisms and Biological Functions of Autophagy. Developmental Cell *6*, 463-477.

Levine, B., and Klionsky, D.J. (2004b). Development by self-digestion: Molecular mechanisms and biological functions of autophagy. Dev Cell *6*, 463-477.

Levine, B., and Yuan, J.Y. (2005). Autophagy in cell death: an innocent convict? J Clin Invest *115*, 2679-2688.

Li, D.N., Matthews, S.P., Antoniou, A.N., Mazzeo, D., and Watts, C. (2003). Multistep autoactivation of asparaginyl endopeptidase in vitro and in vivo. J Biol Chem *278*, 38980-38990.

Li, L.Y., Luo, L., and Wang, X.D. (2001). Endonuclease G is an apoptotic DNase when released from mitochondria. Nature *412*, 95-99.

Liu, C., Sun, C., Huang, H., Janda, K., and Edgington, T. (2003). Overexpression of legumain in tumors is significant for invasion/metastasis and a candidate enzymatic target for prodrug therapy. Cancer Res *63*, 2957-2964.

Lord, S.J., Rajotte, R.V., Korbutt, G.S., and Bleackley, R.C. (2003). Granzyme B: a natural born killer. Immunol Rev *193*, 31-38.

Lorenzo, H.K., and Susin, S.A. (2004). Mitochondrial effectors in caspase-independent cell death. FEBS Lett *557*, 14-20.

Lujan, H.D., Mowatt, M.R., Byrd, L.G., and Nash, T.E. (1996). Cholesterol starvation induces differentiation of the intestinal parasite *Giardia lamblia*. Proc Natl Acad Sci U S A *93*, 7628-7633.

Lum, J.J., Bauer, D.E., Kong, M., Harris, M.H., Li, C., Lindsten, T., and Thompson, C.B. (2005a). Growth factor regulation of autophagy and cell survival in the absence of apoptosis. Cell *120*, 237-248.

Lum, J.J., DeBerardinis, R.J., and Thompson, C.B. (2005b). Autophagy in metazoans: cell survival in the land of plenty. Nat Rev Mol Cell Biol *6*, 439-448.

Madeo, F., Frohlich, E., and Frohlich, K.-U. (1997). A Yeast Mutant Showing Diagnostic Markers of Early and Late Apoptosis. J Cell Biol *139*, 729-734.

Madeo, F., Herker, E., Maldener, C., Wissing, S., Lachelt, S., Herian, M., Fehr, M., Lauber, K., Sigrist, S.J., Wesselborg, S., *et al.* (2002). A caspase-related protease regulates apoptosis in yeast. Mol Cell *9*, 911-917.

Maehr, R., Hang, H.C., Mintern, J.D., Kim, Y.M., Cuvillier, A., Nishimura, M., Yamada, K., Shirahama-Noda, K., Hara-Nishimura, I., and Ploegh, H.L. (2005). Asparagine endopeptidase is not essential for class II MHC antigen presentation but is required for processing of cathepsin L in mice. J Immunol *174*, 7066-7074.

Maeno, E., Ishizaki, Y., Kanaseki, T., Hazama, A., and Okada, Y. (2000). Normotonic cell shrinkage because of disordered volume regulation is an early prerequisite to apoptosis. Proc Natl Acad Sci U S A *97*, 9487-9492.

Maiuri, M.C., Zalckvar, E., Kimchi, A., and Kroemer, G. (2007). Self-eating and self-killing: crosstalk between autophagy and apoptosis. Nat Rev Mol Cell Biol *8*, 741-752.

Manoury, B., Hewitt, E.W., Morrice, N., Dando, P.M., Barrett, A.J., and Watts, C. (1998). An asparaginyl endopeptidase processes a microbial antigen for class II MHC presentation. Nature *396*, 695-699.

Mariante, R.M., Vancini, R.G., and Benchimol, M. (2006). Cell death in trichomonads: new insights. Histochem Cell Biol *125*, 545-556.

Martin, S.J., Amarante-Mendes, G.P., Shi, L., Chuang, T.H., Casiano, C.A., O'Brien, G.A., Fitzgerald, P., Tan, E.M., Bokoch, G.M., Greenberg, A.H., *et al.* (1996). The cytotoxic cell protease granzyme B initiates apoptosis in a cell-free system by proteolytic processing and activation of the ICE/CED-3 family protease, CPP32, via a novel two-step mechanism. EMBO J *15*, 2407-2416.

Mathiasen, I.S., Sergeev, I.N., Bastholm, L., Elling, F., Norman, A.W., and Jaattela, M. (2002). Calcium and calpain as key mediators of apoptosis-like death induced by vitamin D compounds in breast cancer cells. J Biol Chem *277*, 30738-30745.

McClure, H.M., Strobert, E.A., and Healy, G.R. (1980). *Blastocystis hominis* in a pig-tailed macaque: a potential enteric pathogen for nonhuman primates. Lab Anim Sci *30*, 890-894.

McDonald, M.C., Mota-Filipe, H., Paul, A., Cuzzocrea, S., Abdelrahman, M., Harwood, S., Plevin, R., Chatterjee, P.K., Yaqoob, M.M., and Thiemermann, C. (2001). Calpain inhibitor I reduces the activation of nuclear factor-kappaB and organ injury/dysfunction in hemorrhagic shock. Faseb J *15*, 171-186.

Mehlhorn, H. (1988). *Blastocystis hominis*, Brumpt 1912: are there different stages or species? Parasitol Res *74*, 393-395.

Meijer, A.J., and Codogno, P. (2004). Regulation and role of autophagy in mammalian cells. Int J Biochem Cell Biol *36*, 2445-2462.

Meslin, B., Barnadas, C., Boni, V., Latour, C., De Monbrison, F., Kaiser, K., and Picot, S. (2007). Features of apoptosis in *Plasmodium falciparum* erythrocytic stage

through a putative role of PfMCA1 metacaspase-like protein. J Infect Dis *195*, 1852-1859.

Mizushima, N. (2004). Methods for monitoring autophagy. Int J Biochem Cell Biol *36*, 2491-2502.

Moe, K.T., Singh, M., Howe, J., Ho, L.C., Tan, S.W., Chen, X.Q., Ng, G.C., and Yap, E.H. (1997). Experimental *Blastocystis hominis* infection in laboratory mice. Parasitol Res *83*, 319-325.

Munafo, D.B., and Colombo, M.I. (2001). A novel assay to study autophagy: regulation of autophagosome vacuole size by amino acid deprivation. J Cell Sci *114*, 3619-3629.

Muntz, K., and Shutov, A.D. (2002). Legumains and their functions in plants. Trends Plant Sci *7*, 340-344.

Nagata, S. (1999). Fas ligand-induced apoptosis. Annu Rev Genet *33*, 29-55.

Nakagawa, I., Amano, A., Mizushima, N., Yamamoto, A., Yamaguchi, H., Kamimoto, T., Nara, A., Funao, J., Nakata, M., Tsuda, K.*, et al.* (2004). Autophagy defends cells against invading group A *Streptococcus*. Science *306*, 1037-1040.

Nakagawa, T., and Yuan, J.Y. (2000). Cross-talk between two cysteine protease families: Activation of caspase-12 by calpain in apoptosis. J Cell Biol *150*, 887-894.

Nakamura, Y., Hashimoto, T., Yoshikawa, H., Kamaishi, T., Nakamura, F., Okamoto, K., and Hasegawa, M. (1996). Phylogenetic position of *Blastocystis hominis* that contains cytochrome-free mitochondria, inferred from the protein phylogeny of elongation factor 1 alpha. Mol Biochem Parasitol *77*, 241-245.

Nasirudeen, A.M., Hian, Y.E., Singh, M., and Tan, K.S. (2004). Metronidazole induces programmed cell death in the protozoan parasite *Blastocystis hominis*. Microbiology *150*, 33-43.

Nasirudeen, A.M., Singh, M., Yap, E.H., and Tan, K.S. (2001a). *Blastocystis hominis*: evidence for caspase-3-like activity in cells undergoing programmed cell death. Parasitol Res *87*, 559-565.

Nasirudeen, A.M., and Tan, K.S. (2004). Caspase-3-like protease influences but is not essential for DNA fragmentation in *Blastocystis* undergoing apoptosis. Eur J Cell Biol *83*, 477-482.

Nasirudeen, A.M., and Tan, K.S. (2005). Programmed cell death in *Blastocystis hominis* occurs independently of caspase and mitochondrial pathways. Biochimie *87*, 489-497.

Nasirudeen, A.M.A., Tan, K.S.W., Singh, M., and Yap, E.H. (2001b). Programmed cell death in a human intestinal parasite, *Blastocystis hominis*. Parasitology *123*, 235-246.

Nicholson, D.W. (1999). Caspase structure, proteolytic substrates, and function during apoptotic cell death. Cell Death and Differ *6*, 1028-1042.

Niemann, A., Baltes, J., and Elsasser, H.-P. (2001). Fluorescence Properties and Staining Behavior of Monodansylpentane, a Structural Homologue of the Lysosomotropic Agent Monodansylcadaverine. J Histochem Cytochem *49*, 177-186.

Niemann, A., Takatsuki, A., and Elsasser, H.-P. (2000). The Lysosomotropic Agent Monodansylcadaverine Also Acts as a Solvent Polarity Probe. J Histochem Cytochem *48*, 251-258.

Nigro, L., Larocca, L., Massarelli, L., Patamia, I., Minniti, S., Palermo, F., and Cacopardo, B. (2003). A placebo-controlled treatment trial of *Blastocystis hominis* infection with metronidazole. J Travel Med *10*, 128-130.

Nyakeriga, A.M., Perlmann, H., Hagstedt, M., Berzins, K., Troye-Blomberg, M., Zhivotovsky, B., Perlmann, P., and Grandien, A. (2006). Drug-induced death of the asexual blood stages of *Plasmodium falciparum* occurs without typical signs of apoptosis. Microbes Infect *8*, 1560-1568.

O'Brien, E.A., Koski, L.B., Zhang, Y., Yang, L., Wang, E., Gray, M.W., Burger, G., and Lang, B.F. (2007). TBestDB: a taxonomically broad database of expressed sequence tags (ESTs). Nucleic Acids Res *35*, D445-451.

O'Farrell, P.H. (1975). High resolution two-dimensional electrophoresis of proteins. J Biol Chem *250*, 4007-4021.

Okada, H., and Mak, T.W. (2004). Pathways of apoptotic and non-apoptotic death in tumour cells. Nature Rev Cancer *4*, 592-603.

Okamoto, K., Kondo-Okamoto, N., and Ohsumi, Y. (2009). Mitochondria-anchored receptor Atg32 mediates degradation of mitochondria via selective autophagy. Dev Cell *17*, 87-97.

Oliver, E.M., Skuce, P.J., McNair, C.M., and Knox, D.P. (2006). Identification and characterization of an asparaginyl proteinase (legumain) from the parasitic nematode, *Haemonchus contortus*. Parasitology *133*, 237-244.

Pakandl, M. (1999). *Blastocystis* sp. from pigs: ultrastructural changes occurring during polyxenic cultivation in Iscove's modified Dulbecco's medium. Parasitol Res *85*, 743-748.

Pegelow, K., Gross, R., Pietrzik, K., Lukito, W., Richards, A.L., and Fryauff, D.J. (1997). Parasitological and nutritional situation of school children in the Sukaraja district, West Java, Indonesia. Southeast Asian J Trop Med Public Health *28*, 173-190.

Peter, M.E., and Krammer, P.H. (1998). Mechanisms of CD95 (APO-1/Fas)-mediated apoptosis. Curr Opin Immunol *10*, 545-551.

Petiot, A., Ogier-Denis, E., Blommaart, E.F.C., Meijer, A.J., and Codogno, P. (2000). Distinct Classes of Phosphatidylinositol 3'-Kinases Are Involved in Signaling Pathways That Control Macroautophagy in HT-29 Cells. J Biol Chem *275*, 992-998.

Piacenza, L., Irigoin, F., Alvarez, M.N., Peluffo, G., Taylor, M.C., Kelly, J.M., Wilkinson, S.R., and Radi, R. (2007). Mitochondrial superoxide radicals mediate programmed cell death in *Trypanosoma cruzi*: cytoprotective action of mitochondrial iron superoxide dismutase overexpression. Biochem J *403*, 323-334.

Piacenza, L., Peluffo, G., and Radi, R. (2001). L-arginine-dependent suppression of apoptosis in *Trypanosoma cruzi*: contribution of the nitric oxide and polyamine pathways. Proc Natl Acad Sci U S A *98*, 7301-7306.

Picazarri, K., Nakada-Tsukui, K., and Nozaki, T. (2008). Autophagy during proliferation and encystation in the protozoan parasite *Entamoeba invadens*. Infect Immun *76*, 278-288.

Picot, S., Burnod, J., Bracchi, V., Chumpitazi, B.F., and Ambroise-Thomas, P. (1997). Apoptosis related to chloroquine sensitivity of the human malaria parasite *Plasmodium falciparum*. Trans R Soc Trop Med Hyg *91*, 590-591.

Porn-Ares, M.I., Samali, A., and Orrenius, S. (1998). Cleavage of the calpain inhibitor, calpastatin, during apoptosis. Cell Death and Differ *5*, 1028-1033.

Porter, H., Gamette, M.J., Cortes-Hernandez, D.G., and Jensen, J.B. (2008). Asexual blood stages of *Plasmodium falciparum* exhibit signs of secondary necrosis, but not classical apoptosis after exposure to febrile temperature (40 C). J Parasitol *94*, 473-480.

Puthia, M.K., Lu, J., and Tan, K.S. (2008). *Blastocystis ratti* contains cysteine proteases that mediate interleukin-8 response from human intestinal epithelial cells in an NF-kappaB-dependent manner. Eukaryot Cell *7*, 435-443.

Puthia, M.K., Sio, S.W., Lu, J., and Tan, K.S. (2006). *Blastocystis ratti* induces contact-independent apoptosis, F-actin rearrangement, and barrier function disruption in IEC-6 cells. Infect Immun *74*, 4114-4123.

Puthia, M.K., Vaithilingam, A., Lu, J., and Tan, K.S. (2005). Degradation of human secretory immunoglobulin A by *Blastocystis*. Parasitol Res *97*, 386-389.

Rabilloud, T. (2009). Membrane proteins and proteomics: love is possible, but so difficult. Electrophoresis *30 Suppl 1*, S174-180.

Rajah Salim, H., Suresh Kumar, G., Vellayan, S., Mak, J.W., Khairul Anuar, A., Init, I., Vennila, G.D., Saminathan, R., and Ramakrishnan, K. (1999). *Blastocystis* in animal handlers. Parasitol Res *85*, 1032-1033.

Ridgley, E.L., Xiong, Z.H., and Ruben, L. (1999). Reactive oxygen species activate a Ca2+-dependent cell death pathway in the unicellular organism *Trypanosoma brucei brucei*. Biochem J *340 (Pt 1)*, 33-40.

Roberts, L.R., Adjei, P.N., and Gores, G.J. (1999). Cathepsins as effector proteases in hepatocyte apoptosis. Cell Biochem Biophys *30*, 71-88.

Roberts, L.R., Kurosawa, H., Bronk, S.F., Fesmier, P.J., Agellon, L.B., Leung, W.Y., Mao, F., and Gores, G.J. (1997). Cathepsin B contributes to bile salt-induced apoptosis of rat hepatocytes. Gastroenterology *113*, 1714-1726.

Rossignol, J.F., Kabil, S.M., Said, M., Samir, H., and Younis, A.M. (2005). Effect of nitazoxanide in persistent diarrhea and enteritis associated with *Blastocystis hominis*. Clin Gastroenterol Hepatol *3*, 987-991.

Rotari, V.I., Dando, P.M., and Barrett, A.J. (2001). Legumain forms from plants and animals differ in their specificity. Biol Chem *382*, 953-959.

Sajid, M., and McKerrow, J.H. (2002). Cysteine proteases of parasitic organisms. Mol Biochem Parasitol *120*, 1-21.

Sajid, M., McKerrow, J.H., Hansell, E., Mathieu, M.A., Lucas, K.D., Hsieh, I., Greenbaum, D., Bogyo, M., Salter, J.P., Lim, K.C., *et al.* (2003). Functional expression and characterization of *Schistosoma mansoni* cathepsin B and its trans-activation by an endogenous asparaginyl endopeptidase. Mol Biochem Parasitol *131*, 65-75.

Salvesen, G.S., and Dixit, V.M. (1999). Caspase activation: the induced-proximity model. Proc Natl Acad Sci U S A *96*, 10964-10967.

Savill, J., Dransfield, I., Gregory, C., and Haslett, C. (2002). A blast from the past: Clearance of apoptotic cells regulates immune responses. Nat Rev Immunol *2*, 965-975.

Schweichel, J.U., and Merker, H.J. (1973). The morphology of various types of cell death in prenatal tissues. Teratology *7*, 253-266.

Sen, N., Das, B.B., Ganguly, A., Mukherjee, T., Bandyopadhyay, S., and Majumder, H.K. (2004). Camptothecin-induced imbalance in intracellular cation homeostasis regulates programmed cell death in unicellular hemoflagellate *Leishmania donovani*. J Biol Chem *279*, 52366-52375.

Shaw, M.M., and Riederer, B.M. (2003). Sample preparation for two-dimensional gel electrophoresis. Proteomics *3*, 1408-1417.

Shimizu, S., Kanaseki, T., Mizushima, N., Mizuta, T., Arakawa-Kobayashi, S., Thompson, C.B., and Tsujimoto, Y. (2004). Role of Bcl-2 family proteins in a non-apoptotic programmed cell death dependent on autophagy genes. Nat Cell Biol *6*, 1221-1228.

Shintani, T., and Klionsky, D.J. (2004). Autophagy in Health and Disease: A Double-Edged Sword. Science *306*, 990-995.

Shirahama-Noda, K., Yamamoto, A., Sugihara, K., Hashimoto, N., Asano, M., Nishimura, M., and Hara-Nishimura, I. (2003). Biosynthetic processing of cathepsins and lysosomal degradation are abolished in asparaginyl endopeptidase-deficient mice. J Biol Chem *278*, 33194-33199.

Shlim, D.R., Hoge, C.W., Rajah, R., Rabold, J.G., and Echeverria, P. (1995). Is *Blastocystis hominis* a cause of diarrhea in travelers? A prospective controlled study in Nepal. Clin Infect Dis *21*, 97-101.

Silberman, J.D., Sogin, M.L., Leipe, D.D., and Clark, C.G. (1996). Human parasite finds taxonomic home. Nature *380*, 398.

Singh, M., Suresh, K., Ho, L.C., Ng, G.C., and Yap, E.H. (1995). Elucidation of the life cycle of the intestinal protozoan *Blastocystis hominis*. Parasitol Res *81*, 446-450.

Stensvold, C.R., Suresh, G.K., Tan, K.S., Thompson, R.C., Traub, R.J., Viscogliosi, E., Yoshikawa, H., and Clark, C.G. (2007a). Terminology for *Blastocystis* subtypes--a consensus. Trends Parasitol *23*, 93-96.

Stensvold, C.R., Traub, R.J., von Samson-Himmelstjerna, G., Jespersgaard, C., Nielsen, H.V., and Thompson, R.C. (2007b). *Blastocystis*: subtyping isolates using pyrosequencing technology. Exp Parasitol *116*, 111-119.

Stenzel, D.J., and Boreham, P.F. (1991). A cyst-like stage of *Blastocystis hominis*. Int J Parasitol *21*, 613-615.

Stenzel, D.J., and Boreham, P.F. (1996). *Blastocystis hominis* revisited. Clin Microbiol Rev *9*, 563-584.

Stoka, V., Turk, B., Schendel, S.L., Kim, T.H., Cirman, T., Snipas, S.J., Ellerby, L.M., Bredesen, D., Freeze, H., Abrahamson, M., *et al.* (2001). Lysosomal protease pathways to apoptosis - Cleavage of Bid, not pro-caspases, is the most likely route. J Biol Chem *276*, 3149-3157.

Stoka, V., Turk, V., and Turk, B. (2007). Lysosomal cysteine cathepsins: signaling pathways in apoptosis. Biol Chem *388*, 555-560.

Suresh, K., Mak, J.W., Chuong, L.S., Ragunathan, T., and Init, I. (1997). Sac-like pouches in *Blastocystis* from the house lizard *Cosymbotus platyurus*. Parasitol Res *83*, 523-525.

Susin, S.A., Lorenzo, H.K., Zamzami, N., Marzo, I., Snow, B.E., Brothers, G.M., Mangion, J., Jacotot, E., Costantini, P., Loeffler, M., *et al.* (1999). Molecular characterization of mitochondrial apoptosis-inducing factor. Nature *397*, 441-446.

Suzuki, Y., Imai, Y., Nakayama, H., Takahashi, K., Takio, K., and Takahashi, R. (2001). A serine protease, HtrA2, is released from the mitochondria and interacts with XIAP, inducing cell death. Mol Cell *8*, 613-621.

Tafani, M., Minchenko, D.A., Serroni, A., and Farber, J.L. (2001). Induction of the mitochondrial permeability transition mediates the killing of HeLa cells by staurosporine. Cancer Res *61*, 2459-2466.

Takatsuka, C., Inoue, Y., Matsuoka, K., and Moriyasu, Y. (2004). 3-methyladenine inhibits autophagy in tobacco culture cells under sucrose starvation conditions. Plant Cell Physiol *45*, 265-274.

Takeshige, K., Baba, M., Tsuboi, S., Noda, T., and Ohsumi, Y. (1992). Autophagy in yeast demonstrated with proteinase-deficient mutants and conditions for its induction. J Cell Biol *119*, 301-311.

Tan, K.S. (2004). *Blastocystis* in humans and animals: new insights using modern methodologies. Vet Parasitol *126*, 121-144.

Tan, K.S. (2008). New insights on classification, identification, and clinical relevance of *Blastocystis* spp. Clin Microbiol Rev *21*, 639-665.

Tan, K.S., Howe, J., Yap, E.H., and Singh, M. (2001a). Do *Blastocystis hominis* colony forms undergo programmed cell death? Parasitol Res *87*, 362-367.

Tan, K.S., Ibrahim, M., Ng, G.C., Nasirudeen, A.M., Ho, L.C., Yap, E.H., and Singh, M. (2001b). Exposure of *Blastocystis* species to a cytotoxic monoclonal antibody. Parasitol Res *87*, 534-538.

Tan, K.S., and Nasirudeen, A.M. (2005). Protozoan programmed cell death--insights from *Blastocystis* deathstyles. Trends Parasitol *21*, 547-550.

Tan, K.S., Singh, M., and Yap, E.H. (2002). Recent advances in *Blastocystis hominis* research: hot spots in terra incognita. Int J Parasitol *32*, 789-804.

Tan, K.S.W. (2007). *Blastocystis*. In Emerging Protozoan Pathogens, N. Khan, ed. (Taylor and Francis, Oxford, UK).

Tan, S.W., Ho, L.C., Moe, K.T., Chen, X.Q., Ng, G.C., Yap, E.H., and Singh, M. (1996a). Production and characterization of murine monoclonal antibodies to *Blastocystis hominis*. Int J Parasitol *26*, 375-381.

Tan, S.W., Singh, M., Ho, L.C., Howe, J., Moe, K.T., Chen, X.Q., Ng, G.C., and Yap, E.H. (1997). Survival of *Blastocystis hominis* clones after exposure to a cytotoxic monoclonal antibody. Int J Parasitol *27*, 947-954.

Tan, S.W., Singh, M., Thong, K.T., Ho, L.C., Moe, K.T., Chen, X.Q., Ng, G.C., and Yap, E.H. (1996b). Clonal growth of *Blastocystis hominis* in soft agar with sodium thioglycollate. Parasitol Res *82*, 737-739.

Tan, T.C., and Suresh, K.G. (2007). Evidence of plasmotomy in *Blastocystis hominis*. Parasitol Res *101*, 1521-1525.

Tan, Y., Wu, C., De Veyra, T., and Greer, P.A. (2006). Ubiquitous Calpains Promote Both Apoptosis and Survival Signals in Response to Different Cell Death Stimuli. J Biol Chem *281*, 17689-17698.

Taylor, R.C., Cullen, S.P., and Martin, S.J. (2008). Apoptosis: controlled demolition at the cellular level. Nat Rev Mol Cell Biol *9*, 231-241.

Totino, P.R.R., Daniel-Ribeiro, C.T., Corte-Real, S., and Ferreira-da-Cruz, M.D. (2008). *Plasmodium falciparum*: Erythrocytic stages die by autophagic-like cell death under drug pressure. Exp Parasitol *118*, 478-486.

Tresse, E., Kosta, A., Luciani, M.F., and Golstein, P. (2007). From autophagic to necrotic cell death in *Dictyostelium*. Semin Cancer Biol *17*, 94-100.

Tsujimoto, Y., and Shimizu, S. (2005). Another way to die: autophagic programmed cell death. Cell Death Differ *12 Suppl 2*, 1528-1534.

Tsukada, M., and Ohsumi, Y. (1993). Isolation and characterization of autophagy-defective mutants of *Saccharomyces cerevisiae*. FEBS Lett *333*, 169-174.

Turk, B., and Stoka, V. (2007). Protease signalling in cell death: caspases versus cysteine cathepsins. FEBS Lett *581*, 2761-2767.

Turk, B., Turk, D., and Turk, V. (2000). Lysosomal cysteine proteases: more than scavengers. Biochim Biophys Acta *1477*, 98-111.

Ullman, E., Fan, Y., Stawowczyk, M., Chen, H.M., Yue, Z., and Zong, W.X. (2008). Autophagy promotes necrosis in apoptosis-deficient cells in response to ER stress. Cell Death Differ *15*, 422-425.

van Gurp, M., Festjens, N., van Loo, G., Saelens, X., and Vandenabeele, P. (2003). Mitochondrial intermembrane proteins in cell death. Biochem Biophys Res Commun *304*, 487-497.

van Loo, G., Schotte, P., van Gurp, M., Demol, H., Hoorelbeke, B., Gevaert, K., Rodriguez, I., Ruiz-Carrillo, A., Vandekerckhove, J., Declercq, W.*, et al.* (2001). Endonuclease G: a mitochondrial protein released in apoptosis and involved in caspase-independent DNA degradation. Cell Death and Differ *8*, 1136-1142.

Vandenabeele, P., Vanden Berghe, T., and Festjens, N. (2006). Caspase inhibitors promote alternative cell death pathways. Sci STKE *2006*, pe44.

Vardi, A., Berman-Frank, I., Rozenberg, T., Hadas, O., Kaplan, A., and Levine, A. (1999). Programmed cell death of the dinoflagellate *Peridinium gatunense* is mediated by CO(2) limitation and oxidative stress. Curr Biol *9*, 1061-1064.

Vaux, D.L., Haecker, G., and Strasser, A. (1994). An evolutionary perspective on apoptosis. Cell *76*, 777-779.

Wajant, H. (2002). The Fas signaling pathway: More than a paradigm. Science *296*, 1635-1636.

Walderich, B., Bernauer, S., Renner, M., Knobloch, J., and Burchard, G.D. (1998). Cytopathic effects of *Blastocystis hominis* on Chinese hamster ovary (CHO) and adeno carcinoma HT29 cell cultures. Trop Med Int Health *3*, 385-390.

Walker, E.H., Pacold, M.E., Perisic, O., Stephens, L., Hawkins, P.T., Wymann, M.P., and Williams, R.L. (2000). Structural determinants of phosphoinositide 3-kinase inhibition by wortmannin, LY294002, quercetin, myricetin, and staurosporine. Mol Cell *6*, 909-919.

Wang, K.K.W. (2000). Calpain and caspase: can you tell the difference? Trends in Neurosciences *23*, 20-26.

Wang, L.C. (2004). Changing patterns in intestinal parasitic infections among Southeast Asian laborers in Taiwan. Parasitol Res *92*, 18-21.

Waterhouse, N.J., Finucane, D.N., Green, D.R., Elce, J.S., Kumar, S., Alnemri, E.S., Litwack, G., Khanna, K.K., Lavin, M.F., and Watters, D.J. (1998). Calpain activation is upstream of caspases in radiation-induced apoptosis. Cell Death and Differ *5*, 1051-1061.

Weil, M., Jacobson, M.D., Coles, H.S., Davies, T.J., Gardner, R.L., Raff, K.D., and Raff, M.C. (1996). Constitutive expression of the machinery for programmed cell death. J Cell Biol *133*, 1053-1059.

Weiss, W., and Gorg, A. (2008). Sample solublization buffers for two-dimensional electrophoresis. Methods Mol Biol *424*, 35-42.

Welburn, S.C., Dale, C., Ellis, D., Beecroft, R., and Pearson, T.W. (1996). Apoptosis in procyclic *Trypanosoma brucei rhodesiense* in vitro. Cell Death and Differ *3*, 229-236.

Welburn, S.C., and Murphy, N.B. (1998). Prohibitin and RACK homologues are up-regulated in trypanosomes induced to undergo apoptosis and in naturally occurring terminally differentiated forms. Cell Death Differ *5*, 615-622.

Wood, D.E., and Newcomb, E.W. (1999). Caspase-dependent activation of calpain during drug-induced apoptosis. J Biol Chem *274*, 8309-8315.

Wullschleger, S., Loewith, R., and Hall, M.N. (2006). TOR Signaling in Growth and Metabolism. Cell *124*, 471-484.

Xie, Z., and Klionsky, D.J. (2007). Autophagosome formation: core machinery and adaptations. Nat Cell Biol *9*, 1102-1109.

Yin, X.M. (2000). Signal transduction mediated by Bid, a pro-death Bcl-2 family proteins, connects the death receptor and mitochondria apoptosis pathways. Cell Res *10*, 161-167.

Yorimitsu, T., and Klionsky, D.J. (2005). Autophagy: molecular machinery for self-eating. Cell Death Differ *12 Suppl 2*, 1542-1552.

Yoshikawa, H., Kuwayama, N., and Enose, Y. (1995a). Histochemical detection of carbohydrates of *Blastocystis hominis*. J Eukaryot Microbiol *42*, 70-74.

Yoshikawa, H., Satoh, J., Enose, Y., Keenan, T.W., Huang, C.M., and Zierdt, C.H. (1995b). Light and electron microscopic localization of lipids in *Blastocystis hominis*. Comparative analysis of lipid composition in axenic strains of *Blastocystis hominis*. J Electron Microsc (Tokyo) *44*, 100-103.

Yu, L., Alva, A., Su, H., Dutt, P., Freundt, E., Welsh, S., Baehrecke, E.H., and Lenardo, M.J. (2004). Regulation of an ATG7-beclin 1 program of autophagic cell death by caspase-8. Science *304*, 1500-1502.

Yuan, J., Lipinski, M., and Degterev, A. (2003). Diversity in the mechanisms of neuronal cell death. Neuron *40*, 401-413.

Yuan, J.Y., and Yankner, B.A. (2000). Apoptosis in the nervous system. Nature *407*, 802-809.

Zaman, V. (1998). The differential identification of *Blastocystis hominis* cysts. Ann Trop Med Parasitol *92*, 233-235.

Zaman, V., Howe, J., and Ng, M. (1995). A comparative morphology of *Blastocystis hominis* cysts with and without the "fibrillar layer". Southeast Asian J Trop Med Public Health *26*, 801-802.

Zangger, H., Mottram, J.C., and Fasel, N. (2002). Cell death in *Leishmania* induced by stress and differentiation: programmed cell death or necrosis? Cell Death and Differ *9*, 1126-1139.

Zhang, X., Qiao, J.Y., Zhou, X.J., Yao, F.R., and Wei, Z.C. (2007). Morphology and reproductive mode of *Blastocystis hominis* in diarrhea and in vitro. Parasitol Res *101*, 43-51.

Zhang, X.D., Gillespie, S.K., and Hersey, P. (2004). Staurosporine induces apoptosis of melanoma by both caspase-dependent and -independent apoptotic pathways. Mol Cancer Ther *3*, 187-197.

Zierdt, C.H. (1973). Studies of *Blastocystis hominis*. J Protozool *20*, 114-121.

Zierdt, C.H. (1991a). *Blastocystis hominis*--past and future. Clin Microbiol Rev *4*, 61-79.

Zierdt, C.H. (1991b). Pathogenicity of *Blastocystis hominis*. J Clin Microbiol *29*, 662-663.

Zierdt, C.H., Donnolley, C.T., Muller, J., and Constantopoulos, G. (1988). Biochemical and ultrastructural study of *Blastocystis hominis*. J Clin Microbiol *26*, 965-970.

Zierdt, C.H., Rude, W.S., and Bull, B.S. (1967). Protozoan characteristics of *Blastocystis hominis*. Am J Clin Pathol *48*, 495-501.

Zierdt, C.H., and Williams, R.L. (1974). *Blastocystis hominis*: axenic cultivation. Exp Parasitol *36*, 233-243.

Zong, W.X., and Thompson, C.B. (2006). Necrotic death as a cell fate. Genes Dev *20*, 1-15.

Appendices

Appendix I Bioinformatic analysis of Contig 1466 from *Blastocystis* draft genome

GENSCANW output for sequence Contig1466

GENSCAN 1.0 Date run: 6-Jun-109 Time: 08:15:49

Sequence Contig1466 : 5798 bp : 44.77% C+G : Isochore 2 (43 - 51 C+G%)

Parameter matrix: Arabidopsis.smat

Predicted genes/exons:

Gn.Ex	Type	S	.Begin	...End	.Len	Fr	Ph	I/Ac	Do/T	CodRg	P....	Tscr..
1.01	Init	+	87	218	132	2	0	81	61	126	0.269	14.36
1.02	Intr	+	358	493	136	0	1	-18	14	64	0.040	-6.46
1.03	Term	+	1265	2031	767	0	2	19	37	1468	0.146	133.38
1.04	PlyA	+	2071	2076	6							-3.64
2.05	PlyA	-	2101	2096	6							1.05
2.04	Term	-	2397	2149	249	0	0	-27	42	136	0.529	-1.80
2.03	Intr	-	2618	2430	189	2	0	18	3	273	0.620	16.58
2.02	Intr	-	3249	3159	91	2	1	55	51	136	0.724	11.60
2.01	Init	-	4563	3401	1163	0	2	31	46	1722	0.815	160.46
2.00	Prom	-	4644	4605	40							-8.86
3.00	Prom	+	4859	4898	40							-10.35
3.01	Init	+	5123	5788	666	1	0	74	1	990	0.934	89.13

Predicted peptide sequence(s):

Predicted coding sequence(s):

>Contig1466|GENSCAN_predicted_peptide_1|344_aa
MVCISLVAYFVPFFEDILSVVGNFSDVITTFMFPAVMHLWVFRKNRESSPFEIHTQSFRF
DHNLTKEKHRTDPFERFPEDNQDLNRYSCSKSQKKVSKKGKGKKVIDTMAKKEWYDVRAP
NQFLVRDVCKTLVSRTSGLKIASEGLKGRIFEANLGDLSKNEEQGYRKIKLRVEDVQGDK
CITLFYGMDITRDKLGSLIKKWKTLIECNVEVSTTDGYKLRLFCIAFTRKQDNQNKKTCY
AQASQIHRIRAKMVEIITDEVSKCDLATLVPKLYMESIGARIQKECNKIYPLENTLIRKV
KMIKSPKIDTVKLMEQHADVVKKEEEGVKVEETVAPMAGSGGRL

>Contig1466|GENSCAN_predicted_CDS_1|1035_bp
atggtgtgcatctcgctggtcgcttatttcgtgcccttctttgaggatattctgagcgtc
gtcggaaacttcagcgatgtcattaccacgtttatgttcccggcggtgatgcatttgtgg
gtgtttaggaagaatagggaatcttctccattcgaaattcacacacaatcttttcgattt
gatcataatttgacaaaagaaaagcaccgtactgacccttcgagcgattccctgaggac

aaccaagatttaaatcgatattcttgcagcaagtctcagaagaaagtcagtaagaaagga
aagggaaagaaggtgattgataccatggctaagaaggagtggtacgacgtgcgtgccccg
aaccagttcctggtgcgtgatgtttgcaagacgctggtgtctcgtacttcgggattgaaa
atcgcttcggagggtctgaagggacgtattttcgaggccaatctgggtgatctgagcaag
aacgaggagcagggttaccgcaagatcaagctgcgagtggaggacgtgcagggagataag
tgcatcaccctcttctacggaatggacatcacccgcgacaagctgggttctctgatcaag
aagtggaagactctgatcgagtgcaacgtggaggtgtctaccaccgacggttacaagctg
cgtctgttctgcatcgcgttcacccgcaagcaggacaaccagaacaagaagacttgctac
gcgcaggcctctcagatccaccgcattcgtgcgaagatggtggagatcatcacggacgag
gtgtcgaagtgcgatcttgcgacgctggttccgaagctgtacatggagtcgatcggtgct
cgcattcagaaggagtgcaacaagatctatcctctggagaacacgctgatccgcaaggtg
aagatgatcaagtcgcccaagatcgatacggtgaagctgatggagcagcacgccgatgtc
gtgaagaaggaggaagagggcgtgaaggtggaggagactgtggctcccatggctggatcg
ggaggtcgtctataa

>Contig1466|GENSCAN_predicted_peptide_2|563_aa
MKFVSIALLRVLALAAADNWAVLVAGSDGFWNYRHQADVAHAYQIMRRGGIPADHIVTMM
YNDVASSSFNPFPGELYNHPGDESPDVYKGVVVDYEGEDVTPENFMKVLLGDESTGKKVL
KTNENDNIFMFFSDHGGPNVLCFPNGDLSKDDFQATLKKMHEQKKYKHFVLYIEACYSGS
MGVGFPEDLGISIVTAANDSESSWGWYCGEEAVVKGKDIGSCLGDEFSVFWMEDTDKGEQ
RTETLNEQWKRIHDGVTKSHASRYGDVSFESDLIGEYVGYPEEKFNYDHQSSVAWDSRDA
KFLFLLYKYQHTTGSEKAKWEKLYLEEMSLRQQIDRYINSFAKESKLYSARVSGEINMEC
YMAGIEQMVAIFGHNDYQYKYYNVLANMASLRRSISKNTLEDDVLRTSTLRQSDIEKEFL
EYCSRFCEIVVFTASKQEYADRMLDFLDPEKKFIKHRLFRESCTKIGKVYVKDLNRLGRD
LRRTVIIDNSIVSFGYHLDNGIPICSWFDNWKDQEVGFLVGIECSYTTRLASCTLYKQCK
TFVPILLICLDSVKPSIASFVNE

>Contig1466|GENSCAN_predicted_CDS_2|1692_bp
atgaaatttgtgagtatcgccttacttagagttttggctcttgctgctgctgataactgg
gccgtgcttgttgccggttctgatggtttctggaactacagacaccaggctgatgttgcc
cacgcgtatcagatcatgagacgcggaggaattcctgctgatcacattgtgacgatgatg
tacaacgatgttgcttcttcttctttcaatcctttccctggtgagctttacaaccaccct
ggtgacgaatctcctgatgtgtacaagggagtggtcgttgattacgagggagaggatgtg
acccctgagaacttcatgaaggtgctgcttggagacgagtccactggaaagaaggtcctg
aagaccaacgagaacgataacattttcatgttcttctctgaccacggtggcccgaacgtg
ctttgcttccctaacggagatctgtctaaggatgacttccaggctactctgaagaagatg
cacgagcagaagaagtacaagcacttcgtgctgtacattgaggcttgctactctggttcc
atgggtgttggtttccctgaagatttgggcatcagcattgtcaccgctgccaacgactct
gagtccagctggggctggtactgtggagaagaggccgttgtgaagggaaaggacattggt
agctgccttggtgatgagttctccgtgttctggatggaggatactgacaagggcgagcag
agaaccgagactctgaacgagcagtggaagcgcattcacgacggtgtgaccaagagccac
gcttctcgctacggagatgtctccttcgagagcgatctgattggtgagtatgtgggctac
cccgaggagaagttcaactacgaccaccagagctctgttgcctgggattctcgtgatgcc
aagttcctcttccttctgtacaagtatcagcacactactggaagcgagaaggcgaagtgg
gagaagctctatcttgaggagatgagccttcgtcagcagattgatcgctacatcaactcg
tttgctaaggagagcaagctctactctgctagagttagcggtgagatcaatatggagtgc
tacatggctggtattgagcagatggtggctatcttcggtcacaatgattaccagtacaag
tactacaacgtgctggctaacatggctagtttacgaaggtcgatatccaagaatacactt
gaggacgatgttcttcgaacaagcaccttgagacaaagcgacattgaaaaggagtttcta
gagtattgctcccggttttgtgaaatcgtggtcttcacagcatcgaaacaggagtatgcg
gatcgtatgctggacttttggatccggagaagaaattcatcaagcatcgcctgttccgc
gaaagttgtaccaaaatagggaaggtctacgtgaaagatttaaatcgtttgggtcgagat
ttgagacgaactgtgattatcgataactcgatcgtgtcctttggatatcatttagataat
ggaattccgatttgctcatggtttgacaactggaaggatcaagaagtggggtttctagta
ggaatcgagtgtagctatacaacgcggctcgcatcatgtactctttacaagcagtgcaag
acgttcgtccctatattactaatatgtttagactccgtgaaaccatcgattgcttcattt
gtgaatgaataa

>Contig1466|GENSCAN_predicted_peptide_3|222_aa
MHYSMLIQGSPTNGSFTWVNPYKYKNPYITSMTVLFHPNGSMFNNVDTTNVVTNSNDEKV

TIPAGYYTISEIIALLNMMTDTTFSISTNASSFGCIWIQSPHTIDFTDAPDIREILGFDG
RTVILPTSFSGSNVIDITRNRQVIQVYSTIVRSSDLKIANQNNNLLTTMIIDDPTADYVR
SVEDVRIPMITRFDQLMFVFRDMDGKMMRLNGEFELQLTIDD

>Contig1466|GENSCAN_predicted_CDS_3|666_bp
atgcactactccatgcttattcaaggctcacctaccaacggctcatttacatgggttaat
ccgtacaagtacaagaatccctatatcacttccatgactgtgttgtttcatcctaatggt
tcgatgttcaacaacgtagacacgaccaatgtggttactaacagcaatgacgagaaggta
acgatccctgctggttattacacgatcagtgagatcattgccttgctcaatatgatgacc
gatactacattttccatatcgacgaatgcctcgtcgttcggctgtatctggattcagtct
ccacacaccattgatttcacagatgcacctgacattcgtgagatcctcggcttcgatgga
cgaacggtcattctacctacttcgttcagtggatcgaacgtgattgatatcacgcgaaat
cgacaagtgattcaggtctactcgacgatcgtgcgatcatcggacctgaagattgccaac
cagaacaacaacctgctcaccacgatgatcattgacgatccaacggctgactacgtgcga
agtgtggaagacgtgcgtataccaatgatcactcggtttgatcaattgatgttcgtgttc
cgcgatatggatggcaagatgatgcgactgaacggcgaattcgaactccagttgacgatt
gatgac

Explanation

Gn.Ex : gene number, exon number (for reference)
Type : Init = Initial exon (ATG to 5' splice site)
Intr = Internal exon (3' splice site to 5' splice site)
Term = Terminal exon (3' splice site to stop codon)
Sngl = Single-exon gene (ATG to stop)
Prom = Promoter (TATA box / initation site)
PlyA = poly-A signal (consensus: AATAAA)
S : DNA strand (+ = input strand; - = opposite strand)
Begin : beginning of exon or signal (numbered on input strand)
End : end point of exon or signal (numbered on input strand)
Len : length of exon or signal (bp)
Fr : reading frame (a forward strand codon ending at x has frame x mod 3)
Ph : net phase of exon (exon length modulo 3)
I/Ac : initiation signal or 3' splice site score (tenth bit units)
Do/T : 5' splice site or termination signal score (tenth bit units)
CodRg : coding region score (tenth bit units)
P : probability of exon (sum over all parses containing exon)
Tscr : exon score (depends on length, I/Ac, Do/T and CodRg scores)

Comments

The SCORE of a predicted feature (e.g., exon or splice site) is a log-odds measure of the quality of the feature based on local sequence properties. For example, a predicted 5' splice site with score > 100 is strong; 50-100 is moderate; 0-50 is weak; and below 0 is poor (more than likely not a real donor site).

The PROBABILITY of a predicted exon is the estimated probability under GENSCAN's model of genomic sequence structure that the exon is correct.
This probability depends in general on global as well as local sequence properties, e.g., it depends on how well the exon fits with neighboring exons. It has been shown that predicted exons with higher probabilities are more likely to be correct than those with lower probabilities.

Conserved domain searches of Contig1466|GENSCAN_predicted_peptide_2

List of domain hits

Description	PssmId	Multi-dom	E-value
cl02159, Peptidase_C13, Peptidase C13 family	121134	N/A	5e-98

Peptidase C13 family The best-scoring hit on this query sequence is by member pfam01650:

CD Length: 258 **Bit Score:** 353.52 **E-value:** 5e-98

```
                  10        20        30        40        50        60        70        80
               ....*....|....*....|....*....|....*....|....*....|....*....|....*....|....*....|
25185      19 NWAVLVAGSDGFWNYRHQADVAHAYQIMRRGGIPADHIVTMMYNDVASSSFNPFPGELYNHPgdESPDVYKGVVVDYEGE 98
pfam01650   1 LWAVLVAGSNGYYNYRHQADVCHAYQLLKKFGIKDENIIVMMYDDIANNPENPFPGKIFNKP--NGTDVYKGVPIDYTGN 78
                  90        100       110       120       130       140       150       160
               ....*....|....*....|....*....|....*....|....*....|....*....|....*....|....*....|
25185      99 DVTPENFMKVLLGDEST---GKKVLKTNENDNIFMFFSDHGGPNVLCFPNGD-LSKDDFQATLKKMHEQKKYKHFVLYIE 174
pfam01650  79 DVTPRNFLAVLLGDKSAlkgSGKVLKSGPNDNVFIYFTDHGAPGVLGFPELDyLYAKDLAEALKKMHARGKYKKLVFYVE 158
                  170       180       190       200       210       220       230       240
               ....*....|....*....|....*....|....*....|....*....|....*....|....*....|....*....|
25185     175 ACYSGSMGVGFPEDLGISIVTAANDSESSWGWYCGEEAvvkgkdIGSCLGDEFSVFWMEDTDKGEQRTETLNEQWKRIHD 254
pfam01650 159 ACESGSMFEGLPKDINIYATTAANADESSWGTYCPDPE------DGTCLGDLFSVNWMEDSDDHDLSKETLEQQFELVKN 232
                  250       260
               ....*....|....*....|....*
25185     255 GVTKSHASRYGDVSFESDLIGEYVG 279
pfam01650 233 RTTGSHVMQYGDKSIPQLPVSLFQG 257
```

cl02680, NIF, NLI interacting factor-like phosphatase	141620	N/A	2e-31

NLI interacting factor-like phosphatase The best-scoring hit on this query sequence is by member TIGR02251:

CD Length: 162 **Bit Score:** 132.42 **E-value:** 2e-31

```
                  10        20        30        40        50        60        70        80
               ....*....|....*....|....*....|....*....|....*....|....*....|....*....|....*....|
25185     418 EFLEYCSRFCEIVVFTASKQEYADRMLDFLDPEKKFIKHRLFRESCTKIGKVYVKDLNRLGRDLRRTVIIDNSIVSFGYH 497
TIGR02251  49 EFLERVSKWYELVIFTASLEEYADPVLDILDRGGKVISRRLYRESCVFTNGKYVKDLSLVGKDLSKVIIIDNSPYSYSLQ 128
                  90
               ....*....|....*...
25185     498 LDNGIPICSWFDNWKDQE 515
TIGR02251 129 PDNAIPIKSWFGDPNDTE 146
```

Blast search parameters	
Options:	**Database:** CDD **Low complexity filter:** yes **E-value threshold:** 0.010 **Max. hits:** 100
Data Source:	Live blast search **RID =** 2MSPFVE101R
System:	**Search creator:** newblast **Software:** blastp 2.2.20+ **Service:** rpsblast

Appendix II Multiple sequence alignment of legumain sequences from *Blastocystis* and other species

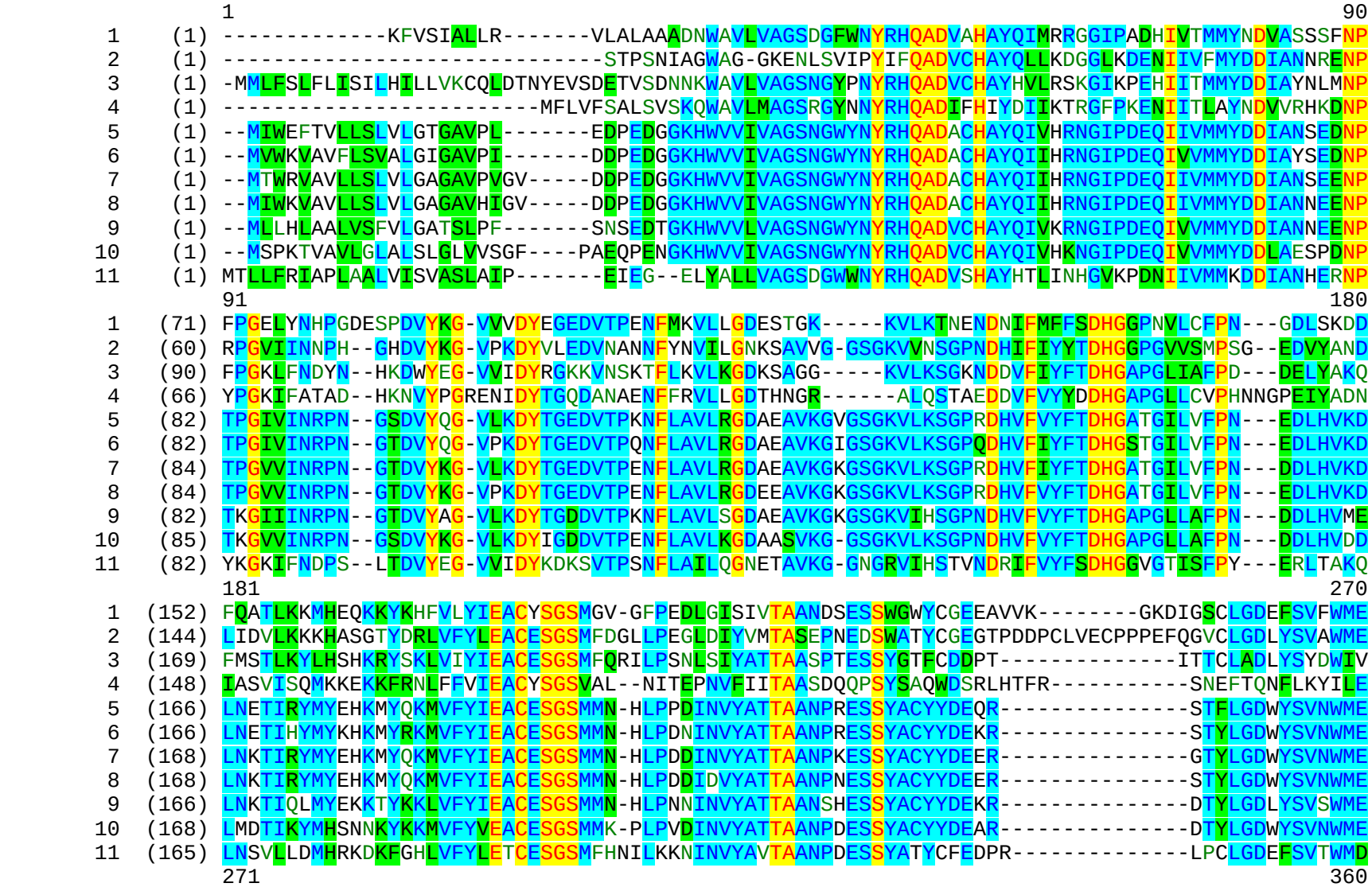

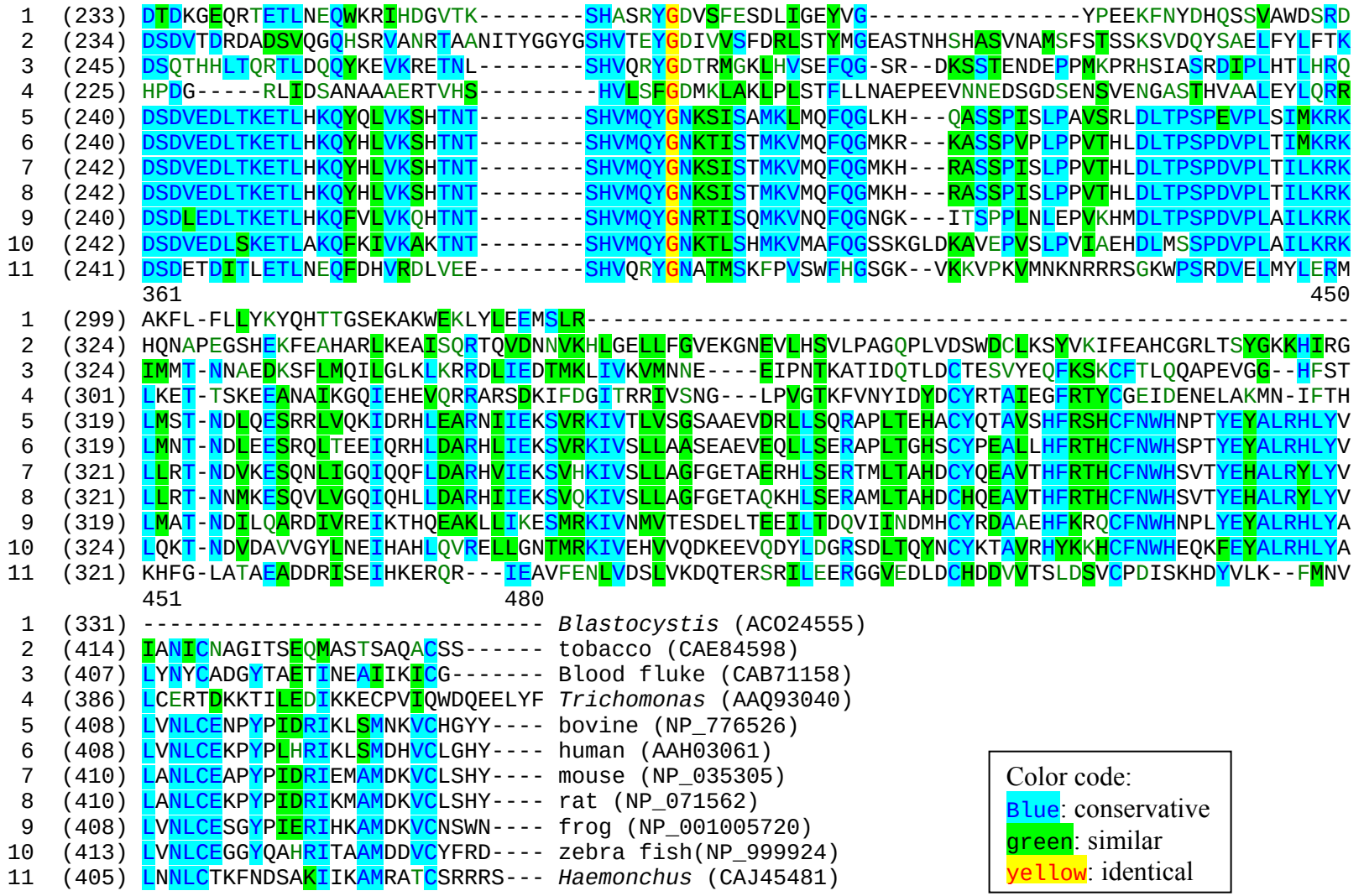
1 (233) DTDKGEQRTETLNEQWKRIHDGVTK-------SHASRYGDVSFESDLIGEYVG----------------YPEEKFNYDHQSSVAWDSRD
2 (234) DSDVTDRDADSVQGQHSRVANRTAANITYGGYGSHVTEYGDIVVSFDRLSTYMGEASTNHSHASVNAMSFSTSSKSVDQYSAELFYLFTK
3 (245) DSQTHHLTQRTLDQQYKEVKRETNL-------SHVQRYGDTRMGKLHVSEFQG-SR--DKSSTENDEPPMKPRHSIASRDIPLHTLHRQ
4 (225) HPDG-----RLIDSANAAAERTVHS---------HVLSFGDMKLAKLPLSTFLLNAEPEEVNNEDSGDSENSVENGASTHVAALEYLQRR
5 (240) DSDVEDLTKETLHKQYQLVKSHTNT-------SHVMQYGNKSISAMKLMQFQGLKH---QASSPISLPAVSRLDLTPSPEVPLSIMKRK
6 (240) DSDVEDLTKETLHKQYHLVKSHTNT-------SHVMQYGNKTISTMKVMQFQGMKR---KASSPVPLPPVTHLDLTPSPDVPLTIMKRK
7 (242) DSDVEDLTKETLHKQYHLVKSHTNT-------SHVMQYGNKSISTMKVMQFQGMKH---RASSPISLPPVTHLDLTPSPDVPLTILKRK
8 (242) DSDVEDLTKETLHKQYHLVKSHTNT-------SHVMQYGNKSISTMKVMQFQGMKH---RASSPISLPPVTHLDLTPSPDVPLTILKRK
9 (240) DSDLEDLTKETLHKQFVLVKQHTNT-------SHVMQYGNRTISQMKVNQFQGNGK---ITSPPLNLEPVKHMDLTPSPDVPLAILKRK
10 (242) DSDVEDLSKETLAKQFKIVKAKTNT-------SHVMQYGNKTLSHMKVMAFQGSSKGLDKAVEPVSLPVIAEHDLMSSPDVPLAILKRK
11 (241) DSDETDITLETLNEQFDHVRDLVEE-------SHVQRYGNATMSKFPVSWFHGSGK--VKKVPKVMNKNRRRSGKWPSRDVELMYLERM
361 450
1 (299) AKFL-FLLYKYQHTTGSEKAKWEKLYLEEMSLR----------
2 (324) HQNAPEGSHEKFEAHARLKEAISQRTQVDNNVKHLGELLFGVEKGNEVLHSVLPAGQPLVDSWDCLKSYVKIFEAHCGRLTSYGKKHIRG
3 (324) IMMT-NNAEDKSFLMQILGLKLKRRDLIEDTMKLIVKVMNNE----EIPNTKATIDQTLDCTESVYEQFKSKCFTLQQAPEVGG--HFST
4 (301) LKET-TSKEEANAIKGQIEHEVQRRARSDKIFDGITRRIVSNG---LPVGTKFVNYIDYDCYRTAIEGFRTYCGEIDENELAKMN-IFTH
5 (319) LMST-NDLQESRRLVQKIDRHLEARNIIEKSVRKIVTLVSGSAAEVDRLLSQRAPLTEHACYQTAVSHFRSHCFNWHNPTYEYALRHLYV
6 (319) LMNT-NDLEESRQLTEEIQRHLDARHLIEKSVRKIVSLLAASEAEVEQLLSERAPLTGHSCYPEALLHFRTHCFNWHSPTYEYALRHLYV
7 (321) LLRT-NDVKESQNLIGQIQQFLDARHVIEKSVHKIVSLLAGFGETAERHLSERTMLTAHDCYQEAVTHFRTHCFNWHSVTYEHALRYLYV
8 (321) LLRT-NNMKESQVLVGQIQHLLDARHIIEKSVQKIVSLLAGFGETAQKHLSERAMLTAHDCHQEAVTHFRTHCFNWHSVTYEHALRYLYV
9 (319) LMAT-NDILQARDIVREIKTHQEAKLLIKESMRKIVNMVTESDELTEEILTDQVIINDMHCYRDAAEHFKRQCFNWHNPLYEYALRHLYA
10 (324) LQKT-NDVDAVVGYLNEIHAHLQVRELLGNTMRKIVEHVVQDKEEVQDYLDGRSDLTQYNCYKTAVRHYKKHCFNWHEQKFEYALRHLYA
11 (321) KHFG-LATAEADDRISEIHKERQR---IEAVFENLVDSLVKDQTERSRILEERGGVEDLDCHDDVVTSLDSVCPDISKHDYVLK--FMNV
451 480
1 (331) ---------- Blastocystis (ACO24555)
2 (414) IANICNAGITSEQMASTSAQACSS------ tobacco (CAE84598)
3 (407) LYNYCADGYTAETINEAIIKICG------- Blood fluke (CAB71158)
4 (386) LCERTDKKTILEDIKKECPVIQWDQEELYF Trichomonas (AAQ93040)
5 (408) LVNLCENPYPIDRIKLSMNKVCHGYY---- bovine (NP_776526)
6 (408) LVNLCEKPYPLHRIKLSMDHVCLGHY---- human (AAH03061)
7 (410) LANLCEAPYPIDRIEMAMDKVCLSHY---- mouse (NP_035305)
8 (410) LANLCEKPYPIDRIKMAMDKVCLSHY---- rat (NP_071562)
9 (408) LVNLCESGYPIERIHKAMDKVCNSWN---- frog (NP_001005720)
10 (413) LVNLCEGGYQAHRITAAMDDVCYFRD---- zebra fish(NP_999924)
11 (405) LNNLCTKFNDSAKIIKAMRATCSRRRS--- Haemonchus (CAJ45481)
Color code:
Blue: conservative
green: similar
yellow: identical